University of Fort Hare
Together in Excellence

Faculty of Science and Agriculture

Department of Pure and Apply Chemistry

PHOTOCATALYTIC ACTIVITY AND ANTIBACTERIAL PROPERTIES OF Ag/N-DOPED TiO_2 NANOPARTICLES ON PVAE-CS NANOFIBRE SUPPORT

A dissertation submitted in fulfilment of the requirement for the degree of Master of Science in Chemistry

Atsile Rosy Ocwelwang

(Student number: 201112347)

Supervisor: Prof. L. Tichagwa

December 2012

Declaration

I, Atsile Rosy Ocwelwang present this thesis as the work done by myself in fulfillment for a Master of Science (MSc) degree in the Department of Chemistry, University of Fort Hare, King Williams Town Road, Alice, 5700 under the supervision of Prof. L. Tichagwa.

I therefore declare that this work has not been submitted in part or in whole to any other university.

Signature:…… Date:…….

Dedication

This work is dedicated to my family, my siblings, Mooketsi, Malebogo and Gopolang for their prayers, love, faithfulness, support, and for their patience with me. They have truly been my strength and *the wind beneath my wings* and I thank God for their lives.

Acknowledgements

First of all I would like to thank my Father, God all mighty, the Alpha and Omega of my life, for giving me the strength, wisdom and for His enduring love, favour and blessings. *Ebenezer*.

My sincere gratitude goes to my supervisor Prof. L. Tichagwa for her belief in me and my work, for her guidance and counsel. Thank you for going beyond the call of duty, I am eternally grateful for the parent I have found in you. I would also like to extend my heartfelt appreciation to my friends and family in the department of Chemistry, my research group to mention a few Mr P. Nyamukamba, Mr M.R. Vala, Mr H. Mungondori, and Mr T. Bunhu, I am forever grateful for all the advice and assistance. To the staff, colleagues and acquaintances in the department I am thankful for all the assistance and kindness you have shown me, as well as for your genuine interest in my work.

Many thanks go to the following people who provided technical assistance and support for me to accomplish the aims and objectives of my project: Mr N. Manene, Mr M. Nwamadi, Mr K. Tshapu, Mr T. Mcako, Ms L. Lubisi (Chemistry Department, UFH); Ms. N. Matyumza (EM unit, UFH), Dr R. Butcher (Ithemba Labs), Dr E. Green (Microbiology Department, UFH), Dr R. Erasmus (Wits University), and Mrs S. Pinchuck (Rhodes University).

I would also like to thank my family, my uncles, aunts, cousins and all my friends for continually keeping me in their prayers and for their words of encouragement.

And finally I would like to thank the National Research Foundation (NRF) and Govan Mbeki Research and Development Centre (GMRDC), UFH for financial support and all their assistance, without your assistance none of this would have been possible, I am humbled and grateful.

Abstract

Lack of potable water is one of the major challenges that the world faces currently and the effects of this are mainly experienced by people in developing countries. This has therefore propelled research in advanced oxidation technologies AOTs to improve the current water treatment methods using cost effective, non toxic and efficient treatment methods. Hence, in this study the sol-gel synthesis method was used to prepare TiO_2 nanoparticles that were photocatalytically active under UV and visible solar light as well as possessing antibacterial properties. Silver and nitrogen doping was carried out to extend the optical absorption of TiO_2. For easy removal and reuse of the photocatalyst the nanoparticles were immobilized on chitosan and poly (vinyl-alcohol-co-ethylene) using the electrospining technique. The synthesized nanomaterials were characterized by FTIR, XRD, SEM/EDS, TEM, DRS, and TGA. FTIR and EDS analysis confirmed the formation and composition of TiO_2 nanopowders for the doped and undoped nanoparticles. XRD analysis showed that the anatase phase was the dominant crystalline phase of the synthesized nanopowders. SEM and TEM respectively illustrated the distribution and size of the electrospun nanofibers and the nanoparticles of TiO_2. DRS results showed that there was a significant shift in the absorption band edge and wavelength of Ag-TiO_2 to 397 nm, followed by N-TiO_2 at 396 nm compared to the commercial titania which was at 359 nm.

The photocatalytic activities and antibacterial properties of these materials were tested on methylene blue dye and *E.coli* microorganism respectively. Ag-TiO_2 immobilized on nanofibers of chitosan and PVAE had the highest photocatalytic activity compared to N-TiO_2. Similar results were observed when the biocide properties of these materials were tested on *E. coli*.

Table of contents

List of Figures

List of Tables

List of Abbreviations

AOTs: Advanced oxidation technologies

MSTs: Membrane separation technologies

Cs: Chitosan

DBPs: Disinfection-by-products

e^-/h^+: Electron hole pair

NPs: Nanoparticles

NOM: Natural organic matter

PVAE: Poly (vinyl-co-ethylene) or

EVOH: Poly (ethylene co vinyl alcohol)

PVA: Poly vinyl alcohol

WHO: World Health Organization

UNICEF: United Nations Children's Fund

CNTs: Carbon nanotubes

CB: Conduction band

VB: Valence band

TiO_2: Titanium dioxide

FTIR: Fourier-transform infrared spectroscopy

XRD: X-ray diffraction

DRS: Diffuse reflectance spectroscopy

TEM: Transmission electron microscopy

SEM: Scanning electron microscopy

EDS: Energy dispersive x-ray spectroscopy

TGA: Thermogravimetric analysis

UV-Vis: Ultraviolet visible spectroscopy

CHAPTER 1: Introduction

1.0 General Overview

Clean, safe drinking water is one of the most essential needs for human health and for the survival of all organisms (Tiwari *et al*., 2009). Water is a basic human right and is considered an essential resource for human life. (Ahuja, 2009). Ensuring availability and supply of potable water is among the major concerns in the world currently. Water pollution is a problem for almost half of the world's population. According to a report by the United Nations (UN), 2.7 billion people will have shortage of water by the year 2025 (Ahuja, 2009; Savage *et al*., 2009).

Water borne diseases contribute to the mortality of fifteen million children every year especially in developing countries in continents such as Africa, Asia and Latin America (Gelover *et al*., 2006; Savage *et al*., 2009). According to the World Health Organization (WHO) 2.4 billion people die each year in the world due to consumption of contaminated water (Institute, 2009). Common waterborne diseases such as gastroenteritis, cholera and typhoid are due to water contamination by pathogens including bacteria, viruses, parasites and faecal matter (Ahuja, 2009).

1.1 Background and rationale

Several methods are used for treatment or disinfection of water contaminated with toxic wastes. Conventional methods include the use of ultraviolet light, reverse osmosis, water sediment filters, chlorination, coagulation and ozone (Christianmangun *et al*., 2001). It has however been discovered that some of the conventional methods are not always very efficient and reliable and they can also result in toxic substances. For example ozone partially degrades natural organic

matter (NOM) found in water to smaller molecules and these particles can also be poisonous. Moreover ozone does not remain in water for a very long time, thus this process is normally used in conjunction with chlorine in order to protect water from bacterial re-growth (Ahuja, 2009; Mamba *et al*., 2009). Likewise during chlorination, chlorine gas tends to react with some of the substances found in natural water to produce halogenated disinfection by-products (DBPs) such as trihalomethanes which are carcinogenic (Li *et al*., 2008; Shannon *et al*., 2008; Mamba *et al*., 2009). With the recognition of side effects and shortcomings associated with the use of conventional water treatment methods, the development of modern water treatment processes, such as advanced oxidation technologies (AOTs) and membrane separation technologies (MSTs) have become important (Choi *et al*., 2007). Extensive research and studies have been done using nanosciences and nanotechnology to purify water (Savage *et al*., 2005). Nanotechnology has gained tremendous attention in the present century because of its capability in allowing for the manipulation of materials and metals into nanosizes, which causes a drastic change in properties (Rai *et al*., 2009).

Recent advances suggest that a great deal of problems in water quality can be resolved or greatly ameliorated by using nanoparticles and nanoscale products developed from nanotechnology (Savage *et al*., 2005). Nanotechnology has enabled the development of a new class of atomic scale materials which are capable of degrading waterborne compounds and disease-causing microbes. Oligodynamic metallic nanoparticles such as silver, copper, zinc, titanium, nickel, and cobalt are among the most promising nanomaterials with bactericidal and viricidal properties (Hashimoto *et al*., 2005). Some nanoscale materials that are being studied and tested as functional materials for water purification include dendrimers, metal-containing nanoparticles, zeolites and carboneous nanomaterials. These materials have a broad range of physicochemical

properties that make them suitable as separation and reactive media for water purification and disinfection (Tiwari *et al*., 2009).

Lately, some of the natural and synthetic nanomaterials that have shown strong antimicrobial properties include chitosan, silver nanoparticles, photocatalytic TiO_2, fullerol, aqueous fullerene nanoparticles, and carbon nanotubes (CNTs). Among the different nanomaterials, TiO_2 is the most studied (Nosaka *et al*., 2005). Photocatalysis of TiO_2 has attracted great attention in the development of efficient water treatment and purification systems. In fact, it has been found that photocatalysis of TiO_2 is highly effective for the complete mineralization of most organic compounds such as pesticides, dyes, aromatic compounds and many more. In addition, the semiconductor has been proven to have the ability to remove cationic and ionic species that are hazardous to human health as well as the ability to inactivate pathogenic microbes found in contaminated water (Hashimoto *et al*., 2005; Choi et al., 2007; Lopez *et al*., 2012). TiO_2 is a also a good photocatalyst due to its biocompatibility, its efficiency, relative low production cost and chemical inertness (Nor *et al*., 2009).

However, it has been found that the photocatalytic activity of TiO_2 does not work effectively under solar radiation; it is mainly activated by ultraviolet (UV) radiation below λ=385 nm (Youji *et al*., 2008). This is a limiting factor for the application of TiO_2 in water disinfection in rural areas where the power grid is either limited or unavailable (Nosaka *et al*., 2005; Kim *et al*., 2008). Therefore, it is necessary to extend the optical properties of TiO_2 to allow the use of visible or indoor light in addition to UV light. Several strategies have been employed in an attempt to extend the absorption of titania and amongst them is metal ion and non metal ion doping which have been proven to be effective in enhancing the photocatalytic properties of TiO_2 (Li *et al*., 2002).

Addition of non metals to titania reduces the band gap by forming a new energy level between the valence band (VB) and the conduction band (CB). Commonly used non metal dopants include carbon, fluorine, phosphorous, sulphur and nitrogen. According to Asahi *et al*., (2001) nitrogen is a more efficient substitutional dopant compared to sulphur because of its smaller ionic radius. Due to the fact that the size of nitrogen is similar to that of oxygen, its incorporation into the crystal structure of titania is therefore easy resulting in reduced band gap by formation of in band gap electronic states (Gao *et al*., 2009).

Another approach that has been widely reported is doping of titania with metal ion dopants. The use of transition metals as dopants is believed to enhance the phototacatalytic activity of titania by acting as electron traps which in turn decreases the electron-hole (e^-/h^+) pair recombination, therefore increasing the life span of these charge carriers (Zaleska, 2008; Sun *et al*., 2010). Metal ions such as chromium, iron, copper, platinum, silver and many other have been widely explored as dopants. Amongst these, silver has been found to be more interesting mainly due to the fact that it has been known and used for centuries as an antibacterial agent (Choi *et al*., 2009; Wong *et al*., 2010). Visible light activation of TiO_2 can facilitate and accelerate the development of more sustainable processes for the remediation of contaminated water resources using solar light. The replacement of UV light irradiation by visible light offers potential for low-cost environmental measures where UV is limited, more so for water treatment (Hashimoto *et al*., 2005). Hence this study explored the effect that doping with silver metal and nitrogen non metal has on the photocatalytic properties of titania, in order to improve the its activity as well as investigate the antibacterial properties.

Another setback in the use of TiO_2 has been the separation of the TiO_2 powder from water after photocatalytic reactions to allow for reuse and for preventing environmental contamination by

the nanoparticles (Nosaka *et al*., 2005; Kim *et al*., 2008). To overcome this predicament, immobilization of the photocatalyst on a polymeric support has often been proposed. Immobilization of titania nanoparticles on electrospun polymer nanofibers has been reported to be practical and efficient and led to improved photocatalytic properties of TiO_2 (Su *et al*., 2003). It is therefore one of the aims of this study to immobilize TiO_2 nanoparticles on a substrate blend of chitosan (Cs) and poly (vinyl alcohol-co-ethylene) (PVAE) polymers for easy recovery and reuse in water treatment. Chitosan is a deacetylated derivative of chitin which is the second most naturally abundant biopolymer. Chitosan is known to possess antibacterial and antifungal properties, and due to its non toxicity, biodegradability as well as biocompatibility nanofibers of this biopolymer can be used in a variety of fields including environmental cleanup. Moreover chitosan is made up of side amino and hydroxyl groups which offer it the possibilities of being modified and functionalized for use as an adsorbent for toxic air and water pollutants (Dutta *et al*., 2004; Pillai *et al*., 2009; Chen *et al*., 2010; Sun *et al*., 2011; AbdElhady, 2012).

Chitosan has high viscosity and this makes it difficult to electrospin for fiber production, therefore to eliminate this shortcoming it is commonly blended with synthetic polymers. Zhang *et al*., (2007) reported that the electrospinnability of chitosan was improved after it was electrospun with the synthetic polymer poly (vinyl alcohol) (PVA). Moreover the mechanical properties and durability of chitosan can be improved by blending it with other synthetic polymers. Hence a blend of this natural polymer and a synthetic polymer PVAE was used in this study as a matrix to immobilize titania nanoparticles.

1.2 Problem Statement

The use of TiO_2 nanotechnology in water treatment promises better prospects because of its efficiency in the degradation of organic pollutants and inactivation of microorganisms in water (Richardson 2003; Hashimoto *et al*., 2005). Large scale application of TiO_2 is hindered by its wide band gap (3.0-3.3 eV) which allows only a small fraction (3-5%) of the solar energy to be used. Also, a high rate of electron hole pair recombination occurs and this reduces photocatalytic reactions, thereby resulting in a decreased rate of pollutant degradation. In addition, separation of nanoparticles from aqueous solution after wastewater treatment is difficult when using TiO_2 in powder form. This means that the photocatalyst cannot be recycled and that poses a risk if the particles are released into the water environment causing more pollution and possible toxicity to living organisms (Hong *et al*., 2006). These problems may be solved by developing an effective TiO_2 photocatalyst with a reduced band gap to allow utilization of UV light, immobilized on a suitable matrix for easy removal from water and with antimicrobial properties.

1.3 Research Aim and Objectives

The main aim of this study was to synthesize UV and visible light (solar light) active TiO_2 nanoparticles with a high photocatalytic activity and antibacterial properties for use in water treatment with the following objectives in mind:

- To prepare silver and nitrogen doped TiO_2 nanoparticles using the sol-gel synthesis method.
- To immobilize the doped nanoparticles onto chitosan (CS) - polyvinyl alcohol-co-ethylene (PVAE) nanofibers using the electrospinning method.

- To evaluate the effect of the dopants (Ag and N) on the photocatalytic activity of TiO_2 nanoparticles immobilized on CS-PVAE nanofibers using Methylene blue (MB) as a model organic pollutant in aqueous medium.
- To establish antimicrobial properties of the doped TiO_2 nanoparticles immobilized on CS-PVAE nanofibers using a strain of *E .coli* as a model pollutant

1.4 Research Hypothesis Statement

Transition metal and non metal ion doping has proved to be an efficient and feasible method for modifying the structure of TiO_2, so that it can easily absorb visible light which makes up about 45% of the solar radiation that reaches the earth surface. Non metal ion doping is responsible for reduction of the band gap by forming in gap states between the Valence Band (VB) and the Conduction Band (CB). Doping TiO_2 with metal ions has been reported to decrease the rate of electron hole pair (e^-/h^+) recombination by acting as electron traps. The lifetime of the e^-/h^+ pairs is increased and the ability for OH radical production is improved, and this is beneficial for oxidation of pollutants (Ho *et al*., 2006; Zaleska, 2008). Therefore metal and non metal ion co-doping seems to be an attractive alternative for improving photocatalytic activity of titanium dioxide.

1.5 Delineations and delimitations of the study

This study was focused on synthesis of silver (Ag) and nitrogen (N) doped TiO_2 nanoparticles using the sol-gel method. The as synthesized nanopowders where immobilized onto a blend of polymers by the electrospinning method. Electrospinning and the sol-gel method have previously been reported on in the research group (Nyamukamba *et al*., 2012). The photocatalytic and antibacterial activities of these nanocomposites were tested using methylene blue dye as a model

organic pollutant and a strain of *E. coli* as a model microorganism pollutant under UV light supplied by a UV lamp of wavelength 365 nm and visible solar light.

1.6 Dissertation outline

This research study is composed of six (6) chapters. Chapter 1 is made up of the introduction, the background and rationale of the study which introduces the research by giving a broad overview of the problems the world is facing in terms of water scarcity and proposed solutions. The chapter ends with the problem statement, research aims, specific objectives, the thesis statement and delineations and delimitations of the study. Chapter 2 is the literature review which gives a review of titanium dioxide, its properties, application in environmental clean-up, the need for modification and modification methods that can be used to improve its photocatalytic activity. Furthermore this chapter outlines the methods of modifications and the synthesis of polymer nanofibers that can be used as immobilization support for TiO_2 nanopowders. Sol-gel synthesis is discussed as the method used for the synthesis of the nanoparticles and electrospinning is reviewed as the method used for nanofibers production.

Chapter 3 is the experimental part of the study which outlines the methodology for synthesis of the doped and undoped titania nanoparticles and the immobilization onto the polymer nanofibers by electrospinning. This chapter is ended by brief outlines of the characterization techniques and their use in this study. Chapter 4 describes how test for the photocatalytic activity and antibacterial properties of the synthesized nanomaterials were carried out. The results are presented and discussed in Chapter 5 and lastly in Chapter 6 a concluding summary is given together with suggestions for future work. Reference list for Chapters one, two and three are at the end of each chapter respectively and for Chapters four, five and six they are listed at the end of the whole document.

References

AbdElhady, M. (2012). Preparation and Characterization of Chitosan/Zinc Oxide Nanoparticles for Imparting Antimicrobial and UV Protection to Cotton Fabric. *International Journal of Carbohydrate Chemistry* , 1-6.

Ahuja, S. (2009). *A handbook of water purity and quality.* New York,USA: Elsevier.

Asahi, R., Morikawa, T., Ohwaki, T., Aoki, K., Taga, Y. (2001). Visible-Light Photocatalysis in Nitrogen-Doped Titanium Oxides. *Science* , 269-271.

Behnajady, M.A., Modirshahla, N., Shokri, M, Rad, B. (2008). Enhancement of photocatalytic activity of TiO2 nanoparticles by Silver doping: Photodeposition versus Liquid impregnation methods. *Global NEST Journal* , 10,1, 1-7.

Castaneda, L., Terrones, M. (2007). Synthesis and structural characterization of novel flower-like titanium dioxide nanostructures. *Physica* , 143-146.

Chen, E., Su, H., Tan, T. (2010). Antimicrobial properties of silver nanoparticles synthesized by bioaffirnity adsorption coupled with TiO2 photocatalysis. *Society of Chemical Industry* , 421-427.

Choi, H., Stathatos, E., Dionysiou, D.D. . (2007). PhotocatalyticTiO2 films and membranes for the development of efficient wastewater treatment and reuse systems. *Desalination, Vol. 202* , 199-206.

Choi, J., Park, H., Hoffmann, M.R. (2009). Effects of Single Metal-Ion Doping on the Visible-Light Photo-reactivity of TiO2. *Journal of Physical Chemistry,C* , 17-55.

Christianmangun, Z., Economy, J. (2001). Removal of Chemical Contaminants from Water to below USEPA MCL using fiber glass supported activated carbon filters. *Environmental Science Technology, Vol. 35* , 2844-2848.

Dutta, P.K., Dutta, J., Tripathi, V.S. (2004). Chitin and chitosan: Chemistry, properties and applications. *Journal of Scienctific & Industrial Research* , 63, 20-31.

Gao, H., Zhou, J., Dai, D.,Qu, Y. (2009). Photocatalytic Activity and Electronic Structure analysis of N-doped Anantase TiO2:A Combined Experimental and Theoretical Study. *Chem. Eng. Technol.* , 32;6:867-872.

Gelover, S., Gomez, L.A., Reyes, K., Leal, M.T. (2006). A practical demonstration of water disinfection using TiO2 films and sunlight. *Water Research, Vol. 40* , 3274-3280.

Hashimoto, K., Irie, H., Fujishima, A. (2005). TiO2 Photocatalysis: A Historical overview and future prospects. *Journal of Applied Physics, Vol. 44* , 8269-8285.

Ho, W., Yu, J.C., Lee, S. (2006). Low-temperature hydrothermal synthesis of S-doped TiO2 with visible light photocatalytic activity . *Journal of Solid State Chemistry, 179* , 1171-1176.

Institute, N. E. (2009). *Water Safety Plan: A manual for pilot study.*

Kim, D.H., Choi, D., Kim, S., Lee, K.S. (2008). The effect of phase type on photocatalytic activity in transition metal metal doped TiO2 nanoparticles. *Catalysis Communicationss, Vol. 9* , 654-657.

Li, F.B., Li, X.Z. (2002). The enhancement of photodegradation efficiency using Pt-TiO2 catalyst. *Chemosphere, Vol. 48* , 1103-1111.

Li, Q., Mahendra, S., Lyon, D.Y., Brunet, L., Liga, M.V., Li, D., Alvarez, P.J.J. . (2008). Antimicrobial nanomaterials for water disinfection and microbial control: Potential applications and implications. *Water Research, 42* , 4591-4602.

Lopez Goeme, T.M., Alvarez Lemus, M.A., Angeles Morales, V., Gomez Lopez E., Castillo Ocampo, P. (2012). Study of Bacterial Sensitivity to Ag-TiO2 Nanoparticles. *J. Nanomedicine & Nanotechnology* , 1-7.

Mamba, B.B., Kruise, R.W., and Haarhoff, J. (2009). Monitoring natural organic matter and disinfection by-products at different stages in two South African water treatment plants. *Water S.A. , Vol. 32* , 121-127.

Nor Hafizar, Iis Sopyan. (2009). Nanosized TiO2 Photocatalyst Powder via Sol-Gel Method: Effect of Hydrolysis Degree on Powder Properties. *International Journal of Photoenergy* , 1-8.

Nosaka, Y., Matsushita, M., Nishino, J., Nosaka, A.Y. . (2005). Nitrogen-doped titanium dioxide photocatalysts for visible response prepared by using organic compounds. *Science and Technology of Advanced Materials, Vol. 6* , 143-148.

Nyamukamba, P., Tichagwa, L., Greyling, C. (2012). The influence of carbon doping on TiO2 nanoparticle size, surface area, anatase to rutile phase transformation and photocatalytic activity. *Materials Science Forum* , 712;49-63.

Rai, M., Yaday, A., Gade, A. (2009). Silver nanoparticles as a new generation of antimicrobials. *Biotechnology Advances, Vol. 27* , 76-83.

Richardson, S. (2003). Disinfection by-products and other emerging contaminants in drinking water. *Trends in Analytical Chemical, Vol. 22, Issue 10* , 666-684.

Savage, N., Diallo, M., Duncan, J., Street, A., Sustich, R. (2009). *Nanotechnology Applications for Clean Water*. Norwich, NY, : William Andrew Inc.

Savage, N.,Diallo, M.S. (2005). Nanomaterials and water purification: Opportunities and challenges. *Journal of Nanoparticles Research, Vol. 7* , 331-342.

Shannon, M.A., Bohn, P.W., Elimelech, M., Georgiadis, J.G., Marinas, B.J. (2008). Science and technology for water purification in the coming decades. *Nature Reviews, 452* , 301-310.

Sun, C., Li, Q., Gao, S., Cao, L., Shang, J.K. . (2010). Photocatalytic Disinfection of Escherichia coli Bacteria by Silver Modification of Nitrogen-Dodep Titanium Oxide Nanoparticle Photocatalyst Under Visible-Light illumination. *American Ceramic Society, 93(11)* , 3880-3885.

Sun, C., Li, Q., Gao, S., Cao, L., Shang, J.K. (2010). Enhanced Photocatalytic Disinfection of Escherichia coli Bacteria by Silver Modification of Nitrogen-Dodep Titanium Oxide Nanoparticle Photocatalyst Under Visible-Light illumination. *American Ceramic Society* , 93;11:3880-3885.

Tiwari, D.K., Sen, P. (2009). Application of Nanoparticles in Waste Water Treatment. *World Applied Sciences Journal, Vol. 3* , 417-433.

Wong, M., Sun, D., Chang, H. (2010). Bactericidal Performance of Visible Light Responsive Titania Photocatalyst with Silver Nanostructures. *Plos One, 5* , 1-7.

Youji, L., Xiaohu, W., Xiaohua, W. (2008). Inactivated properties of activated carbon-supported TiO2 nanoparticles for bacteria and kinetic study. *Journal of Environmental Sciences* , 20; 1528-1533.

Zaleska, A. (2008). Doped- TiO2: A review. *Recent Patents on Engineering, Vol. 2* , 157-164.

Chapter 2 - Literature Review

2.0 Introduction

The supply of clean water is a matter of great concern in the world, most especially in the less developed countries. Even though several successful initiatives have been put in place in the past in order to supply safe, clean drinking water to our urban population, this effort still falls short of the required targets for sustainable development (Gelover *et al.,* 2006). According to a report by WHO and UNICEF, 1.2 billion people lacked an adequate supply of safe drinking water and 2.4 billion did not have access to improved sanitation (WHO, UNICEF, 2000). As a result, 2.2 million people die from diarrhoea related diseases every year, most of whom are children under the age of five (Li *et al.,* 2008; Ahuja, 2009).

The need for provision of clean water and basic sanitation can never be overstated hence they are top of the list on the United Nations Millennium Development Goals (UN-MDGs). The lack of these basic human necessities leads to terrible living conditions, bad hygiene practices and various waterborne diseases (Savage *et al.,* 2005; WHO & Unicef, 2006). Extensive research has been carried out during the past few years to develop heterogeneous photocatalysts which can be applied in air purification, water disinfection, hazardous water remediation and water purification (Yu *et al.,* 2002). The process of heterogeneous photocatalytic oxidation is considered to be one of the most important advanced oxidation processes (AOPs). This is due to the fact that treatment of polluted water with these processes results in complete breakdown of the pollutants to harmless end products such as carbon dioxide, water and inorganic compounds. Photocatalysis can be defined as the acceleration of a photoreaction in the presence of a catalyst. It is mainly focused on using light of appropriate wavelength to enhance the rate of activity of a

solid catalyst. UV and visible light irradiation can be used to excite charge carriers in semiconductors like ZnO, F_2O_3, CdS, ZnS, and TiO_2 which is one of the most commonly used in photocatalysis (Behnajady *et al.,* 2008; Philippopoulos *et al.,* 2010). Photocatalysis involves a variety of reactions such as organic synthesis, water splitting, photo reduction, metal deposition, disinfection, anticancer therapy, gaseous pollutant removal as well as water detoxification. Over the years titanium dioxide (TiO_2) based heterogeneous photocatalysis has gained a lot of attention as an attractive and effective technology for air purification and treatment of wastewaters contaminated with persistent organic compounds (Al-Rasheed, 2005; Gaya *et al*., 2008; Wen *et al*., 2009; Philippopoulos *et al*., 2010).

This review discusses the problems of water contamination due to organics and microorganic pollutants and how heterogeneous photocatalysis under nanotechnology can be part of the solution. General applications of TiO_2 are discussed together with the drawbacks of using TiO_2 for heterogeneous photocatalysis on a larger scale. Furthermore methods of modification in the form of doping the nanoparticles with noble metals to extend their optical absorption band from UV to visible light are reviewed and the use of polymer based nanofibers as supports in water treatment are reported. Electrospinning is also looked at as a method of choice for manufacturing the nanofibers of TiO_2/polymer composites.

2.1 Applications of nano-TiO_2

Titania is one of the most popular commercially available nano-size materials that has found application in a variety of fields to date since its novel properties where published in the early 1970s. Nano materials have shown that they possess different chemical, mechanical, optical and electrical properties compared to their bulk counterparts and they react faster and efficiently.

Among the many photocatalysts, TiO_2 is the most important because of its strong oxidizing power (McCullagh *et al*., 2007; Sirimahachai *et al*., 2009).

Nano structured TiO_2 has found a variety of applications in fields such as optics, electrical insulation, photovoltaic solar cells due to its electron transfer properties, antibacterial coatings and photocatalysis. Some nano sized products can be found commercially as cleaning materials, self-cleaning coatings, sunscreens, toothpastes, air filtration devices, and environmental remediation of pollutants (Hafez *et al*., 2005; Robichaud *et al*., 2009).

In this study nanostructured titania is explored as a photocatalyst for purifying water contaminated with bacteria and organic pollutants. Reports on the antibacterial properties and the photocatalytic activity of TiO_2 are reviewed.

2.1.1 TiO_2 Photocatalysis

Photocatalysis of titanium dioxide (TiO_2) was first discovered in 1972 in an experiment done by Honda and Fujishima. An electrochemical cell which had an inert cathode and TiO_2 rutile phase anode was used to split water into hydrogen and oxygen under UV light. This discovery marked the beginning of a series of research studies and investigations on TiO_2 and its properties as a photocatalyst in a variety of fields such as energy conversion and environmental remediation (Batzill *et al*., 2006; Zaleska, 2008). Titania gained tremendous attention for environmental application after the discovery by Frank and Bard that it was possible to use it for the decomposition of cyanide in water (Sze *et al*., 2008). It has also been reported to be an effective photocatalytic disinfectant of various microorganisms under UV light irradiation (Sun *et al*., 2010).

Although many semiconductors like ZnO, ZrO_2, CdS, MoS_2, Fe_2O_3 and WO_3 can be used as photocatalysts, TiO_2 is considered the most efficient especially for water and air treatment due to

the fact that it has a high oxidising and reducing power, it is relatively non toxic, chemically inert, has low production costs and long term stability against photo-corrosion (Yu *et al*., 2002; Nor *et al*., 2009). TiO_2 is known to exist naturally in three crystalline phases in nature: brookite, anatase and rutile which have the same octahedral $[TiO_6]^{2-}$ structure but different arrangements of atoms. Anatase and rutile are tetragonal and brookite exists in a rhombohedral structure (Nie *et al*., 2009; Chen, 2009; Nolan *et al*., 2010). Figure 2.1 shows a diagram of the commonly studied polymorphs of titanium dioxide showing their distinguished structures, band gap energy and other characteristics:

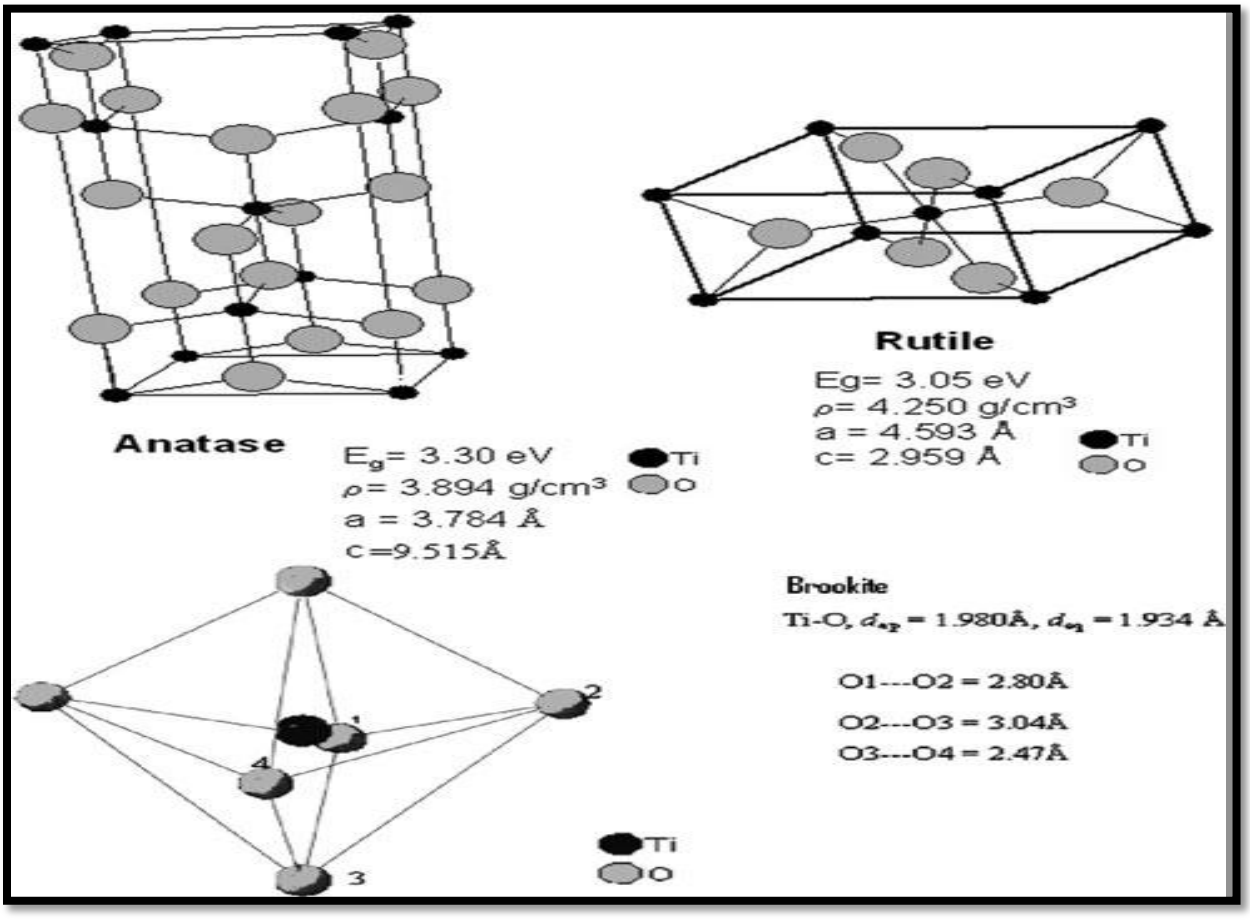

Figure 2.1: Three polymorphs of TiO_2 (Antase, Rutile & Brokite) (Macwan *et al*., 2011)

Studies show that anatase and brookite are the metastable polymorphs of titania unlike rutile which is thermodynamically stable. However anatase is the widely studied phase because it has been found to be the most photocatalytically active. According to literature when titania is exposed to high temperature treatment ranging between 600-700 ºC, it undergoes phase transformation from anatase to rutile (Liqiang *et al*., 2003; Chen *et al*., 2006; Xiao *et al*., 2006; Yu *et al*., 2006; Nolan *et al*., 2010).

The TiO_2 anatase polymorph has the forbidden band gap of ~ 3.3 eV, implying that TiO_2 can only exhibit photocatalytic activity when irradiated with ultraviolet light (wavelength < 400 nm). A band gap is the empty space that extends from the top of the valence band that is filled with electrons to the bottom of the empty conduction band. In terms of the molecular orbital theory (MO), the band gap can be described as the highest occupied molecular orbitals (HOMO) and lowest unoccupied molecular orbital (LUMO). Band gap can be related to electric conductivity of materials, for example metals are known not to have a band gap hence they are good conductors of electricity and insulators have a large band gap therefore electricity cannot pass through them. In contrast semiconductors have an intermediate band gap between insulators and metals (Linsebigler *et al*., 1995; Sung-Mao *et al*., 2007; Zaleska, 2008; Sheng, et al., 2008).

A chain of reactions begins when TiO_2 is irradiated by UV light and it absorbs a photon (hv) with energy greater than that of the band gap energy. The sequence of events is illustrated using equations (1) to (9):

$$TiO_2 + hv \rightarrow TiO_2\,(h^+_{VB} + e^-_{CB}) \qquad (1)$$

Figure 2.2 shows a schematic of the simplified photo-reduction and photo-oxidation reaction mechanisms that occur on the conduction and valence band of titanium dioxide respectively:

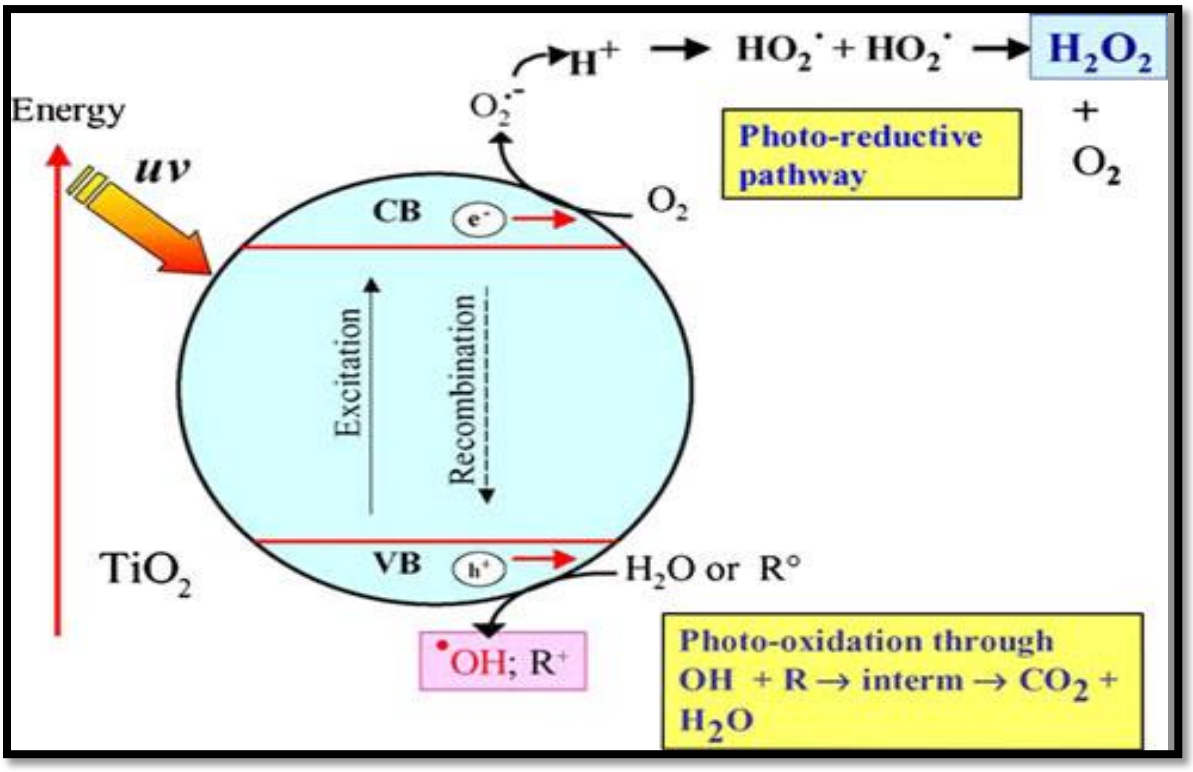

Figure 2.2: Mechanism of TiO_2 photocatalysis (macwan, *et al*., 2011)

An electron-hole pair is then produced from the valence band (VB) of the photocatalyst. The negatively charged electron moves from the VB to the conduction band (CB) leaving the positively charged hole behind. The electron and hole then take part in reduction-oxidation reactions with species that are adsorbed on the surface of titania, such as water, hydroxide (OH^-) ions, organic compounds or oxygen. The conduction band electron (e^-) is highly reducing while the valence band hole (h^+) is highly oxidizing.

$$TiO_2\ (h^+_{VB}) + H_2O_{ads} \rightarrow TiO_2 + \bullet OH_{ads} + H^+ \qquad (2)$$

$$TiO_2\ (h^+_{VB}) + OH^-_{(surface)} \rightarrow TiO_2 + \bullet OH_{ads} \quad (3)$$

The charge carrier h^+ oxidizes H_2O or OH^- ion to the hydroxyl radical (OH•) which is a highly potent, non-selective oxidant. It readily attacks pollutants adsorbed at the surface of titania or in aqueous solution degrading them to water and CO_2.

$$\bullet OH + D_{ads} \rightarrow \quad D^+_{oxid} + H_2O \quad (4)$$

On the conduction band (CB) the electron reduces adsorbed oxygen (O_2) species to superoxide (O_2•), which then undergoes a series of reactions (5-9) to give the OH• radical.

$$TiO_2\ (e_{cb}^-) + O_{2ads} + H^+ \rightarrow TiO_2 + HO_2\bullet \rightarrow O_2\bullet^- + H^+ \quad (5)$$

$$TiO_2\ (e_{cb}^-) + HO_2\bullet + H^+ \rightarrow H_2O_2 \quad (6)$$

$$H_2O_2 + h\nu \rightarrow 2HO\bullet \quad (7)$$

$$H_2O_2 + O_2\bullet^- \rightarrow HO\bullet + O_2 + HO^- \quad (8)$$

$$H_2O_2 + TiO_2\ (e_{cb}^-) \rightarrow HO\bullet + HO^- + TiO_2 \quad (9)$$

Direct or indirect oxidation and reduction of the adsorbed pollutants and other species in aqueous solution by photogenerated charge carriers (h+/e-) eventually leads to the mineralization of the pollutants (Choi *et al*., 2009; Philippopoulos *et al*., 2010). In a case where the above discussed processes do not occur, recombination of the charge carriers results and energy is released in the form of heat and this causes great reduction in efficiency of TiO_2 photocatalysis (Linsenbigler et al., 1995; Al-Rasheed, 2005).

Properties that influence the photocatalytic activity of TiO_2 particles have been suggested to include the surface area, crystallinity; crystallite size and crystal structure (Al-Salim *et al*., 2000). Anatase has been reported to have enhanced photocatalytic activity because of its more open structure compared to rutile (Xiao *et al*., 2006). Extensive research has been conducted to optimize the catalytic properties of titania used in the photodegradation of organic pollutants in water by using modified titania or thin films of titania (Cheng *et al*., 2003). A number of modification strategies commonly employed to improve the photocatalytic efficiency of TiO_2 include:

- Surface sensitization whereby the excitation of a wide band gap semiconductor is achieved by using a light sensitive dye;
- Decreasing the size of titania grains; nanoparticles with reduced size are reported to have a large surface area and this is advantageous because it means there are many active sites for degradation and adsorption of pollutants;
- Addition of electron acceptors to the semiconductor with a wide band gap with another semiconductor with a short band gap that undergoes photo-excitation easily. For example sensitization of TiO_2 with CdS; and
- Doping, this is a widely researched method. It involves introduction of metal or non metal ions as impurities that trap electrons ejected from the valence band in order to prevent charge carrier recombination. This therefore increases the efficiency of photocatalysis (Linsenbigler et al., 1995; Sze *et al*., 2008; Choi *et al*., 2009; Wen *et al*., 2009).

2.1.2 The antibacterial activity of TiO_2

The application of TiO_2 photocatalysis has been reported for over the past two decades as a promising solution to water and air contamination. The photocatalyst has been found to have properties of an antibacterial agent. It has on many occasions been reported to kill both Gram-negative and Gram positive bacterial as well as a variety of viruses (McCullagh *et al*., 2007; Li *et al*., 2008). The antimicrobial property of TiO_2 was first realised by Matsunaga *et al*., in 1985. The photocatalyst was used to inactivate microorganisms under UV irradiation. This study was then followed by a series of investigations on photocatalytic disinfection of various microorganisms such as bacteria, viruses, cancer cells as well as algae (Wong *et al*., 2010; Sun *et al*., 2010).

Irradiation of titania with UV light activates valence band electrons to be transferred to the conduction band leaving behind a positively charged hole. These activated charge carriers create reactive oxygen species (ROS) by reacting with atmospheric oxygen and water molecules. Production of ROS is reported to be the driving force behind the antibacterial activity of titanium dioxide (Amitava *et al*., 2011; Allahverdlyev *et al*., 2011). Doping the photocatalyst with metal and non metal dopant has also proved to be effective in enhancing the inactivation of microorganisms even in the absence of light. A comparative research study between commercial Degussa P25 and a sol-gel synthesized TiO_2 doped with trivalent dopants, aluminium (Al) and boron (B) was undertaken. From the results obtained it was observed that the Al and B doped samples had high antibacterial activity than the commercial photocatalyst (Wei *et al*., 2008; Sirimahachai *et al*., 2009). Using the sol-gel synthesis method and different silver dopant precursors Lopez Goeme *et al*., (2012) reported an enhanced antibacterial activity of Ag doped TiO_2 towards a variety of Gram positive and Gram negative bacterial strains. These results were

in agreement with those of Zhang *et al*., (2009) who reported that good distribution of silver nanoparticles on the surface of titania contributed to the increased antibacterial activity.

2.2 Modifications to improve the Photocatalytic activity of TiO_2

For the past few decades research on TiO_2 has grown tremendously and the photocatalyst has shown great potential for use in various fields, including environmental cleaning, renewable energy production in the form of photovoltaic cells, as well as water and air purification. However, due to the wide band gap of titania (3.2 eV for anatase), many of these applications cannot be carried out under solar light as the semiconductor can only be activated by UV light which accounts for a small fraction of the solar spectrum (Park *et al*., 2006; Ni *et al*., 2007; Shen *et al*., 2009).

To overcome this drawback several modification approaches have been proposed and reported. Some of the approaches include sensitizing titania with a dye or a colourful organic or inorganic compound that can absorb light in the visible region. Secondly, coupling the metal oxide semiconductor with another semiconductor that has lower band gap energy can alter the charge-transfer properties between titania and the surrounding environment, thereby improving the performance of devices made from TiO_2 based nanomaterials as well as doping TiO_2 with metal or non metal ion elements. This method has been widely studied order to produce photocatalysts that can be used under natural sunlight irradiation (Umebayashi *et al*., 2002; Zaleska, 2008; Nah *et al*., 2010; Mahmoud *et al*., 2012).

2.2.1 Doping

Development of TiO_2 materials with high photocatalytic efficiency and sensitivity towards visible light has been the focal research area for scientists around the world for some time. This

has been done by looking into modification methods such as doping. Doping is a form of structural modification in which impurity elements are incorporated into the lattice structure of TiO_2 in order to improve its photocatalytic activity and other related functions. This has been done with both cations and anions and it has been reported to be successful in inducing batho-chromic shift in titania. This approach has been under continuous research for the past decade with promising results towards reducing the band gap energy (Zaleska, 2008; Nie *et al*., 2009; Liao *et al*., 2009; Huang *et al*., 2010).

It is reported that impurity doping alters the structural properties of this photocatalytic semiconductor, thus changing the optical constants and absorption spectra of titania by shifting the optical response from the UV light range (λ< 387 nm) to the visible light (λ>400 nm) range. In the process of doping the ions can occupy a variety positions on the TiO_2 nanostructure, it can either be attached on the surface or be incorporated into the lattice structure of the materials (Li *et al*., 2005). Studies suggest that a doped impurity element can either be an electron scavenger of electrons generated during electron-hole pair production, or it can extend the optical absorption of the semiconductor material to visible light (Esquivel *et al*., 2011). Furthermore the activity of the dopant can differ depending on whether the dopant is on the surface of the nanomaterials, or on the interstitial or substitutional site of the titania lattice structure (Mardare *et al*., 2000; Li *et al*., 2005).

Doping can further increase effective e^-/h^+ pair generation, which are essential for application in photocatalysis. This process has been reported to be successful in increasing the photocatalytic activity of titanium dioxide (Al-Salim *et al*., 2000; Sze *et al*., 2008; Kisanda *et al*., 2010). Successful incorporation of anion and cation dopants has been widely reported on by researchers across all scientific fields. Commonly used transition metals include: Copper, Iron, Platinum,

Gold and Silver. Incorporation of these noble metals into the dielectric matrix of titania provides an absorption feature due to the strong surface plasmon resonance (SPR) that they possess and this is observed in the visible region of the solar spectrum. Extensive research has also been done on non metal ion doping and some of the common non metals used include carbon, nitrogen, and sulphur (Ho *et al*., 2006; Zaleska, 2008; Kanjwal *et al*., 2010). A study by Esquivel *et al*., (2011) suggested that during the doping process the impurities replace the some Ti^{4+} centres on titania thus producing an impure state which reduce the band gap of the photocatalyst. Non metal ion dopants are reported to substitute some of the oxygen atoms in the lattice of TiO_2 thus reducing the band gap of titania by mixing the 2p states of N and O (Ho *et al*., 2006). Figure 2.3 depicts two unit cells of TiO_2; diagram (a) is the undoped rutile polymorph and (b) is the unit cell of metal doped titania with one of the Ti atoms replaced by the metal dopant.

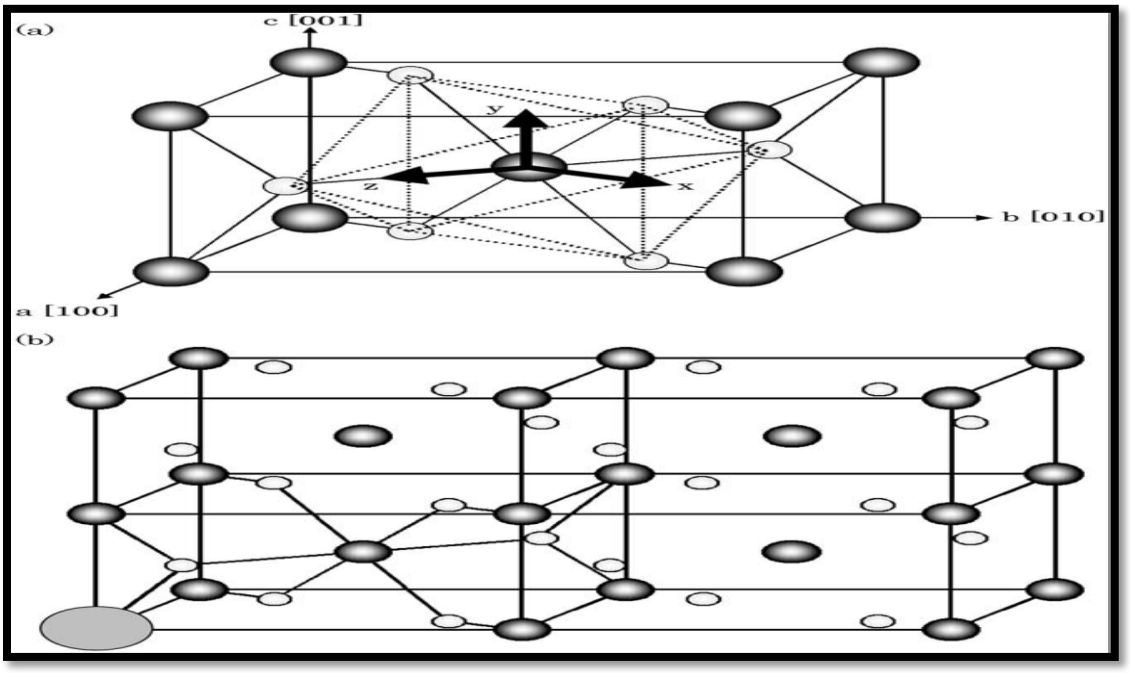

Figure 2.3: Diagram of unit cell undoped (a) and doped (b) rutle TiO_2

2.2.1.1 Silver doping

Extensive research on metal ion doping has shown that certain transition metal ions can extend the light absorption band of a semiconductor to the visible light region. Addition of noble metals such as Ag, Au, Pt, Pd, Cu, and Ni as dopants on titania has shown visible improvement in the photocatalytic activity of the semiconductor. Furthermore, it is reported that due to the work function of the dopants which is higher than that of a semiconductor a Schottky barrier is provided and this assists in the transfer of electrons from the semiconductor to the metal thus improving the catalytic efficiency by preventing charge carrier recombination (Tayade *et al*., 2006; Wei *et al*., 2008).

According to a study in which silver (Ag) and niobium (Nb) were used as dopants to investigate the effect of doping on the structure of titania, it was discovered that these two noble metals have a significant effect on the structure of the photocatalyst as well as on its properties. The phase transformation of TiO_2 from rutile to anatase was found to be mainly enhanced by Ag dopant, whereas Nb stabilized the anatase phase of titania. The activity of Ag was due to the increase in oxygen vacancies at the surface of anatase grains which favours the ionic rearrangement and structural reorganization for the formation of rutile phase (Ahmad *et al*., 2007; Wei *et al*., 2008). Liu *et al*., (2003) reported that during the doping process with silver ion, TiO_2 underwent structural changes and this enhanced the antibacterial activity of the photocatalyst. According to Seery *et al*., (2007) when silver is doped onto titania, it is deposited on the surface of the titania nanoparticles and not into the lattice structure of the photocatalyst. This is due to the fact that Ag ion has a large radius of 126 pm compared to 68 pm of Ti^{4+} ion. As a result these surface attached ions are reported to act as electron traps during photocatalysis, thereby improving the

photocatalytic activity by preventing recombination of charges. Figure 2.4 below shows a schematic diagram of silver doped TiO_2 illustrating the above discussed phenomenon:

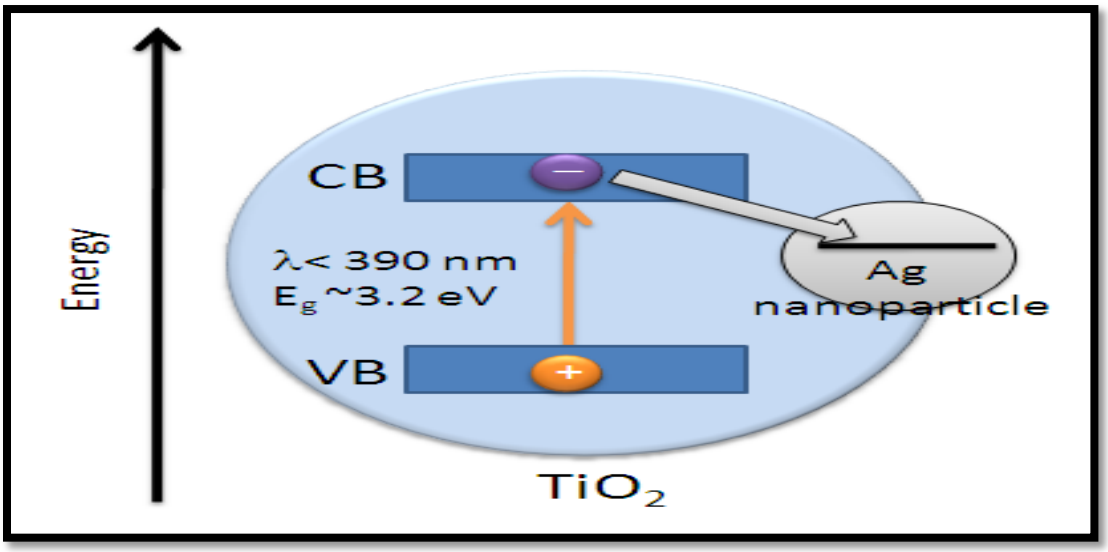

Figure 2.4: A schematic representation of Ag-doped TiO_2 (Seery, 2009)

Elemental silver has long been known and used as an antibacterial agent for decades and it has also been reported to improve the antibacterial activity of TiO_2. Moreover, research on silver and other noble metals such as gold and platinum have shown that they possess distinctive electronic and catalytic properties which in turn are essential in photocatalysis (Song *et al*., 2006; Hamal *et al*., 2007; Li *et al*., 2008). Silver is well known to have strong toxicity towards a wide range of microorganisms including coliforms found in wastewater (Lala *et al*., 2007; Tiwari *et al*., 2008; Wang *et al*., 2009).

2.2.1.2 Nitrogen doping

Non-metal dopants have also been reported to help increase the photocatalytic efficiency of TiO_2. Doping TiO_2 with anions such as nitrogen, boron, carbon and sulphur has received a lot of

attention over recent years in attempts to extend the light absorption band of the catalyst from ultraviolet to the visible light range (Hu *et al*., 2010). The use of nitrogen as a dopant marked the early successes of titania band gap reduction; furthermore this anion is one of the most investigated anionic dopants mainly due to its atomic size which is comparable to that of oxygen. It can easily be substituted into the substitutional sites of TiO_2 and enhance the photocatalytic activity (Nie, 2009; Huang *et al*., 2010).

According to Irie *et al*., (2003) nitrogen 2p states forming on top of the oxygen 2p valence band are responsible for the optical shift of titania from UV to visible light. Co-doping nitrogen with a noble metal has also been reported to enhance photocatalytic activity of titania (Nosaka *et al*., 2005; Sun *et al*., 2010). Figure 2.5 shows a schematic diagram of N doped TiO2 with newly formed in gap states:

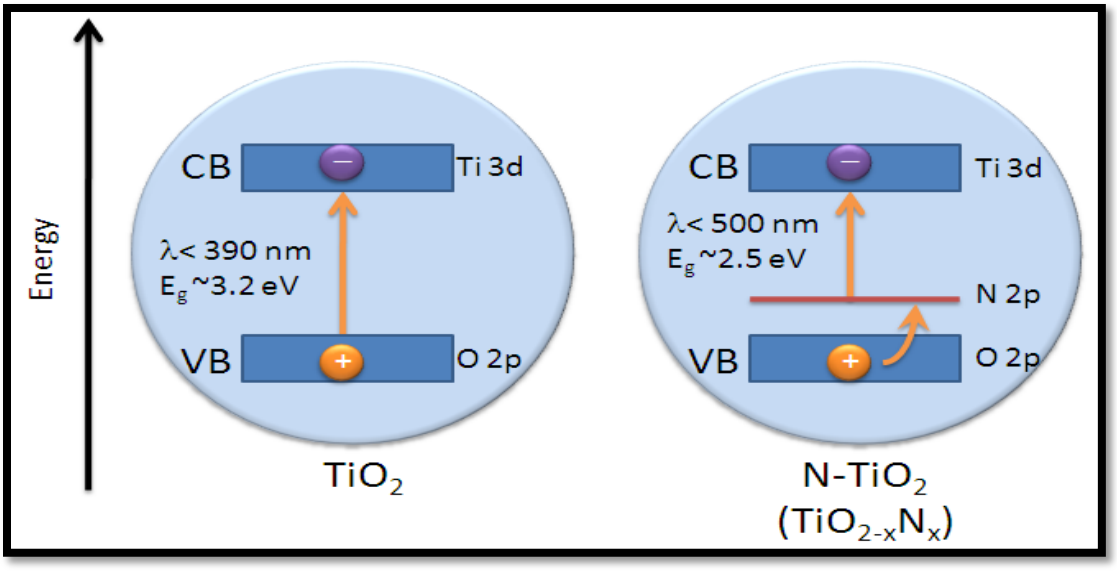

Figure 2.5: A schematic representation of N-doped TiO_2 (Seery, 2009)

Using the density function theory (DFT) calculations, Zhao *et al*., (2011) investigated the effect of nitrogen doping on titania. Their study focused on the effect resulting from electronegativity difference between nitrogen and oxygen and their interaction with the electronic structure and properties of N-doped TiO_2. It was therefore observed that the valence band energy shifted to a valence band maximum value of 0.27 eV and this contributed to an increased photocatalytic activity under visible light. These finding correspond with the study done by Asahi *et al*., (2001) that nitrogen substitutional doping of TiO_2 results in impurities above the valence band maximum (VBM) or below the conduction band minimum (CBM) therefore decreasing the wide band gap of titania. Furthermore the authors reported that this can be attributed to the mixing 2p states of nitrogen and oxygen and their interactions with Ti 3d states.

2.3 Support for TiO_2 nanoparticles

Titanium dioxide is a versatile material due to the potential prospects it possesses in dealing with environmental cleanup and energy challenges among many of its applications (Linsebigler *et al*., 1995; Chen *et al*., 2007). Large scale use of this photocatalyst in environmental cleanup especially in water treatment is however hindered by its use in powder form. A variety of support for TiO_2 photocatalyst have been explored over the years in order to eliminate the tedious exercise of filtering the suspended nanoparticles after treating contaminated water with the powdered photocatalyst. Immobilization on a matrix or coating the TiO_2 on surfaces like glass and ceramic tiles have been widely used and reported to have promising potential (Gaya *et al*., 2008).

2.3.1 TiO_2 immobilization on Polymer substrates

Over the years, the use of nanoparticles for environmental pollution remediation has been growing. However, practical application of these nanosized materials in water or air treatment is

still faced with challenges such as recovery and reuse of suspended nanoparticles after photocatalytic reactions. Failure to separate nanoparticles from fluids exposes the ecosystem and its inhabitants to the risk of nanotoxicity due to the material being released to the environment (Zhao *et al*., 2011). To overcome this predicament, immobilization of the photocatalyst on a polymeric support has often been proposed. Immobilization refers to the attachment or entrapment of a particle onto the chosen supporting matrix (Gorecka *et al*., 2011). Supporting titania nanoparticles with electrospun polymer nanofibers has been reported to be practical and efficient and led to improved photocatalytic properties of TiO_2 (Fang *et al*., 2011). Polymer blends can be synthesized by a variety of methods such as template growth or synthesis, co-electrospinning which involves spinning of two polymers from two needles onto the same collector screen and electrospinning where two or more polymer solutions are mixed together prior to the spinning process (Su *et al*., 2003; Wei *et al*., 2006).

Compared to bulk materials nanosized polymer fibre materials display several useful properties such as high specific surface area due to their small diameters, flexibility in surface functionalities, and good mechanical strength. They are also highly porous materials with better pore interconnection. These properties make polymer nanofiber materials suitable for a variety of applications (Huang *et al*., 2003; Fang *et al*., 2008; Son *et al*., 2009). In a study where TiO_2 was immobilized on polyvinyl pyrolidone/acrylic acid (PVP/AAc), the copolymer hydrogels showed improvement in thermal and chemical stabilities in addition to photocatalytic activity (Hafez *et al*., 2005; Hong *et al*., 2006).

One polymer that has gained attention as a support material or a carrier for various materials in different studies is chitosan. It is often blended with synthetic polymers to synthesize electrospun

polymeric nanofiber composites. Incorporation of chitosan with various polymers such as poly (vinyl alcohol), poly (ethylene oxide), poly (acrylonitrile-co-acrylic acid) and poly (ethylene terepthalate) has been widely reported (Che *et al*., 2008; Son *et al*., 2009). Blending different polymers without altering their individual properties has been shown to be an efficient technique for obtaining new structural materials with improved properties compared to individual components (Bajpai *et al*., 2008). Figure 2.6 presents a schematic image of two different polymers blended together:

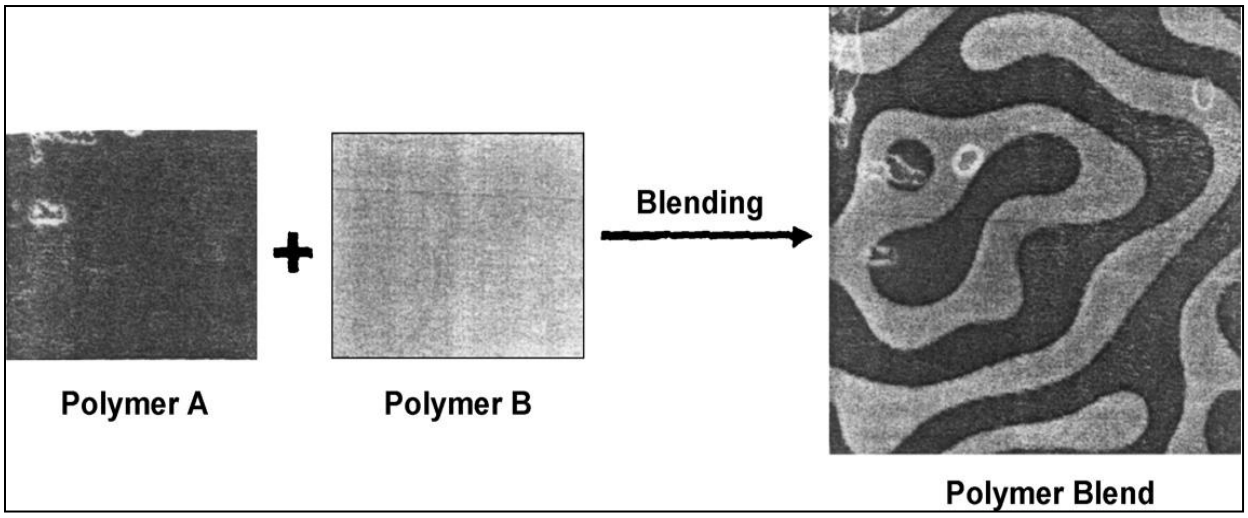

Figure 2.6: Hypothetic schematic for polymer blend preparation (Bajpai *et al*., 2008)

Nanofibers made from blended polymers offer functional materials which can be used in many applications. These functionalized electrospun nanofibers are advantageous because of their large surface area to volume ratio, and they have a potential to modify the photocatalytic activity of the TiO_2 (Wei *et al*., 2006; Kanjwal *et al*., 2010).

2.3.1.1 Properties of chitosan (CS)

Chitosan, whose structure is shown in Figure 2.7 is a (1-4) - linked 2-amino-2-deoxy-D-glucopyranose, is one of the most abundant natural polyelectrolyte that is derived from chitin by deacetylation (Homayoni *et al*., 2009). Chitin can be extracted from many living organisms such as from the skeleton of crustaceans and some insects. This biopolymer is well known for its unique properties like biodegradability, non-toxicity, antimicrobial and antifungal activities and it is also used in the field of biomedicine. Furthermore chitosan has been reported to have the affinity to bind toxic metal ions, and this renders it useful for air and water purification systems (Che *et al*., 2008; Sun *et al*., 2011).

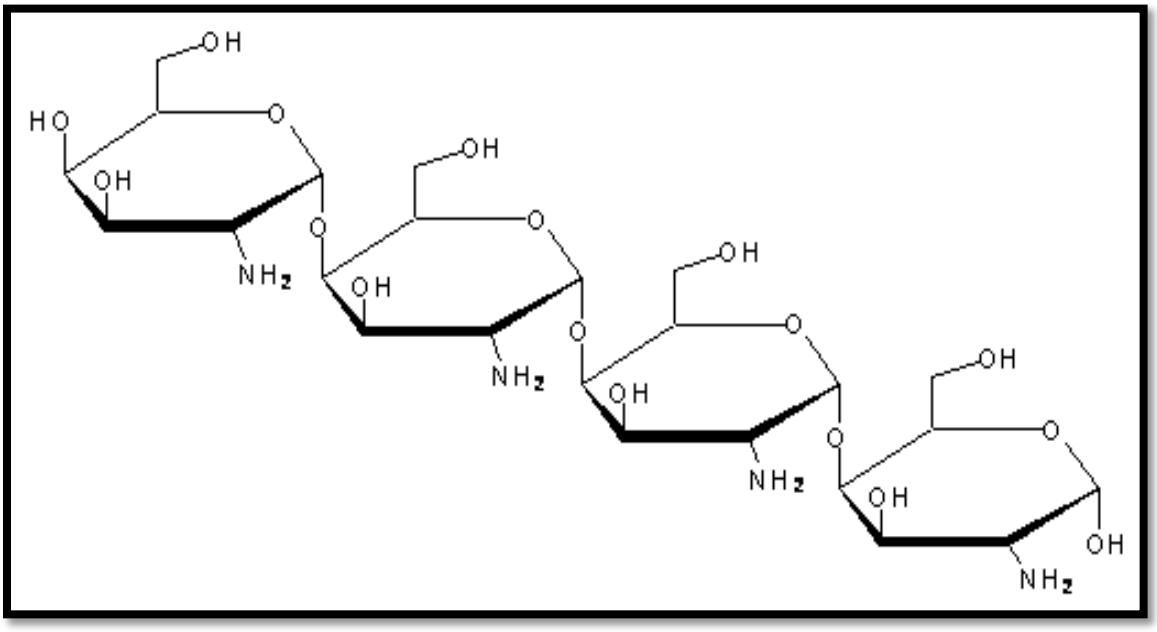

Figure 2.7: Structure of Chitosan (1-4 linked 2-amino-2deoxy-D-glucopyranose)

Electrospun chitosan nanofibers have recently attracted a lot of attention as adsorbents. Honarkar *et al*., (2009) reported effective degradation of organic compounds and adsorption of heavy metals was reported after wastewater was treated with a chitosan/TiO_2 composite. Adsorbent properties of chitosan are mainly due to its high content of amino and hydroxyl functional groups on its molecular structure (Homayoni *et al*., 2009).

2.3.1.2 Properties of polyvinyl alcohol-co-ethylene (PVAE)

Polyvinyl alcohol-co-ethylene (PVAE) is a biocompatible, semi-crystalline copolymer made from polyvinyl alcohol (PVA) and poly-ethylene (PE). It can be derived from the hydrolysis of poly (ethylene-co-vinyl acetate). This copolymer can be found in commercial markets and often the main component being PVA; as a result its properties mainly resemble those of polyvinyl alcohol. PVAE bonds with other materials by strong hydrogen interactions through the hydroxyl groups from the PVA (Arboleda *et al*., 2004).

PVAE is a hydrophilic copolymer because of the PVA repeat units and is highly resistant to a variety of chemicals. This copolymer is largely used in industries as a packaging material for spices, food, oil, agricultural chemicals, fruits and many more. In addition it is widely used as a component of many plastic containers. These properties of PVAE render it suitable for application in a variety of areas. One of the common areas where this polymer is used is in skin wound treatment and tissue engineering because it has good mechanical strength; it is biocompatible and biodegradable. Using the electrospining technique, Xu et al., (2011) successfully synthesized poly (etheylene-co-vinyl alcohol) (EVOH) nanofibers loaded with Ag nanoparticles. Composites of this copolymer with antibacterial active material like silver nanoparticles can be used as filters for water treatment as well as in protective clothing when electrospun into fibers or processed into films. Nanofibrous materials offer a larger surface area compared to bulk material and in turn this enhances the exposure of pollutants to the antimicrobial active nanofibers (Wang *et al*., 2011; Xu *et al*., 2011; Liu *et al*., 2012).

Bana *et al*., (2009) prepared a nanocomposite film of PVAE and wood dust and they observed that its mechanical properties and barrier properties we improved. From the TGA results it was observed that the thermal stability of the composite film was better compared to that of individual wood dust or PVAE. More over the biodegradability of this composite material was also greatly enhanced. Figure 2.8 is a representation of PVAE made up of the co ethylene group and the vinyl alcohol moiety with the hydroxyl group that promote hydrogen interactions:

Figure 2.8: Structure of polyvinyl alcohol-co-ethylene

2.4 Synthetic methods for nano-TiO_2

Various methods have been developed and reported for the synthesis of nanostructured powdered titanium dioxide. They include methods such as: pulsed laser deposition, hydrothermal synthesis, metal organic chemical vapour deposition (MOCVD), and template synthesis. However some of these techniques are exhaustive and complex when compared to sol-gel synthesis method which was used in this study.

2.4.1 Sol-gel synthesis

Generally the sol-gel process is defined as a chemically based route for the synthesis of high purity solid materials from a liquid at a relatively low temperature. This process was first applied in the mid 1800s for synthesis of glass and ceramics and extensively exploited for the last several decades, mainly to produce thin film and powder catalyst. The sol-gel synthesis method is favourable for the synthesis of titania nanoparticles because it is flexible and not complex. Compared to other methods, this technique is low in operation costs and it does not need high

temperature treatment. Moreover, this method gives an opportunity to control the chemical and physical properties of the materials by changing the composition of the solution. It is thus a method of choice especially when preparing doped titania nanoparticles (Wen *et al*., 2001; Mao *et al*., 2007; Charbonneau *et al*., 2009; Othman *et al*., 2010).

The sol gel process also provides for the possibility of varying the properties of the as synthesized material by changing the ingredients (Wen *et al*., 2001; Akpan *et al*., 2010). Over the past few years the sol-gel method has advanced as a promising technique for the synthesis of TiO_2 nanocomposites with noble metals and non-metal ion dopants. Basically sol-gel synthesis occurs in three steps:

- Hydrolysis,
- Condensation,
- Growth or gelation

A metal-organic or inorganic based precursor is reacted with an aqueous solvent to form a dispersion of colloidal particles commonly referred to as a sol. The sol is made up of solid particles with diameters of 1-100 nm ($1x10^{-9}$ m). The sol undergoes a condensation reaction to form a gel which is a porous network with bonds between the colloidal suspensions. The particles in the suspension undergo growth and polymerization and finally agglomerate to give a thick network of gel. Transformation of the sol to a gel is referred to as the gelation process (Lakshmi *et al*., 1997; Zhang *et al*., 2006; Mackennzie *et al*., 2007; Madani *et al*., 2010).

2.5 Electrospinning

Electrospinning is a simple and cost-effective method used for the production of non-woven fibers with large surface area to volume ratio. This versatile fibre forming process can be dated

back to the early 1930s, and it only became famous in 1934 after the discovery made by Formhals. Through his modified electrospinning process he managed to produce parallel aligned nanofibers on to the collecting screen (Subbiah *et al*., 2005). In 1971 its use for production of ultrafine fibers with a diameter less than a micron was also reported. It was only the mid 1990s that researchers in the fields of nanosciences and nanotechnology realized a great potential that electrospinning has for the production of nanofibers.

The interest of nanotechnologists in this fiber forming technique is fuelled by the application potential that this process has in a variety of fields such as: biosensors, filtration, drug delivery and enzyme immobilization (Bhardwaj *et al*., 2010; Kulkarni *et al*., 2010; Sun *et al*., 2011). Reviews done by Fang *et al*., (2008) and Sun *et al*., (2011) on fuctionalized electrospun polymeric nanofibers have reported that these nanomaterials have been successfully employed in environmental remediation processes such as air and water filtration, metal ion recovery and many more. This is owed to the fact that electrospining produces high surface to volume ratio and large porosity fibers with excellent pore interconnectivity. In addition nanofibers with large surface-to-volume ratio are advantageous as good immobilization supports for enzymes and other nanomaterials.

The electrospinning process involves the use of electrostatic force to synthesize polymeric nanofibers with a diameter scale range from submicron level down to tens of nanometers (Hong *et al*., 2006; Lee *et al*., 2009). In this process the electric force is applied between the spinneret tip and the grounded collector few centimetres away, this induces surface charge on the polymer fluid. Once the applied electric field overcomes the surface tension of the polymer solution, the charged droplet is ejected from the tip of the Taylor cone. The jet is subjected to instability due

to the applied electrostatic forces and it is whipped and attracted to the collector as fibers. The solvent used is evaporated and dry polymer fibers are deposited onto the collector (Geng *et al*., 2005; Bhardwaj *et al*., 2010). Figure 2.9 shows a schematic of the electrospinning set up with all the basic elements required during the process:

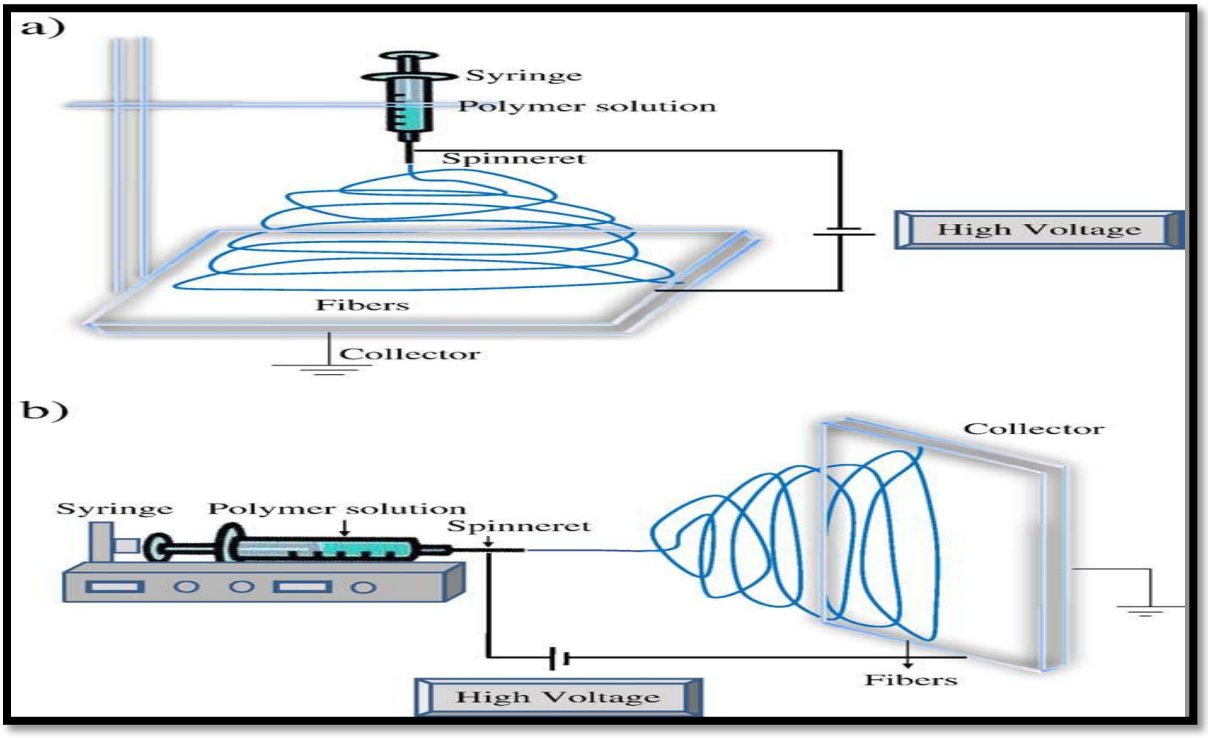

Figure 2.9: Basic components of used during the electrospinning process (Bhardwaj *et al*., 2010)

Various nanofiber synthesis methods have been reported, these include template synthesis, drawing, self-assembly, phase separation and others (Fang *et al*., 2008). However the electrospinning technique has been recognised as more efficient compared to these other methods due to the fact that it is simple to use and set-up and it easily forms fibers. Moreover electrospinning is flexible; it can be used to form fibers from a wide range of materials such as polymers, composites, semiconductors and many more. More than 200 polymer nanofibers with

a variety of applications have been produced through this method over the years. A study by Geng *et al*., (2005) reported a successful synthesis of chitosan nanofibers. Process conditions including molecular weight of chitosan, acid concentration and electric field used during electrospining were varied. By varying the parameters of nanofiber synthesis such as solution or solvent concentration, applied voltage and solution flow rate, the size of the polymer fibers can be controlled and the uniform nanofibers can be produced (Teo *et al*., 2006; Stoilova *et al*., 2010; Bhardwaj *et al*., 2010).

Numerous studies report that electrospinning is highly efficient for the production of functionalized nanofibers. Functionalized nanofibers are usually a composite of polymers with a functional material like nanoparticles, carbon nanotubes, catalysts, enzymes and many more. Using the electrospining technique, Kanjwal *et al*., (2010) successfully produced functionalized poly(vinyl acetate) and titanium dioxide nanofibers loaded with silver nanoparticles. These functionalized nanofibers were found to be highly efficienct in degrading the colour of methylene blue and methylene red dyes. In a similar study chitosan and PVA nanofibers loaded with $AgNO_3$ and TiO_2 were successfully electrospun and their antibacterial activity was tested on *Staphylococcus aureus* and *Escherichia coli*. The synthesized nanofibers of chitosan/PVA showed improved antibacterial activity after functionalization with titania and $AgNO_3$. Moreover, polymeric materials loaded with inorganic materials or catalyst are widely reported on due to their ability to enhance the mechanical strength of the nanocomposite. They are also more efficient in comparison to nanoparticles alone in terms of reusability and recycling of the material (Ali *et al*., 2005; Lu *et al*., 2008; Wang *et al*., 2009; Son *et al*., 2009).

References

AbdElhady, M. (2012). Preparation and Characterization of Chitosan/Zinc Oxide Nanoparticles for Imparting Antimicrobial and UV Protection to Cotton Fabric. *International Journal of Carbohydrate Chemistry* , 1-6.

Ahmad, A., Thiel, J., Shah, S.I. (2007). Structural effects of niobium and silver doping on titanium dioxide nanoparticles. *Journal of Physics: Conference Series* , 11-15.

Ahuja, S. (2009). *A handbook of water purity and quality.* New York,USA: Elsevier.

Akpan, U.G., Hameed, B.H. (2010). The advancements in sol–gel method of doped-TiO2 photocatalysts. *Applied Catalysis* , 1-11.

Ali, I.M., El-Zahhar, A.A., Zakaria, E.S. (2005). Thermal and sorption behavior of polyacrylonitrile supported hydrous titanium dioxide. *Journal of Radioanalytical and Nuclear Chemistry, 264, 3* , 637-644.

Allahverdlyev, A.M., Abamor, E.S., Bagirova, M., Rafallovich, M. (2011). Antimicrobial effects of TiO2 and Ag2O nanoparticles againsts drug-resistant bacteria and leishmania parasites. *Future Microbiology* , 6, 8, 1-8.

Al-Rasheed, R. A. (2005). Water Treatment by Heterogenous Photocatalysis An Overview. *SWCC(Saline Water Conversion Corporation) Acquired Experience Symposium.* Jeddah: Saline Water Desalination Research Institude.

Al-Salim, N.I., Bagshaw, S.A., Bittar, A.,Kemmitt, T., McQuillan, A.J., Mills,A.M., Ryan, M.J. (2000). Characterisation and activity of sol-gel prepared TiO2 photocatalysts modified with Ca, Sr, or Ba ion additives. *Materials Chemistry, 10* , 2358-2363.

Amitava, M., Mohammed, S.I., Prathna, T.C., Chandrasekaran, N. (2011). Antimicrobial activity of alumium oxide nanoparticles for potential clinical applications. *Science against microbial pathogens: communicating current research and technological advances* , 245-251.

Arboleda E.,C., Mejia G., A.I., Lopez O., B.L. (2004). Poly (Vinylalcohol-Co-Ethylene) Biodegradation on Semi Solid Fermantation by Phenrochaete Chrysosporium. *Acta Farmaceutica Bonaerense* , 123-128.

Asahi, R., Morikawa, T., Ohwaki, T., Aoki, K., Taga, Y. (2001). Visible-Light Photocatalysis in Nitrogen-Doped Titanium Oxides. *Science* , 269-271.

Ashkarran, A. (2011). Antibacterial properties of silver -doped TiO2 nanoparticles under solar simulated light. *Journal of Theoretical and Applied Physics* , 4-4, 1-8.

Bajpai, A.K., Shukla, S.K., Bhanu, S., Kankane, S. (2008). Responsive polymers in controlled drug delivery. *Progress in Polymer Science* , 1088-1118.

Bana, R., Banthia, A.K. (2009). Preparation and characterisation of green nanocomposites of biodegradable poly (vinyl-alcohol-co-ethylene) and wood dust. *Pigment & Resin Technology* , 275-279.

Batzill, M., Moralles, E.H., Diebold, U. (2006). lnfluence of Nitrogen Doping on the Defect Formation and Surface Properties of TiO2 Rutile and Anatase. *Physical Review Letters, 96* , 026103(1-4).

Behnajady, M.A., Modirshahla, N., Shokri, M, Rad, B. (2008). Enhancement of photocatalytic activity of TiO2 nanoparticles by Silver doping: Photodeposition versus Liquid impregnation methods. *Global NEST Journal* , 10,1, 1-7.

Bhardwaj, N., Kundu, S.C. (2010). Electrospinning: A fascinating fiber forming technique. *Biological Advances* , 28; 325-347.

Castaneda, L., Terrones, M. (2007). Synthesis and structural characterization of novel flower-like titanium dioxide nanostructures. *Physica* , 143-146.

Chang, H., Su, C., Lo, C., Chen, L., Tsung, T., Jwo, C. (2004). Photodecomposition and Surface Adsorption of Methylene Blue on TiO2 Nanofluid Prepared by ASNSS. *Materials transactions* , 45, 12, 3334-3337.

Charbonneau, C., Gauvin, R., Demopoulos, G.P. (2009). Nucleation and growth of self-assembled nanofibre-structured rutile (TiO2) particles via controlled forced hydrolysis of titanium tetrachloride solution. *Journals of Crystal Growth* , 86-94.

Che, A., Liu, Z., Huang, J., Wang, Z., Xu, Z. (2008). Chitosan-Modified Poly(acrylonitrile-co-acrylic acid) Nanofibrous Memebranes for the immobilization of Concanavalin A. *Biomacromolecules, 9* , 3397-3403.

Chen, D.,Yang, D., Wang, Q., Jiang, Z. (2006). Effects of Boron Doping on Photocatalytic Activity and Microstructure of Titanium Dioxide Nanoparticles. *Ind. Eng. Chem. Res., 45* , 4110-4116.

Chen, E., Su, H., Tan, T. (2010). Antimicrobial properties of silver nanoparticles synthesized by bioaffirnity adsorption coupled with TiO2 photocatalysis. *Society of Chemical Industry* , 421-427.

Chen, Q., Cao, H. (2004). Ab initio calculation of electronic structure of anatase TiO2. *Chinese Physics Society* , 2121-05.

Chen, X. (2009). Titanium dioxide nanomaterials and their energy applications. *Chinese Journal of Catalysis* , 30, (8); 839- 851.

Chen, X., Lou, Y., Samia, A.C.S., Burda, C., Gole, J.L. (2005). Formation of Oxynitride as the Photocataltic Enhancing Site in Nitrogen-Doped Titania Nanocatalysts: Comparison to a Commercial Nanopowder. *Advanced Functional Materials* , 15;41-49.

Chen, X., Mao, S.S. (2007). Titanium Dioxide Nanomaterials: Synthesis, Properties, Modifications, and Applications. *Chemical Reviews* , 2891-2959.

Cheng, P., Zheng, M., Jin, Y., Huang, Q. and Gu, M. . (2003). Preparation and characterization of silica-doped titania photocatalyst through sol-gel method. *Materials Letters, 57* , 2989-2994.

Choi, H., Stathatos, E., Dionysiou, D.D. . (2007). PhotocatalyticTiO2 films and membranes for the development of efficient wastewater treatment and reuse systems. *Desalination, Vol. 202* , 199-206.

Choi, J., Park, H., Hoffmann, M.R. (2009). Effects of Single Metal-Ion Doping on the Visible-Light Photo-reactivity of TiO2. *Journal of Physical Chemistry,C* , 17-55.

Christianmangun, Z., Economy, J. (2001). Removal of Chemical Contaminants from Water to below USEPA MCL using fiber glass supported activated carbon filters. *Environmental Science Technology, Vol. 35* , 2844-2848.

Esquivel, K., Garcia, M.G., Rodriquez, F.J., Gonzalez, M.V., Escobar-Alarcon, L., Ortiz-Frade, L.,Godinez, L.A. (2011). Titanium dioxide doped with transition metals (MxTi1-xO2,M:Ni, Co): synthesis and characterization for its potential application as photoanode. *Journal Nanoparticle Research* , 1-13.

Fang, J., Nui, H., Lin, T., Wang, X. (2008). Applications of electrospun nanofibers. *Chinese Science Bulletin, 15* , 2265-2286.

Fang, J., Wang, X., Lin, T. (2011). Functional Applications of Electrospun Nanofibers. *Nanofibers-Production, Properties and Functional Applications* , 287-327.

Gao, H., Zhou, J., Dai, D.,Qu, Y. (2009). Photocatalytic Activity and Electronic Structure analysis of N-doped Anantase TiO2:A Combined Experimental and Theoretical Study. *Chem. Eng. Technol.* , 32;6:867-872.

Gaya, U.I., Abdullah, A.H. (2008). Heterogeneous photocatalytic degradation of organic contaminants over titanium dioxide: A review of fundamentals, ;rogress and problems. *Journal of Photochamistry and Photobiology* , 1-12.

Gelover, S., Gomez, L.A., Reyes, K., Leal, M.T. (2006). A practical demonstration of water disinfection using TiO2 films and sunlight. *Water Research, Vol. 40* , 3274-3280.

Geng, X., Kwon, O., Jang, J. (2005). Electrospinning of chitosan dissolved in concentrated acetic acid solution. *Journal of Biomaterials* , 5427-5432.

Gorecka, E., Jastrzebska, M. (2011). Immobilization techniques and biopolymer carriers. *Biotechnology Food Sci.* , 75; 65-86.

Hafez, H.S., Ali, A.E., Mottaleb, M.S.A. (2005). Photocatalytic efficiency of titanium dioxide immobilized on PVP/AAc hydrogel membranes: A comparative study for safe disposal of wastewater of Remazol Red RB-133 textile dye. *International Journal of Photoenergy, 7* , 181-185.

Hamal, D.B., Klabunde, K.J. (2007). Synthesis, characterization and visible light activity of new nanoparticle photocatalysts based on silver, carbon and sulfur doped TiO2. *Journal of colloidal inface science, 311* , 514-522.

Hashimoto, K., Irie, H., Fujishima, A. (2005). TiO2 Photocatalysis: A Historical overview and future prospects. *Journal of Applied Physics, Vol. 44* , 8269-8285.

Ho, W., Yu, J.C., Lee, S. (2006). Low-temperature hydrothermal synthesis of S-doped TiO2 with visible light photocatalytic activity . *Journal of Solid State Chemistry, 179* , 1171-1176.

Homayoni, H., Abdolkarim, S., Ravandi, H., Valizadeh, M. (2009). Electrospinning of chitosan nanofibers: Processing Optimization. *Journal of Carbohydrate Polymers, 77* , 656-661.

Honarkar, H., Barikani, M. (2009). Applications of biopolymers I: Chitosan. *Monatsh Chem, 140* , 1403-1420.

Hong, Y., Li, D., Zheng, J., Zou, G. (2006). Sol-gel growth of titania from electrospun polyacrylonitrile nanofibers. *Nanotechnology, 17* , 1986-1993.

Hu, Y., Zhang, X., Wei, C. (2010). Simple preparation of Mn-N codoped titania photocatalyst with visible light response. *Research Chem. Intermed, 36* , 95-101.

Huang, B., Chang, F., Wei, M. (2010). An efficient composite growing N-doped TiO2 on multi-walled carbon nanotubes through sol-gel. *Nanoparticle Research,12* , 2503-2510.

Huang, Z-M., Zhang, Y.Z., Kotaki, M., Ramakrishna, S. . (2003). A review on polymer nanofibers by electrospinning and their applications in nanocomposites. *Journal of Composites Science and Technology* , 2223-2253.

Institute, N. E. (2009). *Water Safety Plan: A manual for pilot study.*

Jagadale, T.C., Takale, S.P., Sonawane, R.S., Joshi, H.M., Patil, S.I., Kale, B.B., Ogale, S.B. (2008). N-Doped TiO2 Nanoparticle Based Visible Light Photocatalyst by Modified Peroxide Sol-Gel Method. *Journal Phys. Chem.* , 14596-14602.

Jaiswal, S., Duffy, B., Jaiswal, A.K., Stobie, N., McHale, P. (2010). enhancement of the antibacterial properties of silver nanoparticles using beta-cyclodextrin as a capping agent. *International Journal of Antimicrobial Agents* , 1-5.

Jaiswal, S., Duffy, B., Jaiswal, A.K., Stobie, N., McHale, P. (2010). Enhancement of the antibacterial properties of silver nanoparticles using beta-cyclodextrin as a capping agent. *International Journal of Antimicrobial Agents* , 1-5.

Juntanon, K., Niamlang, S., Rujiravanit, R., Sirivat, A. (2008). electrically controlled release of sulfosalicylic acid from crosslinked poly (vinyl alcohol) hydrogel. *International Journal of Pharmaceutics* , 356, 1-2, 1-11.

Kanda-Nishikicho. *Measurement of Band Gap in Compound Semiconductors-Band Gap determination from Diffuse Reflectance Spectra.* Tokyo, Japan: SHUMADZU CORPORATION International Marketing Division.

Kanjwal, M.A., Barakat, N.A.M., Sheikh, F.A., Khil, M.S., Kim, H.Y. (2010). Functionalization of Electrospun Titanium Oxide Nanofibers with Silver Nanoparticles: Strongly Effective Photocatalyst. *Journal of Applied Ceramic Technology* , E54-E63.

Kasuga, T., Hiramatsu, M., Hoson, A., Sekino, T., Niihara, K. (1998). Formation of Titanium Oxide Nanotube. *Langmuir, 14* , 3160-3163.

Kim, D.H., Choi, D., Kim, S., Lee, K.S. (2008). The effect of phase type on photocatalytic activity in transition metal metal doped TiO2 nanoparticles. *Catalysis Communicationss, Vol. 9* , 654-657.

Kisanda, V., Joost, U., Reedo, V., Parna, R., Tatte, T., Shulga, J., Saar,A.,Matisen, L., Kikas, A., Kink, I. (2010). Influence of the heating temperature on the properities of nickel doped TiO2 films prepared by sol-gel method. *Applied Surface Science, 26* , 4538-4542.

Kong, H., Song, J., Jang, J. (2010). Photocatalytic Antibacterial Capabilities of TiO2-Biocidal Polymer Nanocomposites Synthesized by a Surface-Initiated Photopolymerization. *Environmental Science and Technology* , 44;5672-5676.

Krishna Rao, K.S.V., Vijaya Kumar Naidu, B., Subha, M.C.S., Sairam, M., Aminabhavi, T.M. (2006). Novel chitosan-based pH-sensitive interpenetrating network hydrogels for the controlled release of cefadroxil. *Carbohydrate Polymers* , 66, 333-344.

Kulkarni, A., Bambole, V.A., Mahanwar, P.A. (2010). Electrospinning of Polymers, Their Modeling and Applications. *Polymer-Plastics Technology and Engineering, 49* , 427-441.

Kumar, R.V., Raza, G. (2009). Photocatalytic disinfection of water with Ag-TiO2 nanocrystalline composite. *Ionics* , 15;579-587.

Kusumawardani, C., Kartini, I., Narsito. (2009). Synthesis of visible light active N-doped Titania photocatalyst. *International Conference on Chemical, Biological and Environmental Engineering* (pp. 115-118). Singapore: World Scientific Publishing Co. Pte. Ltd.

Lakshmi, B.B., Patrissi, C.J., Martin, C.R. (1997). Sol-Gel Template synthesis of Semiconductor Oxide Micro- and Nanostructures. *Chemical Material* , 2544-2550.

Lala, N.L., Ramaseshan, R., Bojun, L., Sundarrajan, S., Barhate, R.S., Ying-jun, L., Ramakrishna, S. (2007). Fabrication of nanofibers with Antimicrobial functionality used as filter:Protection against contaminants. *Biotechnology and Bioengineering* , 1357-1365.

Lee, D.W., Lim, H., Chong, H.N., Shim, W. (2009). Advances in Chitosa Material and its Hybrid Derivatives: A Review. *Open Biomaterials Journal, 1* , 10-20.

Li, F.B., Li, X.Z. (2002). The enhancement of photodegradation efficiency using Pt-TiO2 catalyst. *Chemosphere, Vol. 48* , 1103-1111.

Li, Q., Mahendra, S., Lyon, D.Y., Brunet, L., Liga, M.V., Li, D., Alvarez, P.J.J. . (2008). Antimicrobial nanomaterials for water disinfection and microbial control: Potential applications and implications. *Water Research, 42* , 4591-4602.

Li, Q., Mahendra, S., Lyon, D.Y., Brunet, L., Liga,M.V., Li, D., Alvarez, P.J.J. (2008). Antimicrobial nanomaterials for water disinfection and microbial control: Potential applications and implications. *Water Research, Vol. 42* , 4591-4602.

Li, W., Frenkel, A.I., Woicik, J.C., Ni, C., Shah, S.I. (2005). Dopant location identification in Nd3+ doped TiO2 nanoparticles. *Physical Review* , 1-6.

Liang, H., Li, X., Nowotny, J. (n.d.). Photocatalytical Properities of TiO2 Nanotubes.

Liao, B., Qin, L., Wu, X., Hou, X., Cheng, K., Liu, A. (2009). Calculation of Electronic Structure of Anatase TiO2 Doped With Transition Metal V, Cr, Fe, and Cu Atoms by the Linearized Augmented Plane Wave Method. *Chinese Journal of Structural Chemistry* , 869-873.

Liao, H., Qi, R., Shen, M., Cao, X., Guo, R., Zhang, Y., Shi, X. (2011). Improved cellular response on multiwalled carbon nanotube-incorporated electrospun polyvinyl alcohol/chitosan nanofibrous scaffolds. *Colloids and Surfaces B: Biointerfaces, 84* , 528-535.

Linsebigler, A.L., Lu, G., Yates, J.T. Jnr. (1995). Photocatalysis on TiO2 surfaces: Principles, Mechanisms and selected Results. *Chemical Reviews* , 95, 735-758.

Linsenbigler, A.M., Lu, G., Yates, J.T. Jnr. (1995). Photocatalysis on tiO2 Surfaces: Principles, Mechanisms and Selected Results. *Chemical Reviews* , 95, 735-758.

Liqiang, J., Xiaojun, S., Weinmin, C., Zili, X., Yaoguo, D., Honggang, F. (2003). 1The preparation and characterization of nanoparticle TiO2/Ti films and their photo-catalytic activity. *Journal of Physics and Chemistry of Solids, 64* , 615-623.

Liu, H.-L., Yang, T.C.-K. . (2003). Photocatalytic inactivation of Escherichia coli and Lactobacillus helveticus by ZnO and TiO2 activated with ultraviolet light. *Process Biochemistry* , 39, 475-481.

Liu, W.C., Kang, Z., Bai, S. (2012, May 30th). *Qinhuangdao Xiang Qi New material science and technology limited co.* . Retrieved May 22nd, 2012, from http://www.qhdxiangqi.com

Lopez Goeme, T.M., Alvarez Lemus, M.A., Angeles Morales, V., Gomez Lopez E., Castillo Ocampo, P. (2012). Study of Bacterial Sensitivity to Ag-TiO2 Nanoparticles. *J. Nanomedicine & Nanotechnology* , 1-7.

Lopez, R.,Gomez, R. (2012). Band-gap energy estimation from diffuse reflectance measurements on sol-gel and commercial TiO2:A comparative study. *Journal of Sol-Gel Sci Technol* , 1-7.

Lu, P. , Ding, B. (2008). Applications of electrospun fibers. *Recent patents on Nanotechnology* , 2; 169-182.

Mackennzie, J.D., Bescher, E.P. (2007). Chemical Routes in the Synthesis of Nanomaterials using the Sol-Gel process. *Accounts of Chemical Research* , 810-819.

Macwan, D.P., Dave, P.N., Chaturvedi, S. (2011). A review on nano-TiO2 sol–gel type syntheses and its applications. *Journal of Material Science* , 3669-3686.

Madani, S.M., Ehteshamzadeh, M., Rafsanjani, H.H., Mansoori, S.S. (2010). The effect of calcination on the corrosion performance of TiO2 sol-gel coatings dioed with benzotriazole on steel CK45. *Materials and Corrosion* , 1-6.

Mamba, B.B., Kruise, R.W., and Haarhoff, J. (2009). Monitoring natural organic matter and disinfection by-products at different stages in two South African water treatment plants. *Water S.A. , Vol. 32* , 121-127.

Mao, Y., Park, T., Zhang, F., Zhou, H., Wong, S.S. (2007). Environmentally friendly methodologies of nanostructure synthesis. *Small Journal* , 1122-1139.

Mardare, D., Tasca, M., Delibas, M., Rusu, G.I. (2000). On the structural properties and optical transimittance of TiO2 r.f. sputtered thin films. *Applied Surface Science* , 200-206.

Martinez-Castanon, G.A., Nino-Martinez, N., Maritinez-Gutierrez, F., Martinez-Mendoza, J.R., Ruiz, F. (2008). Synthesis and antibacterial activity of silver nanoparticles with different sizes. *J. Nanopart. Res.* , 10, 1343-1348.

Masuda, N., Sakagawa, E., Ohya, S. (1995). Outer Membrane Proteins Responsble for Multiple Drug Resistance in Pseudomonas aeruginosa. *Antimicrobial agents and Chemotherapy* , 645-649.

McCullagh, C., Robertson, J.M.C., Bahnemann, D.W., Robertson, P.K.J. (2007). The application of TiO2 photocatalysis for disinfection of water contaminated with pathogenic micro-organisms: A review. *Journal Research Chem. Intermed.* , 359-375.

Morgan, D.L., Waclawik, E.R., Frost, R.L. (2006). Relationship of Titania Nanotube Binding Energies and Raman Spectra. *ICONN* , 60-63.

Nah, Y., Paramasivam, I., Schmuki, P. (2010). Doped TiO2 and TiO2 Nanotubes: Synthesis and Applications. *ChemPhysChem* , 2698-2713.

Nasr-Esfahani, M., Habibi, M.H. (2008). Silver Doped TiO2 Nanostructure Composite Photocatalyst Film Synthesized by Sol-Gel Spin and Dip Coating Technique on Glass. *International Journal of Photoenergy* , 1-11.

Nave, R. (n.d.). *Band Theory for Solids.* Retrieved October 09, 2012, from Hyperphysics - Condensed Matter: http://hyperphysics.phy-astr.gsu.edu/hbase/solids/band.html

Ni, M., Leung, M.K.H., Leung, D.Y.C., Sumathy, K. (2007). A review and recent developments in photocatalytic water-splitting using TiO2 for hydrogen production. *Renewable and Sustainable Energy Reviews* , 11; 401-425.

Nie, X., Zhuo, S., Maeng, G., Sohlberg, K. (2009). Doping of TiO2 Polymorphs for Altered Optical and Photocatalytic Properties. *International Journal of Photoenergy* , 1-22.

Nolan, N.T., Seery, M.K., Hinder, S.J., Healy, L.F., Pillai, S. (2010). A Systematic Study of the Effect of Silver on the Chelation Formic Acid to a Titanium Precursor and the Resulting Effect on the Anatase to Rutile Transformation of TiO2. *Journal of Phys. Chem.* , 1-10.

Nor Hafizar, Iis Sopyan. (2009). Nanosized TiO2 Photocatalyst Powder via Sol-Gel Method: Effect of Hydrolysis Degree on Powder Properties. *International Journal of Photoenergy* , 1-8.

Nosaka, Y., Matsushita, M., Nishino, J., Nosaka, A.Y. . (2005). Nitrogen-doped titanium dioxide photocatalysts for visible response prepared by using organic compounds. *Science and Technology of Advanced Materials, Vol. 6* , 143-148.

Ohno, T., Akiyoshi, M., Umebayashi, T., Asia, K., Mitsui, T., Matsumura, M. (2004). Preparation of S-doped TiO2 photocatalysts and their photocatalytic activities under visible light. *Applied Catalysis A: General 265* , 115-121.

Othman, S.H., Rashid, S.A., Ghazi, T.I., Abdullah, N. (2010). Effect of Fe Doping on Phase Transition of TiO2 nanoparticles Synthesized by MOCVD. *Journal of Applied Sciences* , 1044-1051.

Park, H., Choi, W. (2006). Visible-Light-Sensitized production of Hydrogen Using Perfluorosulfonate Polymer-Coated TiO2 Nanoparticles: An Alternative Approach to Sensitizer Anchoring. *Langmuir* , 2906-2911.

Park, H., Kim, H. (2010). Characterizations of Highly Ordered Arrays Obtained by Anodic Oxidation. *Transactions on Electrical and Electronic Materials, 11* , 112-115.

Park, H.K., Kim, D.K., Kim, C.H. (1997). Effect of Solvent on Titania Particle Formation and Morphology in Thermal Hydrolysis of TiCl4. *Journal American Ceramic Soc.* , 743-749.

Pawlak, A., Mucha, M. (2003). Thermogravimetric and FTIR studies of chitosan blends. *Tehmochimica Acta* , 396, 153-166.

Philippopoulos, C.J., Nikolaki, M.D. (2010). *Photocatalytic processes on the oxidation of organic compounds in water.* Greece: New trends in technology.

Pillai, C.K.S. & Sharma, C.P. (2009). Electrospinning of Chitin and Chitosan Nanofibres. *Trends Biomater. Artif. Organs* , 22, 3, 179-201.

Qu, X., Wirsen, A., Albertsson, A.-C. (2000). Effect of lactic/glycolic acide side chains on the thermal degradation kinetics of chitosan derivatives. *Polymer* , 41, 4841-4847.

Rai, M., Yaday, A., Gade, A. (2009). Silver nanoparticles as a new generation of antimicrobials. *Biotechnology Advances, Vol. 27* , 76-83.

Rao, K.V.S., Lavedrine, B., Boule, P. (2003). Influence of metallic species on TiO2 for the photocatalytic degradation of dyes and dye intermediates. *Journal of Photochemistry and Photobiology A: Chemistry* , 154; 189-193.

Ren, L., Huang, X., Sun, F., He, X. (2007). Preparation and characterization of doped TiO2 nanodandelion. *Materials letters* , 61;427-431.

Ribbens, S., Meynen, V., Van Tendeloo, G., Ke, X., Mertens, M., Maes, B.U.W., Cool, P., Vansant, E.F. (2008). Development of photocatalytic efficient Ti-based nanotubes and nanoribbons by conventional and microwave assisted synthesis strategies. *Microporous and Mesoporous Materials, 114* , 401-409.

Richardson, S. (2003). Disinfection by-products and other emerging contaminants in drinking water. *Trends in Analytical Chemical, Vol. 22, Issue 10* , 666-684.

Robichaud, C.O., Uyar, A.E., Darby, M.R., Zucker, L.G., Wiesner, M.R. (2009). Estimates of Upper Bounds and Trends in Nano-TiO2 production As a Basis for Exposure Assessment. *Environmental Science and Technology* , 1-7.

Sathish, M., Viswanathan, B., Viswanath, R.P., Gopinath, C.S. (2005). Synthesis, Characterization, Electrosnic Structure, and Photocatalytic Activity of Nitrogen-Doped TiO2 Nnaocatalyst. *Chemical Materials* , 17;6349-6353.

Savage, N., Diallo, M., Duncan, J., Street, A., Sustich, R. (2009). *Nanotechnology Applications for Clean Water*. Norwich, NY, : William Andrew Inc.

Savage, N.,Diallo, M.S. (2005). Nanomaterials and water purification: Opportunities and challenges. *Journal of Nanoparticles Research, Vol. 7* , 331-342.

Schirmer, R.H., Adler, H., Pickhardt, M., Mandelkow, E. (2011). Lest we forget you- methylene blue. *Neurobiology of Ageing* , 1-10.

Seery, M. (2009, 09 30). *The Photochemistry Portal*. Retrieved 11 13, 2012, from http://photochemistryportal.net/home/index.php/2009/09/30/metal-oxide-photocatalysis/

Seery, M.K., George, R., Floris, P., Pillai, S.C. (2007). Silver doped titanium dioxide nanomaterials for enhanced visible light photocatalysis. *Journal of Photochemistry and Photobiology A: Chemistry* , 189; 258-263.

Serpone, N.&Salinaro, A. (1999). Terminology, Relative photonic efficiencies and quantum yields in heterogeneous photocatalysis. Part I: Suggested Protocol. *Pure&Appl. Chem.* , 71, 2, 303-320.

Shannon, M.A., Bohn, P.W., Elimelech, M., Georgiadis, J.G., Marinas, B.J. (2008). Science and technology for water purification in the coming decades. *Nature Reviews, 452* , 301-310.

Shen, Y., Xiong, T., Du, H., Jin, H., Shang, J., Yang, K. (2009). Phosphorous, nitrogen, and molybdenum ternary co-doped TiO2: preparation and photocatlytic activities under visible light. *Journal of Sol-Gel Science Technology* , 98-102.

Shen, Y., Xiong, T., Du, H., Jin, H.,Shang, J., Yang, K. (n.d.).

Sheng, M., Jun, R., Efthimios, K. (2008). Natural dyes adsorbed on TiO2 nanowire for photovoltaic applications: Enhanced light absorption and ultrafast electron injection. *Nano Letters* , 8; 10; 3266-3272.

Sirimahachai, U., Phongpaichit, S., Wongnawa, S. (2009). Evaluation of bacterial activity of TiO2 photocatalysts: A comparative study of laboratory made and commercial TiO2 samples. *Songklanakarin Journal of Science and Technology* , 517-525.

Sobana, N., Muruganadham, M., Swaminathan, M. (2006). Nano-Ag particles doped TiO2 for efficient photodegradation of Direct azo dyes. *Journal of Molecular Catalysis A: Chemical* , 258, 124-132.

Son, B., Yeom, B., Song, S.H., Lee, C., Hwang, T.K. (2009). Antibacterial Electrospun Chitosan/Poly(vinyl alcohol) Nanofibers Containing Silver Nitrate and Titanium Dioxide. *Journal of Applied Polymer Science, 111* , 2892-2899.

Song, H.Y., Ko, K.K., Oh, I.H., Lee, B.T. (2006). Fabrication of Silver Nanoparticles and their Antimicrobial mechanisms. *Europeans Cells and Materials, 11* , 58.

Stoilova, O., Manolova, N., Gabrovska, K., Marinov, I., Godjevargova, T., Gustavo, D., Rashkov, I. (2010). Electrospun Polyacrylonitrile Nanofibrous Membranes Tailored for Acetylcholinesterase Immobilization. *Journal of Bioactive and Compatible Polymers* , 40-57.

Su, B., Liu, X., Peng, X., Xiao, T., Su, Z. (2003). Preparation and characterization of the TiO2/polymer complex nanomaterial. *Materials Science and Engineering, A349* , 59-62.

Subbiah, T., Bhat, G.S., Tock, R.W., Parameswaran, S., Ramkumar, S.S. (2005;96). Electrospinning of Nanofibers. *Journal of Applied Polymer Science* , 557-569.

Sun, C., Li, Q., Gao, S., Cao, L., Shang, J.K. (2010). Enhanced Photocatalytic Disinfection of Escherichia coli Bacteria by Silver Modification of Nitrogen-Dodep Titanium Oxide Nanoparticle Photocatalyst Under Visible-Light illumination. *American Ceramic Society* , 93;11:3880-3885.

Sun, K., Li, Z.H. (2011). Preparations, properties and applications of chitosan based nanofibers fabricated by electrospinning. *Express Polymer Letters, 5, 4* , 342-361.

Sung-Mao,C., Zhi-Sheng, C., Kuo-Yuan, Y., Yu-Lung, H., Dershin, G. . (2007). Photocatalytic activity of doped TiO2 coatings prepared by sputtering deposition. *Materials Processing Technology,192-193* , 60-67.

Suwanchawalit, C., Chanhom, P., Sriprang, P., Wongnawa, S. (2011). A Ag-Doped TiO2 Photocatalyst for Dye Decolorization under UV. *Pure and Applied Chemistry International Conference* , (pp. 375-405).

Sze, M.Lam, Jin, C.Sin, Abdul, R. Mohamed . (2008). Recent Patents on Photocatalysis over Nanosized Titanium Dioxide. *Recent Patents on Chemical Engineering* , 209-219.

Tayade, R. J., Kulkarni, R.G., Jasra, R.V. (2006). Transition Metal Ion Impregnated Mesoporous TiO2 for Photocatalytic Degradation of Organic Contaminants in Water . *Ind. Eng. Chem. Res.* , 45,5231-5238.

Tayade, R.J., Key, D.L. (2010). Synthesis and Characterization of Titanium Dioxide Nanotubes for Photocatalytic Degradation of Aqueous Nitrobenzene in the presence of Sunlight. *Materials Science Forum, 657* , 62-74.

Teo, W.E., Ramakrisna, S. (2006). A review on electrospinning design and nanofibers assemblies . *Nanotechnology* , 17; R89-R106.

Tiwari, D.K., Behari,J., and Sen,P. . (2008). Application of Nanoparticles in Waste Water Treatment. *World Applied Sciences Journal, 3* , 417-433.

Tiwari, D.K., Sen, P. (2009). Application of Nanoparticles in Waste Water Treatment. *World Applied Sciences Journal, Vol. 3* , 417-433.

Umebayashi, T., Yamaki, T., Itoh, H., Asai, K. (2002). Analysis of electronic structures of 3d transition metal-doped TiO2 based on band calculations. *Journal of Physics and Chemistry of Solids* , 1909-1920.

Wang, D., Xu, W., Sun, G., Chiou, B. (2011). Radical Graft Polymerization of an Allyl Monomer ont oHydrophilic Polymers and Their Antibacteial Nanofibrous Membranes. *Applied Materials and Interfaces* , 2838-2844.

Wang, H., Fu, G., Li, X. (2009). Functional Polymeric Nanofibers from Electrospinning. *Recent Patents on Nanotechnology, 3* , 21-31.

Wei, M. Kang, B., Sung, C., Mead, J. (2006). Core-Sheath Structure in Electrospun Nanofibers from Polymer Blends. *Macromolecular Materials and Engineering* , 1307-1314.

Wei, S., Peng, B., Chai, L., Liu, Y., Li, Z. (2008). Separation of doping titania antibacterial powder by ultrasonic spray pyrolysis. *Trans. Nonferrous Met. Society of China, 18* , 1145-1150.

Wen, L., Liu, C., Zhao, X. (2009). Preparation, Characterization and Photocatalytic Property of Ag-loaded TiO2 Powders using photodeposition method. *Journal of Wuhan University of Technology-Material Science Ed.,24* , 258-263.

Wen, T., Gao, J., Shen, J. (2001). Preparation and characterization of TiO2 thin films by the sol-gel process. *Journal of Materials Science* , 5923-5926.

WHO, UNICEF. (2000). *Global Water Supply and Sanitation Assessment 2000 Report* . World Health Organization and United Children's Fund.

Wong, M., Sun, D., Chang, H. (2010). Bactericidal Performance of Visible Light Responsive Titania Photocatalyst with Silver Nanostructures. *Plos One, 5* , 1-7.

Xiao, J., T. Peng, T., Li, R., Peng, Z. and Yan, C. (2006). Preparation, phase transformation and photocatalytic activities of cerium-doped mesoporous titania nanoparticles. *Journal of Solid State Chemistry, 179* , 1161-1170.

Xiao, P., Liu, D., Garcia, B.B., Sepehri, S., Zhang, Y.,Cao, G. (2008). Electrochemical and photoelectrical properties of titania nanotubes annealed in different gases. *Sensors and Actuators* , 367-372.

Youji, L., Xiaohu, W., Xiaohua, W. (2008). Inactivated properties of activated carbon-supported TiO2 nanoparticles for bacteria and kinetic study. *Journal of Environmental Sciences* , 20; 1528-1533.

Yu, J.C., Lee, S., Ho, W. . (2006). Low-temperature hydrothermal synthesis of S-doped TiO2 with visible light photo-catalytic activity. *Journal of Solid State Chemistry, 179* , 1171-1176.

Yu, J.C., Yu, J., Ho, W., Jiang, Z., Zhang, L. (2002). Effects of F- Doping on the Photocatalytic Activity and Microstructure of Nanocrystlline TiO2 Powders. *Chemical materials, 14* , 3808-3816.

Zaleska, A. (2008). Doped- TiO2: A review. *Recent Patents on Engineering, Vol. 2* , 157-164.

Zhang, H., Chen, G. (2009). Potent Antibacterial Activities of Ag/TiO2 Nanocomposte Powders Synthesized by a One-Pot Sol-Gel Method. *Environ. Sci. Technol.* , 43, 2905-2910.

Zhang, J., Zhang, Y., Yu, L., Zhong, X., Wang, W. (2011). Preparatin of Ag-modified nano-titanium and their photocatalytic activity. *Rare Metals* , 30; 267-270.

Zhang, L., Liu, P., Su, Z. (2006). Low Tempereature Preparation of Titania Coated PAN Fiber and Its Photocatalytical Property. *Journal of the Chinese Chemical Society* , 319-324.

Zhang, Y., Huang, X., Duan, B., Wu, L., Li, S., Yuan, X. (2007). Preparation of electrospun chitosan/poly(vinyl alcohol) membranes. *Colloid Polym. Sci.* , 285, 855-863.

Zhao, X., Lv, L., Pan, B., Zhang, W., Zhang, S., Zhang, Q. (2011). Polymer-supported nanocomposites for environmental application: A review. *Chemical Engineering Journal* , xxx-xxx.

Chapter 3- Experimental

3.0 Introduction

The main aim of this research project was to synthesize titanium dioxide nanoparticles doped with silver (Ag) and nitrogen (N) respectively and to immobilize the photocatalyst on a blend of polymer fibers using the electrospining method. The sol-gel synthesis method was chosen because it is a versatile method, it is relatively easy and practical; it does not require expensive complex instruments. Furthermore in this method the size, morphology, and distribution of the nanostructured material can be controlled. The dopant can directly interact with sol during the gelation period therefore promoting incorporation of the dopants (Lakshmi *et al*., 1997; Zaleska, 2008). This chapter gives an overview of the experimental procedures that were followed to achieve the aim and objective of this study. The analytical techniques used for characterization of the synthesized nanomaterials are also outlined.

3.1 TiO_2 Sol-gel synthesis

3.1.1 Chemical reagents/Materials

The following commercial reagents supplied by Merck were used in this project: $TiCl_4$ (99%), TiO_2 (Degussa P25), $AgNO_3$, Urea ($(NH_2)_2CO$), and deionised water (DW) was obtained from the O Purite (Select) deioniser supplied by Lasec, South Africa (Pty) LTD.

3.1.2 Preparation of pure TiO_2 nanoparticles

Titanium tetrachloride ($TiCl_4$) was the main starting material and was used as received from the supplier without any further purification. A precursor, 0.1 M of 99% titanium (IV) chloride (11 mL) was slowly added to 200 mL of distilled water in a 250 mL Erlenmeyer flask immersed in

an ice bath with a thermometer reading of 0 ºC and stirred vigorously to give a Ti^{4+} concentration of 0.495 M. This was done under a fume hood because the reaction was vigorous and generated white hydrochloric gas fumes. The resultant aqueous solution was rapidly heated to 100 ºC on stirrer coupled hot plate to eliminate more chloride ions as hydrogen chloride. The temperature was closely monitored on a thermometer and maintained for 10 minutes so as to completely carry out hydrolysis and condensation. The solution was then allowed to cool and neutralized to a pH of 8.0 using 10 M NaOH to aid the process of gelation, approximately 50 mL of the solution was used. Subsequently a white gel was formed and it was separated from solution by centrifugation. The precipitate was washed repeatedly with deionised water until most of the chloride ions were removed. This was tested by adding a few drops of $AgNO_3$ solution. After a thorough wash the precipitate was filtered and allowed to dry at 150 ºC overnight in a Memmert oven supplied by Lasec, South Africa (Pty) Ltd. Using a mortar and pestle the dried material was pulverized into a powder and then taken for calcination at a temperature of 600 ºC at a rate of 5 ºC per minute for 2 hours in a programmable furnace supplied by MET-UED, South Africa. Figure 3.1 shows the flow chart diagram for the method followed for the synthesis of doped and undoped TiO_2 nanopowders. The obtained nanopowders were then taken for characterization on XRD, SEM, EDX, TEM, DRS and FTIR.

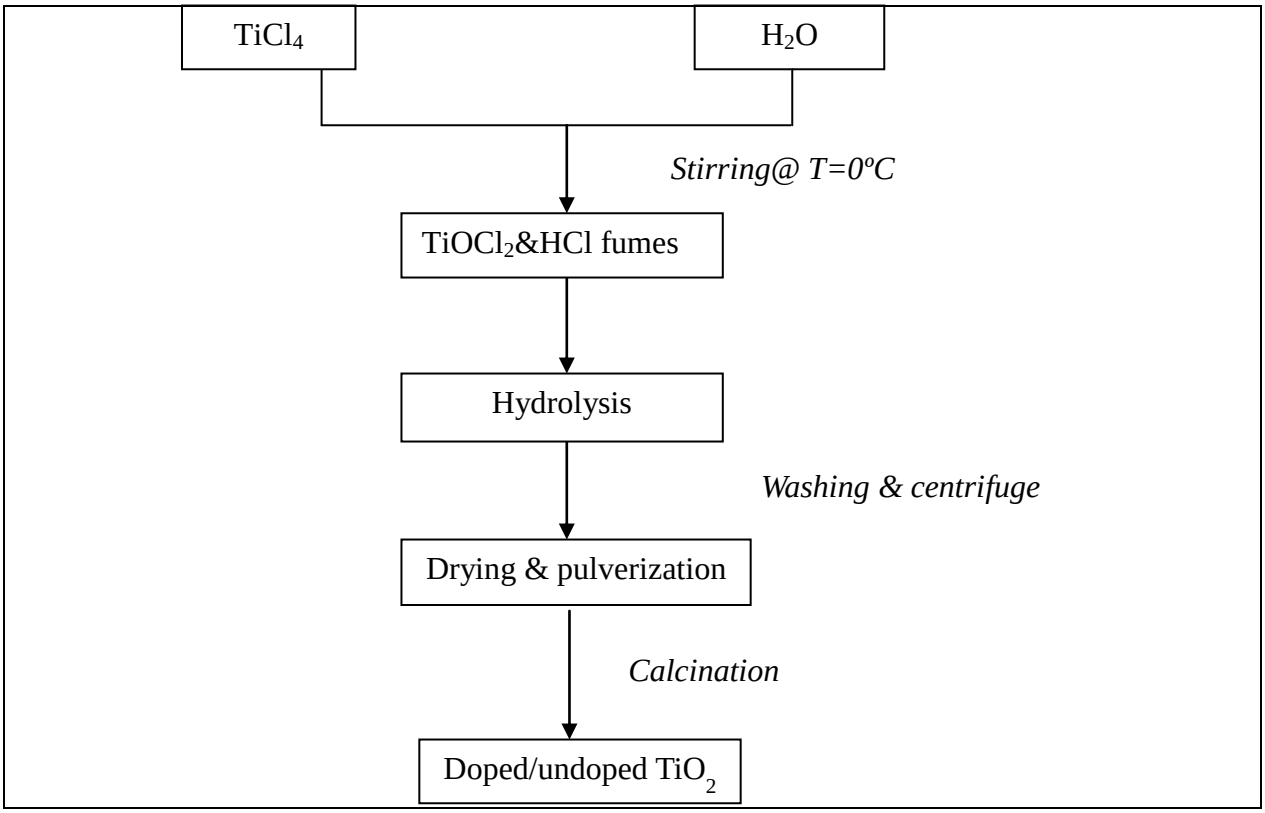

Figure 3.1: Flow diagram of the Sol-gel synthesis

3.1.3 Preparation of Ag doped TiO_2 nanoparticles

Following the method described in Section 3.1.2 and the flow chart diagram in Figure 3.1, silver doped titania nanoparticles were prepared. The commercial silver nitrate ($AgNO_3$) was used as received from the supplier (RADCHEM) without any further purification. One gram (0.01 mols) of $AgNO_3$ crystal salt was weighed and dissolved in 200 mL of deionised water (DW) in a 250 mL Erlenmeyer flask immersed in an ice bath as in Section 3.1.2. In a drop-wise manner 11 mL of titanium tetrachloride was subsequently added to the solution of $AgNO_3$ under a fume hood. The solutions were kept under continuous magnetic stirring, and rapidly heated to 100 ºC and maintained for 10 minutes. The colour of the sol turned from cream to colourless during the heating process. After cooling the sol was neutralised with a solution of NaOH and stirred for some time. The resultant white precipitate was then centrifuged, washed and filtered until it was

chloride free. The products were dried in a Memmert oven supplied by Lasec South Africa overnight at 150 ºC, after which the material was crushed and grounded into fine powder. The crushed powder was evenly spread on a watch glass placed into an empty 500 mL beaker covered with aluminium foil then irradiated with UV light using a Camag 365 nm lamp supplied by Labotec for two hours for *in situ* reduction of Ag^{+} ions to Ag^{0} nanoparticles (Duplessis, 2011). After 2 hours of exposure to UV light, the powder turned to a grey-brownish colour and calcined in a programmable furnace supplied by MET-UED at a rate of 5 ºC to 600 ºC for 2 hours and the colour of the final product was grey due to the presence of silver oxide (Lopez Goerne *et al*., 2012). The products were characterized with FTIR, XRD, DRS, SEM/EDX and TEM.

3.1.4 Preparation of N doped TiO_2 nanoparticles

A similar procedure as above was followed for the synthesis of N-doped TiO_2. Urea ($(NH_2)_2CO$) was used as the nitrogen source and it was used as received from supplier. Five grams (0.083 mols) of urea was dissolved in 200 mL of deionised water in a 250 mL Erlenmeyer flask with continuous magnetic stirring. This was followed by a drop-wise addition of 11 mL of 0.1 M $TiCl_4$ into the Erlenmeyer flask immersed in an ice bath maintained at a temperature of 0º C, and stirred continuously. This reaction was done under a fume hood since white fumes presumed to be hydrogen chloride were being released. The reaction solution turned yellow upon contact of water and $TiCl_4$, and subsequently became colourless as the temperature was rapidly raised to 100 ºC and maintained for 10 minutes. The colourless sol was allowed to cool down and neutralised with a solution of 10M sodium hydroxide (NaOH) to pH 8. The solution precipitated and turned cream white upon addition of NaOH. The sol solution was washed repeatedly with deionised water, centrifuged and filtered to remove any chlorine ions left. The precipitated gel

was dried at 150 ºC overnight in a Memmert oven supplied by Lasec South Africa (Pty) Ltd and the products were pulverised into a fine powder using a mortar and pestle. The powder was then calcined in a programmable furnace supplied by MET-UED at 600 ºC for 2 hours to remove moisture and any organic residues from the dopant source. After calcination the colour of the powder was yellowish and this was believed to be due to the formation of nitrogen doped TiO_2. The products were characterized with FTIR, XRD, DRS, SEM/EDX and TEM.

3.2 Preparation of a Chitosan and PVAE polymer blend

3.2.1 Reagents and materials

Polyvinyl alcohol-co- ethylene (PVAE) with 32 mol% ethylene in granular form were supplied by Stellenbosch University, and Chitosan (Batch number: CAS 9012-76-4) with > 75% degree of deacetylation (%DD) supplied by Sigma-Aldrich, 70% Acetic acid (AA) prepared from 99.5% AA by RADCHEM, and 70% Propan-1-ol prepared from absolute n-Propyl alcohol supplied by Hopkin&Williams LTD. Deionised water was obtained from the O-Purite deioniser supplied by Lasec S.A. housed in the department of chemistry, University of Fort Hare. The polymers chitosan and PVAE were used as received from the supplier without any further processing.

3.2.2 Preparation of chitosan and PVAE polymer blend

The polymer blend was prepared by first dissolving the polymers in separate reaction flasks and subsequently mixed to give a homogeneous chitosan-polyvinyl alcohol-co-ethylene (PVAE) blend. A solution of 70% acetic acid was initially prepared by transferring 70 mL of 99.5% acetic acid into a 100 mL volumetric flask and filled up to the mark with DW. A measured amount of chitosan flakes (1.4 grams) was dissolved in 70% acetic acid (70 mL) to prepare 2% (w/v) of the polymer. This was done under continuous stirring in a 100 mL double neck round

bottom flask connected to a condenser in an oil bath. The temperature of the flask was kept at 60º C and the reaction was allowed to run under reflux in air for 12 hours.

Polyvinyl alcohol-co-ethylene (PVAE) (2.5 grams) was dissolved in 25 mL of 70% propan-1-ol to make 10% (w/v) of the polymer. The solution was stirred continuously in a double neck flask immersed in an oil bath at 80º C for 2 hours and this reaction was also refluxed under air.

The two polymer solutions were allowed to cool down before being blended together in reaction vessels labeled C1, C2, C3 and C4 for different volume ratios of Cs/PVAE. The two miscible solutions were mixed at different volume ratios of chitosan/PVAE to give (C1 10/90; C2 20/80; C3 25/75 and C4 30/70) presented in volume percentages. Different runs were carried out in order to find the most suitable solution for electrospining and in the end 80:20 % (v/v) of PVAE:Cs blend ratio gave a suitable viscosity and was found to be the most appropriate and used. The polymer blends were taken for electrospining under conditions outlined in Section 3.3, after which they were characterized on FTIR, SEM and TGA.

3.2.3 Preparation of doped and undoped TiO_2 immobilized on chitosan-PVAE blend

The chitosan-polyvinyl alcohol co ethylene (PVAE)-doped TiO_2 nanocomposite was prepared by adding 0.025 g, 0.05 g and 0.1 g of Ag/TiO_2 and N/TiO_2 nanopowders respectively to labelled reaction vessels of the polymer blends containing chitosan-PVAE solution. The doped TiO_2 nanopowder particles were soaked in the chitosan-PVAE blend and continuously stirred for an hour using a magnetic stirrer. After an hour the composite was taken for electrospining under the set-up outlined on Section 3.3. The same procedure was followed for the preparation of the undoped TiO_2 polymer immobilized blend.

3.3 Electrospinning of doped and undoped TiO_2 and chitosan-PVAE mixture

Over the years, electrospinning has become a powerful and effective method for the preparation of nanofibrous materials from different polymers. Such materials offer many advantages when used as support for biocatalysts and drug delivery. To carry out the process of electrospinning in the laboratory, the following elements were used: a high voltage power supplier that could generate up to 50 kV direct current voltages, a 25 mL syringe connected to a capillary pipette, a metal wire and a collecting screen with aluminium foil which also acted as the grounded electrode. The metal wire was connected to the positive terminal of the power supply and passed through the capillary glass pipette. The tip of the pipette was kept 15 cm away from the grounded aluminium foil collector. The flow of the polymer blend solution was dependent on gravity and the viscosity of the solution was adjusted by changing the volume ratio of chitosan: PVAE. A voltage of 15-20 kV was applied and the polymer solution was stretched out into fibers which were then collected onto a grounded collector. Several trials were done before fibers started forming and the nanofibers were allowed to dry in air overnight and then taken for characterization by FTIR, SEM, EDX and TGA.

3.4 Characterization Techniques

This section gives a brief outline of the analytical techniques that were used for the characterization of the nanoparticles and nanofibers synthesized in this study.

3.4.1 Fourier Transform Infrared spectroscopy (FTIR)

The Fourier transform infrared spectroscopy is one of the most popular spectroscopic techniques that have been successfully used by chemists to identify organic and inorganic compounds. In this study the Perkin Elmer System 2000 Fourier transform infrared (FTIR) was used to determine the newly formed functional groups in the doped and undoped TiO_2 nanoparticles.

About 2 mg of the synthesized titania nanopowder was mixed with a binder potassium bromide (KBr) to make transparent pellets using a bolt and a nut pelletizer. Each sample was analysed in the wavenumber range 4000-350 cm^{-1} with a resolution of 4 cm^{-1}, 16 scans were done for each sample.

3.4.2 X-ray diffraction (XRD)

X-ray diffraction is a versatile, non-destructive analytical technique that is primarily used for the characterization of natural and manufactured crystalline materials. It is used to study the structure of the material, including atomic arrangement, crystallite size and atomic spacing. XRD is based on the interaction of monochromatic X-rays with a crystalline sample. X-rays are generated in the cathode ray tube, and then filtered to produce monochromatic radiation which goes through the collimator to increase their intensity and finally directed to the sample. Bombardment of the target sample with the incident X-ray beam produces a diffracted ray which is detected, processed and converted to count rates provided Braggs's Law conditions are satisfied.

In this study X-ray diffractometer XRD-D8 Bruker AXS Advance, fitted with a LynxEye detector, with Cu $K\alpha_1$ (λ=1.5406 Å) radiation was used to determine the crystalline phase of the synthesized titania nanopowder materials. The instrument was also programmed with software of EVA and Diffrac. Suite for identification of crystallographic phases and calculations of the crystallite sizes using the Scherrer equation:

$$D = \frac{0.9\lambda}{\beta cos\theta}$$

where D is the crystallite size, β is the full width at half maximum (FWHM) of a peak, λ is the wavelength X-ray radiation, θ represents Bragg's diffraction angle (Chen *et al*., 2005). The samples were scanned in a two theta angle (2θ) range of 5º C to 90 ºC at room temperature. From

this characterization technique the crystalline phases, particles size and structure were identified. Analysis was done with the help of the laboratory technitian at the department of chemistry, University of Fort Hare where the instrument is housed.

3.4.3 Scanning Electron Microscopy (SEM)

The scanning electron microscopy takes images of the surface of a sample by scanning it with a high energy beam of electrons. SEM images yield information about the topography, morphology (size and shape), composition and crystallographic information of the sample. Unlike the conventional light microscopes that use light waves to create their images, the SEM uses a beam of highly energetic electrons. When a beam of electrons from the electron gun hits the surface of the specimen, it interacts with the atoms of the sample to produce signals in the form of secondary electrons, backscattered electrons and diffracted backscattered electrons that are used to determine the crystal structures and orientations of minerals. Basically the SEM produces images of a sample surface, revealing details about the size of the sample.

In this study SEM images were obtained from JEOL JSM-6390LV scanning electron microscope fitted with secondary electron detector. The SEM was equipped with the Energy dispersive X-ray spectroscopy (EDS). The samples were first mounted on a metal sample holder called a stub using a carbon double sided tape and then sputter coated with gold and palladium (ratio 80:20) using an Eiko IB 3 Ion coater. After this they were ready for SEM observation. The accelerating Voltage used was between 10-15kV at different magnifications.

3.4.4 Energy dispersive X-ray spectroscopy (EDS)

The EDS is a micro-analytical technique used in conjunction with SEM. It is used to provide qualitative information about the sample. This technique uses the characteristic spectrum of x-rays emitted by the specimen after excitation by high-energy electrons to obtain information

about the elemental composition of a sample. In this study EDS technique was used to determine and quantify the elemental composition of the synthesized compounds.

3.4. 5 Transmission Electron Microscopy (TEM)

Transmission electron microscopy is another form of electron microscope similar to SEM in that they both use electrons to obtain images. However, in TEM a high-powered beam of electrons is passed through an ultra thin object, interacting with the sample as it is transmitted. An image is formed from the interaction of the electrons transmitted through the specimen; the image is magnified and focused onto an imaging device, such as a fluorescent screen, on a layer of photographic film, where the final image is observed. Since the beam of electrons passes entirely through the sample, the pattern of scatter gives a comprehensive view of the interior of the specimen. TEMs are capable of imaging at a significantly higher resolution than light microscopes, and give higher resolution images of the inner structure of the sample compared to the SEM.

In this study TEM used was accessed at Rhode University, RSA. It was supplied by Zeiss Libra 120, operated at an accelerating voltage of 80 kV at room temperature. The nanoparticles were first prepared by being dispersed onto absolute ethanol and then deposited onto a carbon coated Formvar copper grid and dried before being analysed.

3.4. 6 Diffuse Reflectance Spectroscopy (DRS)

The UV-vis diffuse reflectance spectroscopy is one of the commonly employed optical methods for describing the electronic behaviour present in the structure of a solid material. The spectra obtained give information about the electronic transitions of the different orbitals of the solid sample (Lopez *et al*., 2012). In this study the diffuse reflectance spectroscopy (DRS), Cary 500 UV-Vis-NIR spectrophotometer equipped with an integrating sphere accessory for diffuse

reflectance spectra was employed to determine shifts in the optical absorption band edge of the synthesized and commercial titania nanoparticles. The samples were analysed at room temperature in the wavelength range of 800 nm to 200 nm and $BaSO_4$ was used as a reference. This instrument was accessed at the department of chemistry, Wits University, RSA.

3.4.7 Thermal Gravimetric analysis (TGA)

Thermal gravimetric analysis is a technique in which the change in the weight of a substance is monitored and recorded as a function of temperature in an inert gas controlled atmosphere. This analytical technique is commonly employed to determine the characteristics of substances such as thermal stability, degradation temperature, moisture and solvent content of materials and the filler content in polymers. A TGA consists of a sample pan that is supported by a precision balance. That pan resides in the furnace and is heated or cooled during the experiment. The weight of the sample is monitored during the experiment. A sample purge gas controls the sample environment.

In this study a PerkinElmer thermogravimetric analyzer (TGA7) fitted with a thermal analysis controller (TAC7/DX) was used to determine thermo-gravimetric analysis. The machine was operated under a nitrogen gas atmosphere and the samples were heated from 20 °C to 900 °C at a heating rate of 20 °C/min. About 5 mg of sample was weighed into the pan and run accordingly.

3.4.8 Ultraviolet Visible spectroscopy (UV-vis)

Ultraviolet-visible spectroscopy is an analytical technique that is widely employed for the quantitative analysis of a variety of analytes. Analysis using spectroscopic methods are commonly done with liquid samples, however solids and gases can also be analysed using this technique. Common analysed samples include transition metal ions, highly conjugated organic

compounds and biological macromolecules. A UV-vis spectrophotometer measures transmittance (%*T*) which is the ratio of the intensity of light that passes through a sample (*I*) and the intensity of the light before it passes through a sample (I_o) at a given wavelength. Since absorbance is based on transmittance, the Beer-Lambert law can be applied to determine concentration of species in solution:

$$A = Log_{10} (I_o/I) = \varepsilon . c.L$$

Where *A* is the measured absorbance, *%T = (Io/I)*, *L* is the path length through the sample, and *c* is the concentration of the absorbing species. And ε is the molar absorptivity constant which differs from one element to the next.

In this study, the Perkin Elmer Lambda 25 UV-visible spectrophotometer was used to determine the change in concentration of methylene blue (MB) during the photocatalytic degradation experiments with Cs-PVAE immobilized Ag/N doped TiO_2 nanomaterials. Methylene blue (MB) is a heterocyclic aromatic chemical compound with the formula $C_{16}H_{18}N_3SCl$. Before testing the photocatalytic activity of the prepared material, the UV-vis spectrum of methylene blue solution was obtained to see the range in which it absorbed the ultraviolet light. According to literature (Chang *et al*., 2004) MB has a maximum absorption wavelength in the range 660-665 nm, however in this study using the above mentioned instrument maximum wavelength was measured to be at 615 nm.

In a solid form MB appears as a dark green, odourless powder and it turned blue when dissolved in water. Under catalytic red-ox cycle MB can be reduced to a colourless compound (Schirmer *et al*., 2011). Figure 3.2 depicts the UV-vis spectra of the maximum absorbance of the 10 mg/L methylene blue (MB) solution used in this study:

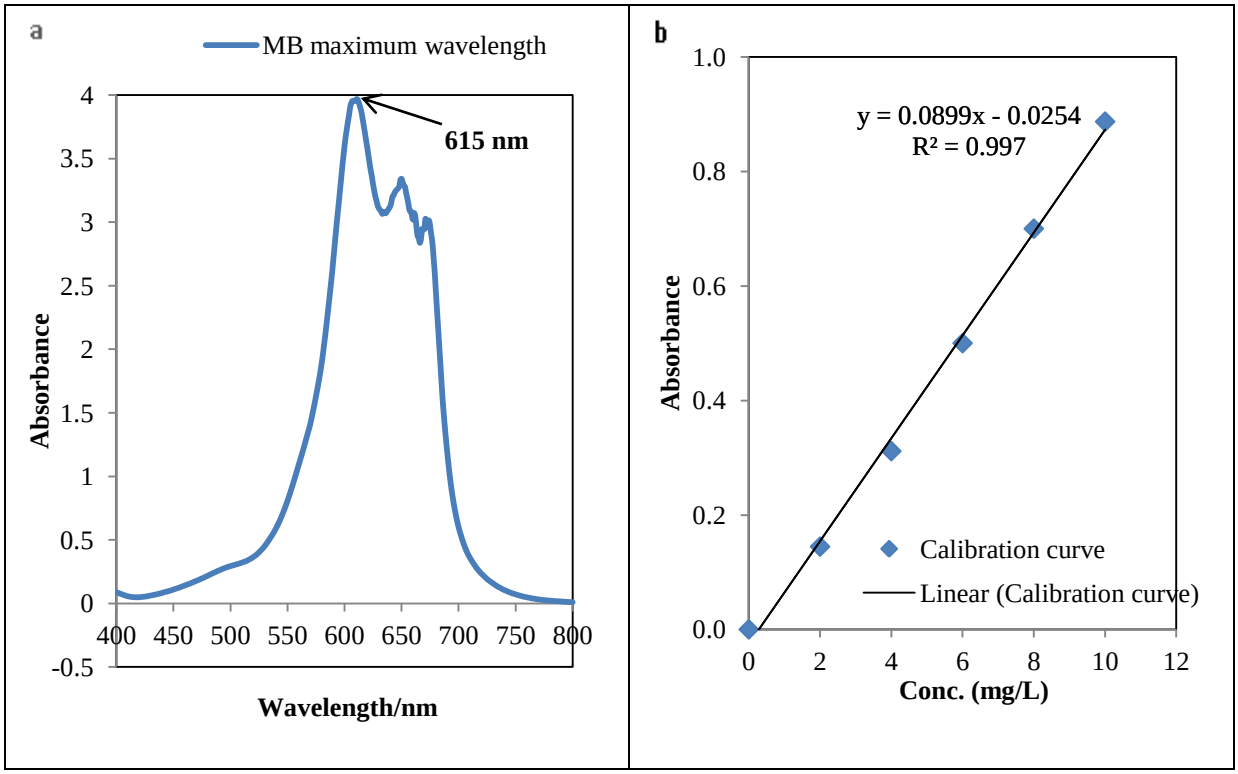

Figure 3.2: (a) Maximum absorption spectra of methylene blue and the calibration curve of MB at wavelength 615 nm (b)

3.5 Conclusion

Preparation of Ag and N doped titanium dioxide immobilized on Cs-PVAE nanofibers was successfully done and results are presented and discussed in Chapter 5. This was confirmed by the characterization techniques discussed in Section 3.4. In Chapter 4 properties of the synthesized materials were tested by evaluating the photocatalytic activity as well as the antibacterial activity.

References

Chen, X., Lou, Y., Samia, A.C.S., Burda, C., Gole, J.L. (2005). Formation of Oxynitride as the Photocataltic Enhancing Site in Nitrogen-Doped Titania Nanocatalysts: Comparison to a Commercial Nanopowder. *Advanced Functional Materials* , 15;41-49.

Duplessis, D. (2011). *Fabrication and characterization of anti-microbial and biofouling resistant nanofibers with silver nanoparticles and immobilized enzymes for application in water filtration.* Stellenbosch,RSA: Stellenbosch University.

Lopez Goeme, T.M., Alvarez Lemus, M.A., Angeles Morales, V., Gomez Lopez E., Castillo Ocampo, P. (2012). Study of Bacterial Sensitivity to Ag-TiO2 Nanoparticles. *J. Nanomedicine & Nanotechnology* , 1-7.

Lopez, R.,Gomez, R. (2012). Band-gap energy estimation from diffuse reflectance measurements on sol-gel and commercial TiO2:A comparative study. *Journal of Sol-Gel Sci Technol* , 1-7.

Schirmer, R.H., Adler, H., Pickhardt, M., Mandelkow, E. (2011). Lest we forget you- methylene blue. *Neurobiology of Ageing* , 1-10.

Zaleska, A. (2008). Doped- TiO2: A review. *Recent Patents on Engineering, Vol. 2* , 157-164.

Chapter 4: Photocatalytic and Antibacterial activity tests

4.0 Introduction

After synthesis and characterization of the immobilized nanofibers was complete, evaluation of the photocatalytic and antibacterial activities of the as synthesized nanomaterials was carried out

4.1 Photocatalytic activity

To test the photocatalytic activity of the modified photocatalyst, methylene blue (MB) was chosen as a model organic pollutant. The dye was dissolved in deionised water to mimic a pollutant in an aqueous medium. Methylene Blue is a cationic tri-cyclic aromatic compound with the structure illustrated in Figure 4.1.

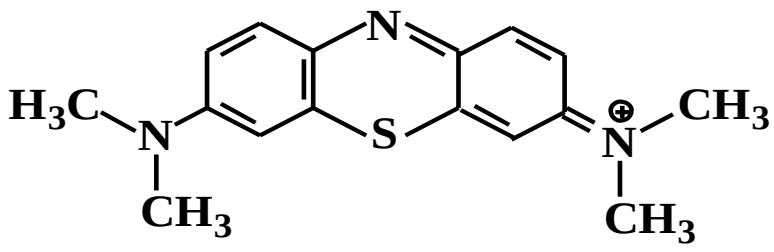

Figure 4.1: Chemical structure of Methylene Blue

The concentration of the dye was first measured on a UV-vis spectrophotometer at a maximum absorption wavelength of 615 nm. A 10 mg/L solution of MB was used for the photocatalytic activity tests; 100 mL of the aqueous dye solution was measured into a beaker containing 5g of nanofibers made from a composite of Cs/PVAE-doped TiO_2. The reaction mixture was kept under continuous stirring and kept in the dark for 30 minutes to allow equilibration. After 30 minutes the flask was exposed to UV irradiation at λ=365 nm using a Camag UV lamp and kept under continuous stirring. At 2 hours intervals, 5 mL aliquots were drawn and taken for measurement on the UV-vis spectrophotometer to evaluate the concentration after exposure to

the photocatalyst and light. This experiment was run concurrently with the visible light (solar light) in place of the UV tests. Figure 4.2 presents photographs taken during the photocatalytic degradation of MB.

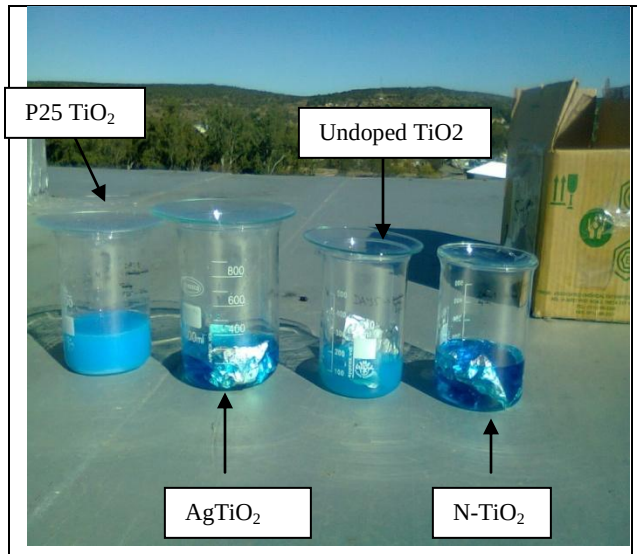

(a)At time zero

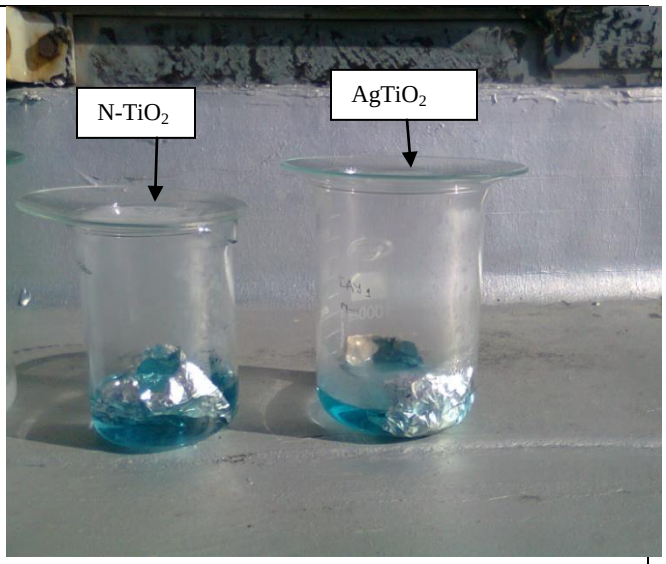

(b) After 4 hours

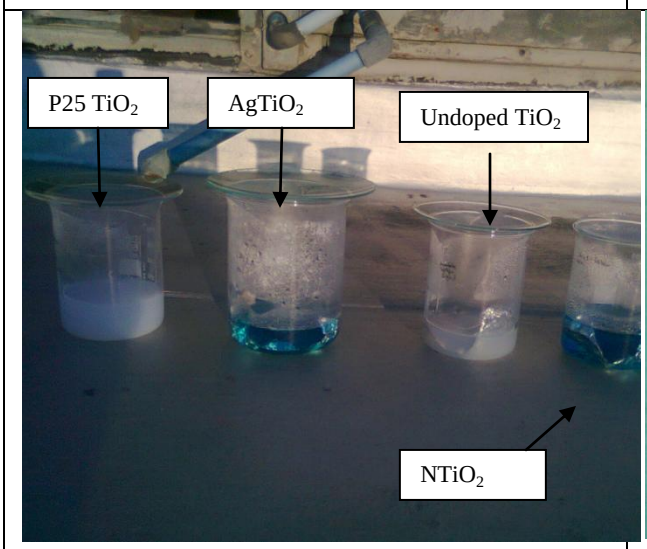

(c)After 6 hours of sunlight exposure

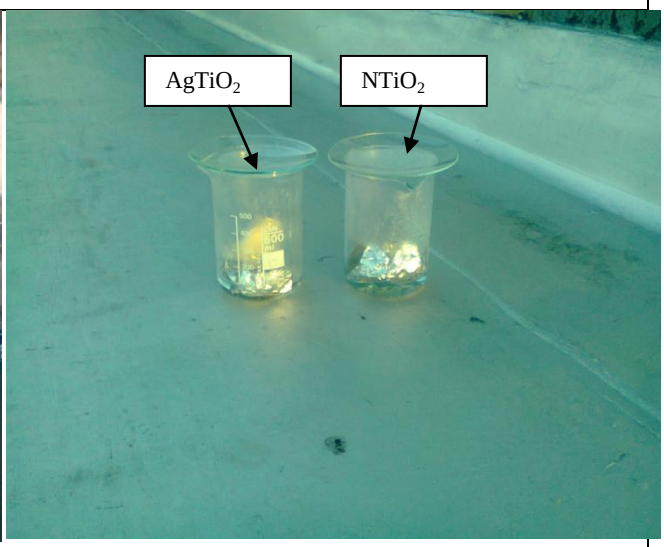

(d)After 3 days of exposure to sunlight

Figure 4.2: Images taken during the test of the photocatalytic degradation of MB under solar light radiation

4.2 Antibacterial tests

Determination of antibacterial properties of the as synthesized nanomaterials tests was carried out in the Microbiology and Biochemistry department at the University of Fort Hare.

4.2.1 Growth of microorganism

A strain of *Escherichia coli* (*E. coli*) was chosen as the model bacterial contaminant and cultivated on nutrient medium. A series of cell dilutions was made from the cell culture of *E. coli* sample under study to obtain a suspension of suitable colony forming unit (cfu/mL). The isolate of *E.coli* was grown overnight in a nutrient broth medium at 37 ºC.

4.2.2 Reaction system set-up

A reactor system to carry out antibacterial tests under direct solar light was set up on a sunny day with a temperature above 28 ºC on the roof of Chemistry Department University of Fort Hare. The photocatalyst materials that were tested were N-doped TiO_2 and Ag-doped TiO_2, immobilized on Cs-PVAE nanofibers, undoped TiO_2 and commercial P25 Degussa TiO_2 nanopowders. All the tests were done in duplicates. Eight sterilized 600 mL beakers with lids, each containing the photocatalytic nanomaterials were labelled accordingly and placed on a magnetic stirrer for mixing.

4.2.3 Experimental procedure

To each of the prepared 600 mL beakers 150 mL of nutrient broth was transferred and stirring was resumed. This was followed by the addition of 1000 µL of the organism and the mixture was continuously swirled on a magnetic stirrer. The control of the experiment was made up of the similar set-up but placed in a darkroom. At regular 30 minutes intervals, aliquots of 200 µL were withdrawn from the reaction mixture and inoculated onto the prepared nutrient agar plates using

sterile swaps. The experiment was run for 3 hours, from t = 0 to t = 180 minutes and inoculated agar plates were incubated at 37ºC for 18-24 hours. After 24 hours colony counts were taken and recorded. The mean of the colonies for the duplicate plates was calculated and the number of surviving colonies was plotted against time. All these tests were done in duplicates, following the experiments reported by other researchers (Liu *et al*., 2003; Coleman *et al*., 2005). In both the solar light and dark room experimental setups, a mixture of broth and organism without the nanomaterials served as the blank.

Chapter 5: Results and Discussion

5.0 Introduction

Chapter 5 covers results that were obtained after characterization of the synthesized TiO_2 nanopowders, undoped and doped as well as the composites and nanofibers. Section 5.1 outlines characterization results before electrospining, Section 5.2 covers characterisation results of the electrospun nanofibers while Section 5.3 reports on the results obtained for photocatalytic and antimicrobial tests of the synthesized materials.

5.1 Results of characterization of the doped and undoped TiO_2

This section reports and discusses the results obtained for doped and undoped TiO_2 prepared by the sol-gel synthesis. The characterization techniques used were FTIR spectroscopy, XRD, SEM, EDS, TEM and DRS.

5.1.1 FTIR results

Figure 5.1 shows spectra of the undoped, nitrogen and silver doped titanium dioxide nanopowders obtained after calcination. All three graphs show a broad band in the region from 440-900 cm^{-1} due to Ti-O stretching vibration and O-Ti-O lattice corresponding to what has been reported in the literature as a characteristic of TiO_2. The peak observed in all three spectra in regions 1620-1640 cm^{-1} and 3396-3500 cm^{-1} respectively correspond to the O-H bending and O-H vibration of the adsorbed water molecules and hydroxyl ions. The latter peak also corresponds to the O-H stretch region and has been attributed to the interactions between the hydroxyl groups of titania (Park *et al*., 1997; Chen *et al*., 2005; Jagadale *et al*., 2008; Suwanchawalit *et al*., 2011). These adsorbed OH ions play a significant role in photocatalysis by trapping charge carriers to produce reactive OH radicals which are the driving force behind the process. Furthermore they

act as adsorbents and active sites for the reactant molecules or the pollutant (Maira *et al*., 2001). The distinct broadness of the peak in region 3379-3500 cm^{-1} in nitrogen doped titania can also be attributed to N-H symmetric and asymmetric stretching vibrations (Ren *et al*., 2007; Kong *et al*., 2010).

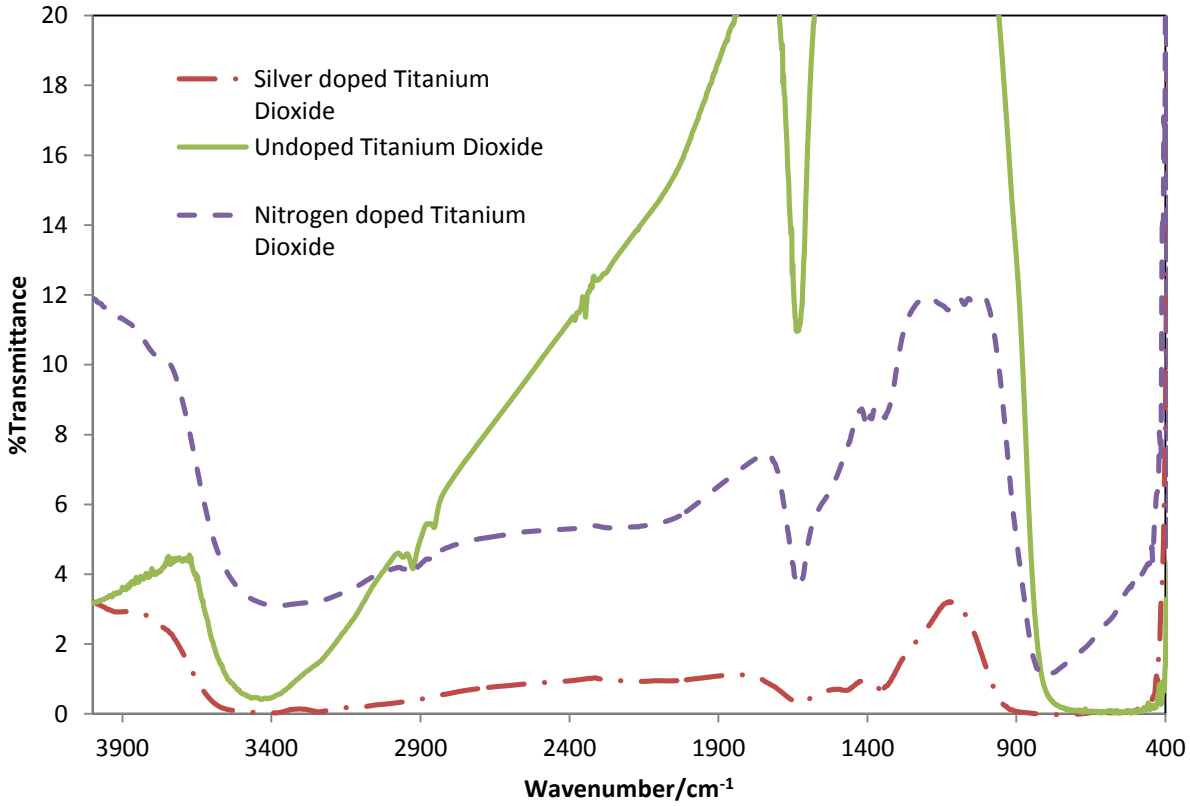

Figure 5.1: FTIR spectra of doped and undoped Titanium dioxide (TiO_2)

5.1.2 XRD results

The phase composition and crystallite sizes of the synthesized titanium dioxide nanopowders were determined by XRD analysis. The XRD patterns of the undoped, as well as silver and nitrogen doped titanium dioxide nanoparticles after calcination are shown in Figure 5.2. The samples were all calcined at 600 ºC. The XRD pattern shows that all three samples consisted of mixed crystalline phases; anatase, rutile and a small percentage of the mineral halite (NaCl)

suspected to be an impurity due to the materials used in the synthesis process (Yalcin *et al*., 2012).

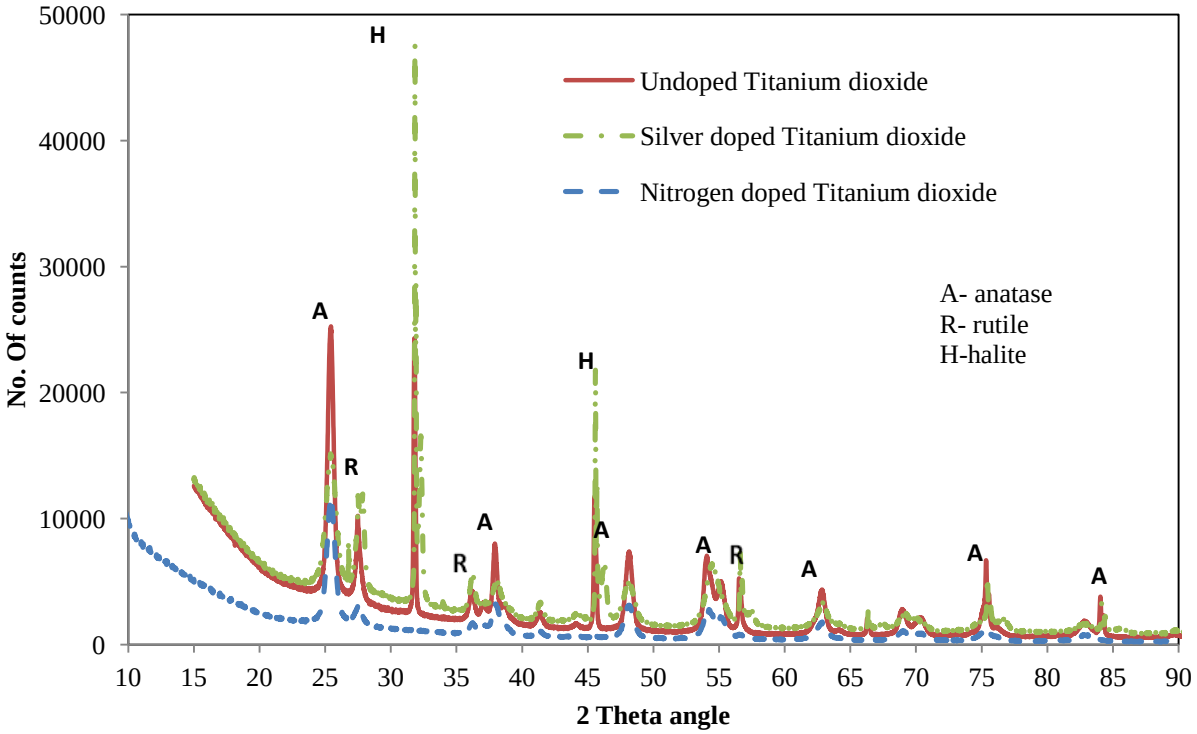

Figure 5.2: XRD Pattern of doped and undoped TiO_2 nanopowders

From all the three spectra strong diffraction peaks representing the anatase phase are observed at 2θ values of 25.5º, 37.9º, 47.5º, 53.89º, 62.44º, 75.3º and 84.1º. This shows that the anatase is the dominant phase and this is beneficial since anatase is reported to be more photocatalytically active than rutile (Ding *et al*., 2000; Akpan *et al*., 2010). Traces of the rutile phase are observed at 27.5º, 36.1º and 56.8º. From the sharpness of the peaks in the spectra it can be deduced that the calcination process induced high crystallinity (Chen *et al*., 2007; Thamaphat *et al*., 2008). On the contrary, the N-TiO_2 peak broadened after doping and the size of the crystals also decreased compared to the pure and Ag-TiO_2. This can be attributed to formation of nanoparticles and aggregation of the crystallites as they get smaller which agrees with other reported studies

(Sathish *et al*., 2005; Chen *et al*., 2005). In a similar study Wang *et al*. (2005) used Scherrer equation to estimate the average sizes of the nitrogen doped titania nanoparticles and it was deduced that a decrease in peak width is directly proportional to the size of nanoparticles.

Silver doped TiO_2 spectrum does not show any noticeable change in the number of peaks due to the presence of the silver dopant. Nasr-Esfahani *et al*., (2008) suggests that this could imply that the Ag nanoparticles were well scattered on the surface of TiO_2. Behnajady *et al*., (2008) points out that this could be due to what has been reported by other researchers that silver attaches on the surface of titania since it has a large radius to be incorporated into the lattice structure (Sobana *et al*., 2006; Choi *et al*., 2009).

Table 5.1 presents the average nanocrystallite sizes of titania as estimated by the Scherrer equation which is explained in Section 3.4.2. Nitrogen doped titania has an average grain size of 8.2 nm, and this was the smallest size compared to undoped titania and Ag doped TiO_2 with 9.23 nm and 10.52 nm respectively. These estimated results confirm what has been reported that peak broadening in nitrogen doped TiO_2 implies formation and agglomeration of nanoparticles (Sathish *et al*., 2005; Kusumawardani *et al*., 2009). The size of nanoparticles has been reported to have an inversely proportional relationship with the surface area, implying that N-doped TiO_2 has a larger surface area compared to the undoped and Ag-doped nanoparticles (Sobana *et al*., 2006).

Table 5.1: Crystalline sizes of doped and undoped TiO_2 calculated by Scherrer equation

Sample ID	**Crystallite size (nm)**
Undoped TiO_2	9.23
Ag-TiO_2	10.52
N-TiO_2	8.22

5.1.3 SEM results

SEM analysis was carried out in order to examine the morphology and diameter size of the electrospun nanofibers and the sol gel synthesized undoped TiO_2 nanoparticles. The micrograph of these nanomaterials is shown in Figure 5.3. The images were obtained from JEOL JSM-6390LV SEM fitted with secondary electron detector, and equipped with an attachment for the Energy dispersive X-ray spectroscopy (EDS) to enable compositional analysis to be carried out.

Figure 5.3a shows the electrospun nanofibers made from a polymer blend of chitosan/ PVAE and titania nanoparticles. The average size of the nanofibers was found to be in the range 234-270 nm, and appeared to be uniform. Figure 5.3b shows that the shape of pure titania nanoparticles was spherical and evenly distributed. TEM analysis was used to obtain the sizes of the nanoparticles since the SEM micrographs were not clear for size measurement at high magnification.

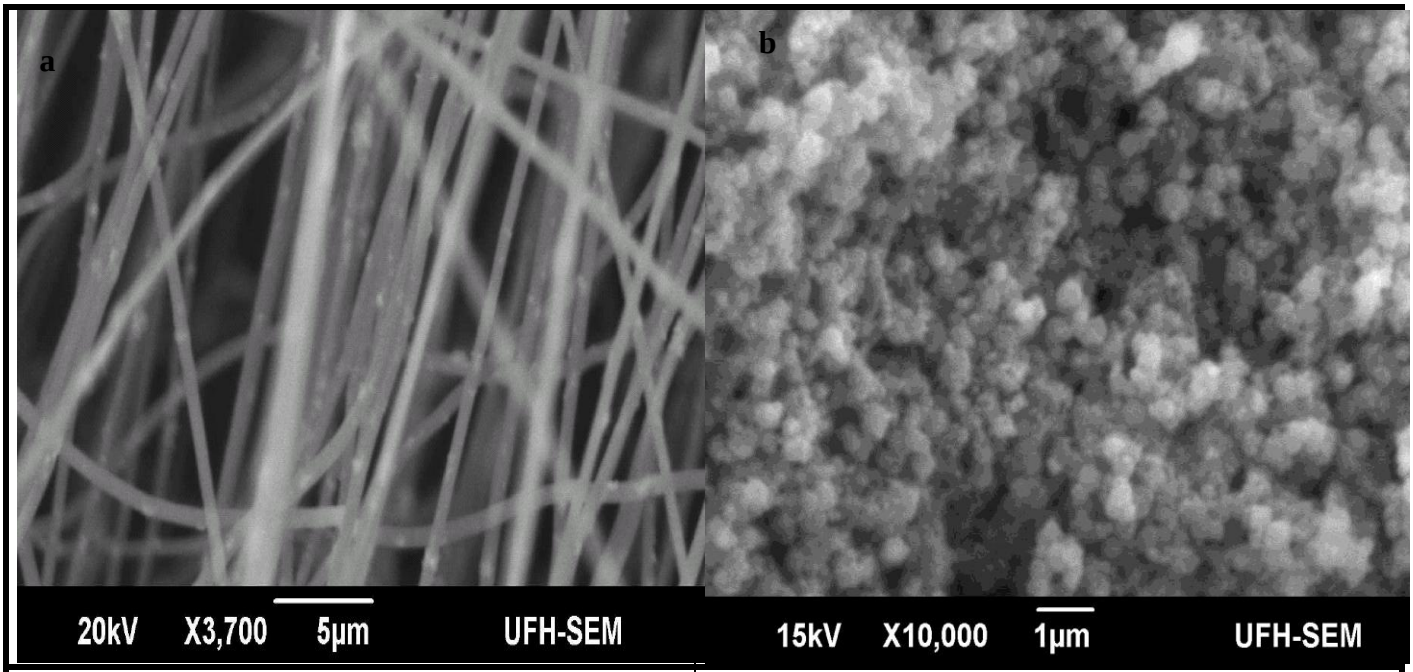

(a)SEM image of TiO_2-Cs/PVAE nanofibers

(b)SEM image of undoped TiO_2 spherical nanoparticles

Figure 5.3: SEM images of (a) titania immobilized on a polymer blend of Cs-PVAE (b) undoped TiO_2 spherical nanoparticles

5.1.4 EDS results

Elemental composition of the undoped titania, nitrogen and silver doped titania was determined using EDS. Table 5.2 shows the percent loadings of all the elemental components making the nanomaterials and it can be deduced from the high weight % of titanium and oxygen that they are the main components. The weight % loading of Ag-TiO_2 was much higher compared to that of N-TiO_2, and this can be suggested to be due to silver dopant attaching onto the surface of titania and not incorporated into the crystal lattice where it would be shadowed from detection. Nitrogen has a small radius which is comparable to that of oxygen; therefore it can easily undergo interstitial substitution into titania (Choi *et al*., 2009; Sobana *et al*., 2006). Hence, only a small fraction of nitrogen weight % was detected compared to the silver weight %.

Table 5.2: Energy dispersive X-ray spectroscopy results

Sample	**Titanium (Ti) w%**	**Oxygen (O) w%**	**Dopants (Ag&N) w%**
Undoped TiO_2	53.02	19.89	
Ag-TiO_2	41.83	19.27	11.99
N-TiO_2	53.54	25.75	3.18

5.1.5 TEM results

Figure 5.4 depicts TEM images of doped and undoped TiO_2 nanoparticles (images a-d) after calcination. The micrographs show that nanoparticles are of spherical shape for both the doped and undoped samples. The average size determined from the diameter of randomly selected nanoparticles ranges from 6.4 nm to 21 nm and this is comparable to the estimated nanoparticles sizes as calculated from the XRD results. Figure 5.4(a) shows N-doped TiO_2 nanoparticles which appear to have a crystalline monodisperse orientation compared to Ag-doped TiO_2 in Figure 5.4(b) and the undoped titania in images (c) and (d) which appear to be aggregated and polydisperse. The size of the undoped titania in Figures 5.4 (c & d) is comparable to the reported size of commercial P25 TiO_2 which ranges between 21-30 nm (Bakardjieva *et al*., 2005).

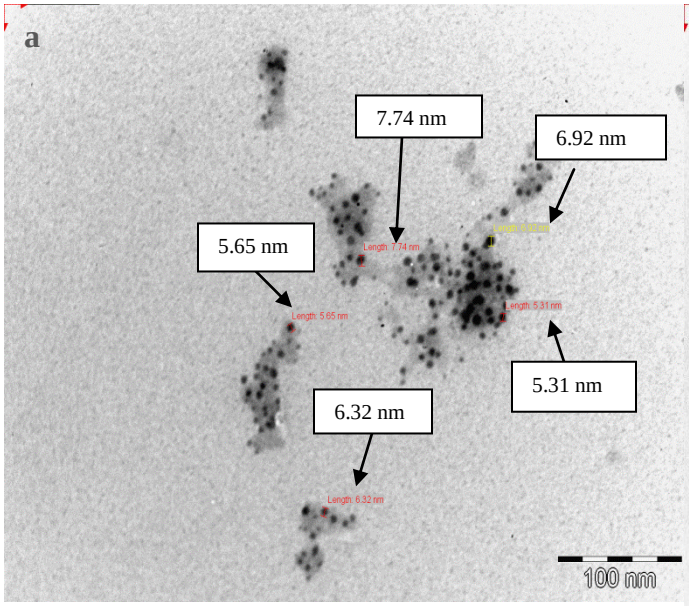

(a) TEM image N doped TiO_2 nanoparticles

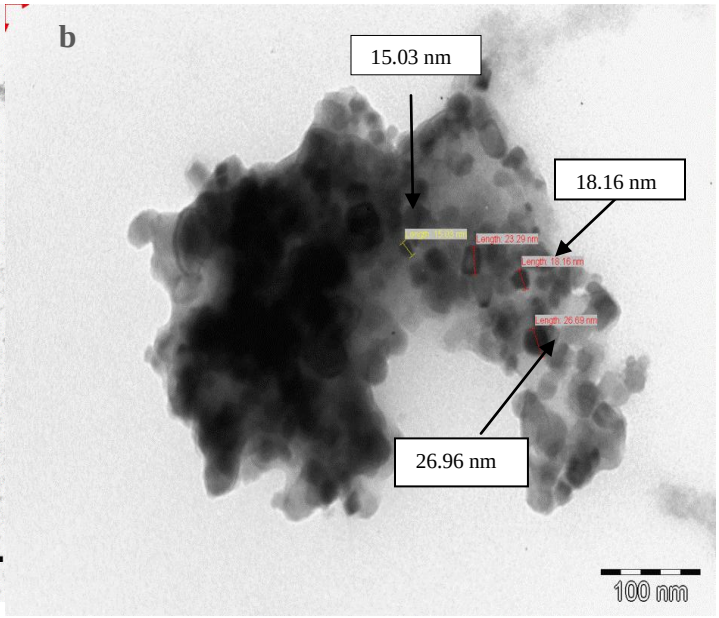

(b) TEM image of Ag doped TiO_2 nanoparticles

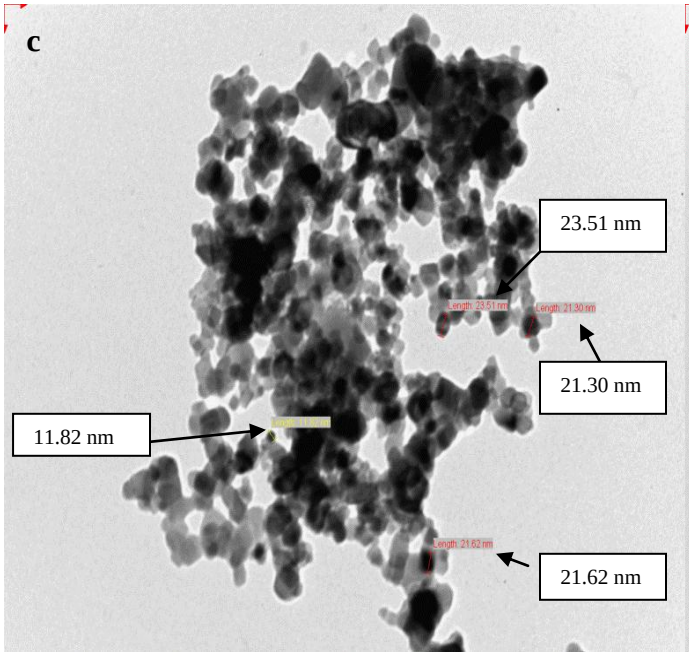

(c)TEM image of undoped TiO_2 nanoparticles (zoomed)

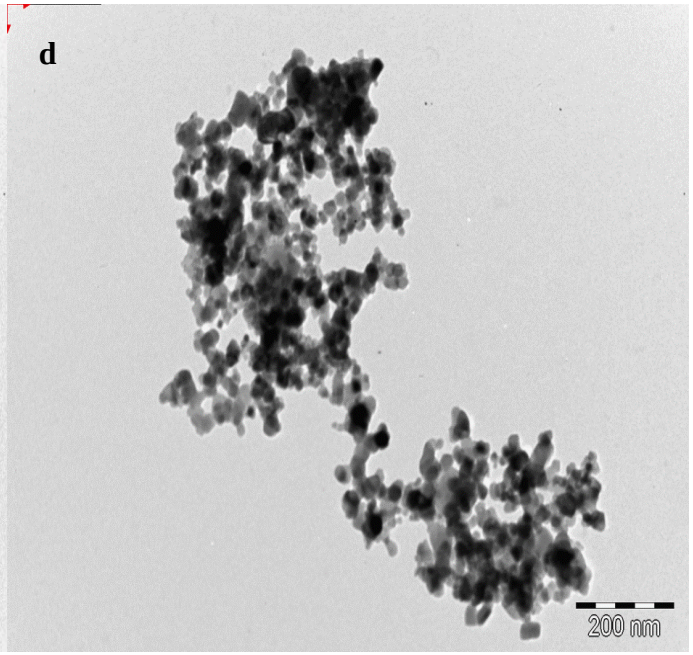

(d) TEM image of undoped sol-gel synthesized TiO_2 nanoparticles

Figure 5.4: TEM images of doped and undoped TiO2 nanoparticles

5.1.6 DRS results

Diffuse reflectance spectroscopy was used to determine the band gap energy of the synthesized doped and undoped titanium dioxide nanoparticles, the commercial Degussa P25 TiO_2 was also analysed for comparison. Figure 5.5 shows the DRS spectra of all the analysed nanopowder particles. From the spectra it is observed that the commercial undoped TiO_2 P25 Degussa is the least absorbed and Ag-doped TiO_2 shows higher absorbance compared to all the nanomaterials. This shift absorption band edge corresponds to what has been reported in literature that silver doping increases the optical properties of TiO_2 to a higher wavelength (Sobana *et al*., 2006).

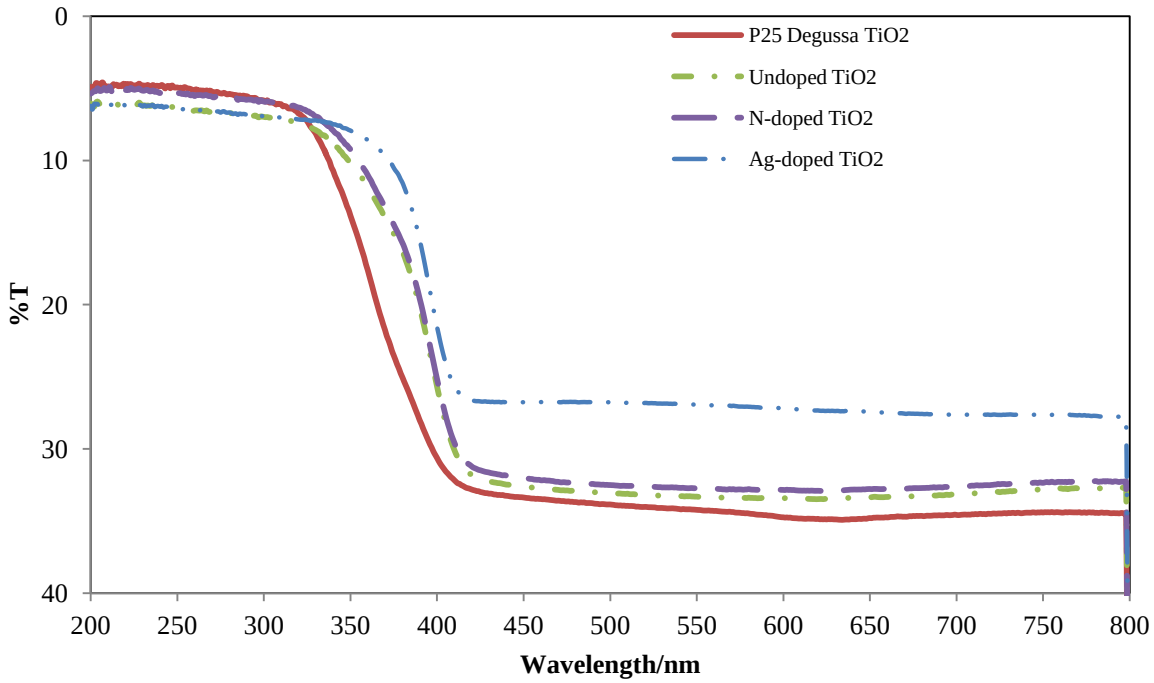

Figure 5.5: DRS spectra of the doped and undoped TiO_2

Figure 5.6(a-d) shows the DRS spectra and derivative plots of all the samples from which absorption band edges were deduced. Figure 5.6(a-c) represents the spectra of undoped titania, N-doped titania and Ag-doped titania respectively. Their absorption band edges appear to have shifted to longer wavelengths in the visible region compared to the commercial titania shown in Figure 5.6(d) of the DRS differential spectra, the commercial photocatalyst Degussa P25

absorption band edge was observed to be in the UV region at 359 nm while the synthesized samples showed a large shift in the wavelength towards visible region (~400 nm). However, there was a small difference in the absorption shift amongst the synthesized nanomaterials.

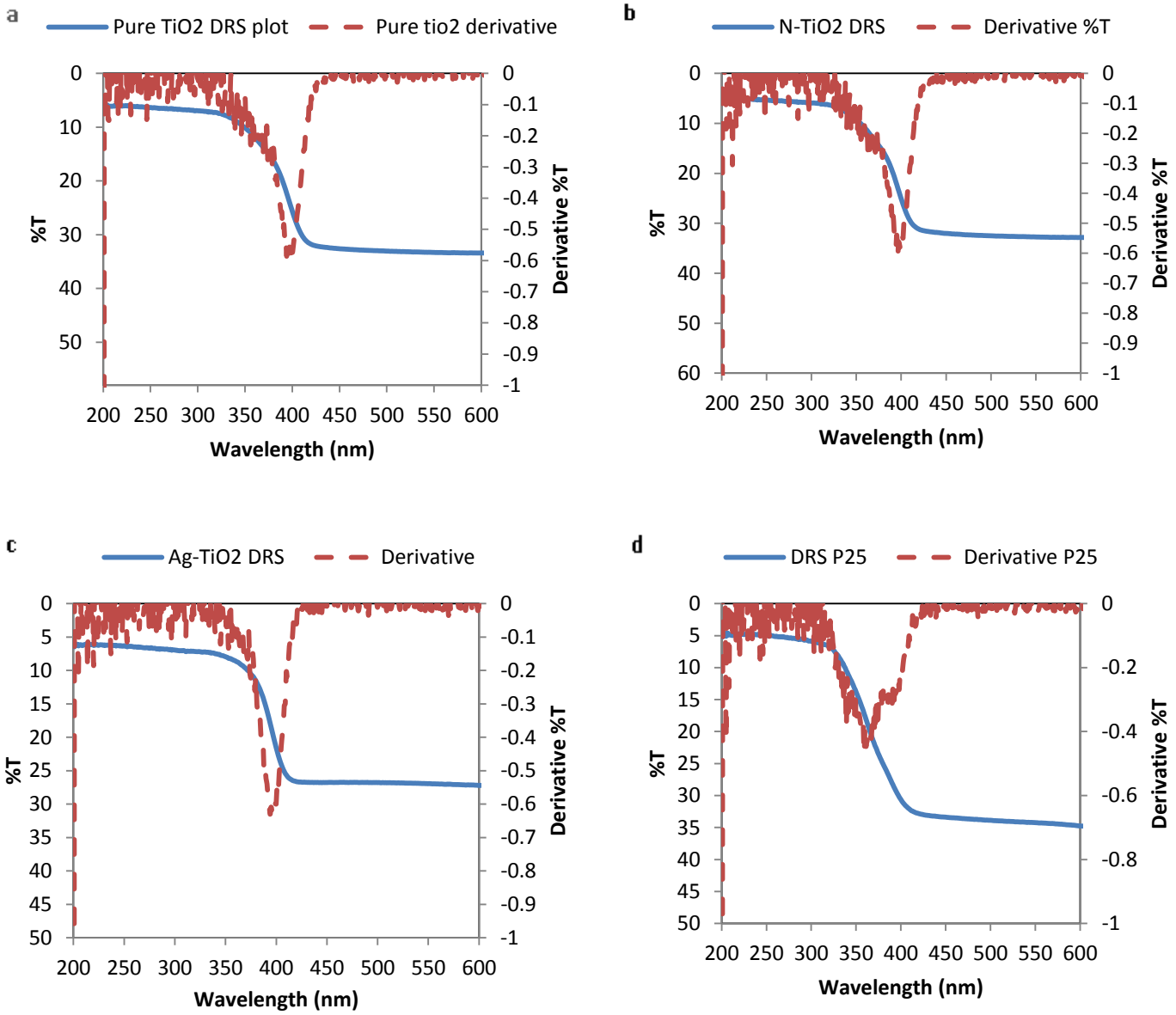

Figure 5.6: DRS spectra and differential spectra of undoped TiO_2 (a), (b) N doped TiO_2, (c) Ag doped TiO_2 and (d) commercial Degussa P25 TiO_2

Using the observed absorption band edge values the band gap energies (EG) of the samples were calculated according to the equation:

$$\text{Band gap energy } (Eg) = hc/\lambda$$

Where $h = 4.135 \times 10^{-6}$ eV.s is the Planck's constant, $c = 3 \times 10^{8}$ m/s is the velocity of light, λ is the absorption band edge wavelength in nm (Tayade *et al*., 2006). Table 5.3 shows the results of the calculated band gap energies. And it can be seen that the band gap energies of the synthesized samples are narrower compared to the commercial titania. There is also an observed difference in the band gap energy of the synthesized catalysts even though it is not large.

Table 5.3: Calculated results of the DRS band gap energy of the TiO_2 nanoparticles

Sample ID	Wavelength/ nm	Band gap energy/eV
N-doped TiO_2	396	3.13
Ag-doped TiO_2	397	3.12
P-25 TiO_2 (commercial)	359	3.45
Pure TiO_2(lab-synthesized)	394	3.15

5.2 Characterization results of the electrospun nanofibers

This section presents characterization results of the FTIR, TGA and SEM results obtained for analysis of electrospun chitosan-PVAE nanofibers before and after immobilization of the doped TiO_2 nanoparticles. The SEM image for the nanofibers is shown in Figure 5.3, Section 5.1.3, the FTIR and TGA results are shown below in Section 5.2.1 and 5.2.2 respectively.

5.2.1 FTIR results

FTIR analysis was done for identification of structural changes that took place during synthesis. Figure 5.7 depicts the FTIR spectra of pure chitosan (curve A), the 90:10% (v/v) (curve B) and 80:20 % (v/v) (curve C) blends of PVAE and chitosan. Figure 5.7 spectrum A show peaks that are characteristic of chitosan, a sharp peak observed in the wavenumber range from 1018 cm^{-1} correspond to the C-O stretching vibration and peaks in the range 842-1120.6 cm^{-1} are assigned to the saccharide structure of chitosan. Peaks at 1332 cm^{-1} and 1363 cm^{-1} are characteristic of the CH_3 symmetric deformation and stretching vibration of C-H bonds. Another C-H stretching vibration observed at the peak 2889 cm^{-1}. These peaks can also be attributed to symmetric or asymmetric CH_2 stretching from the pyranose ring. The peaks at 1577 cm^{-1} and 1654 cm^{-1} respectively correspond to the stretching vibration of the amino and amide group of chitosan. The broad but not intense peak in the range 3200-3400 cm^{-1} is due to the amine NH symmetric vibration (Pawlak *et al*., 2003; Krishna Rao *et al*., 2006; Anicuta *et al*., 2010).

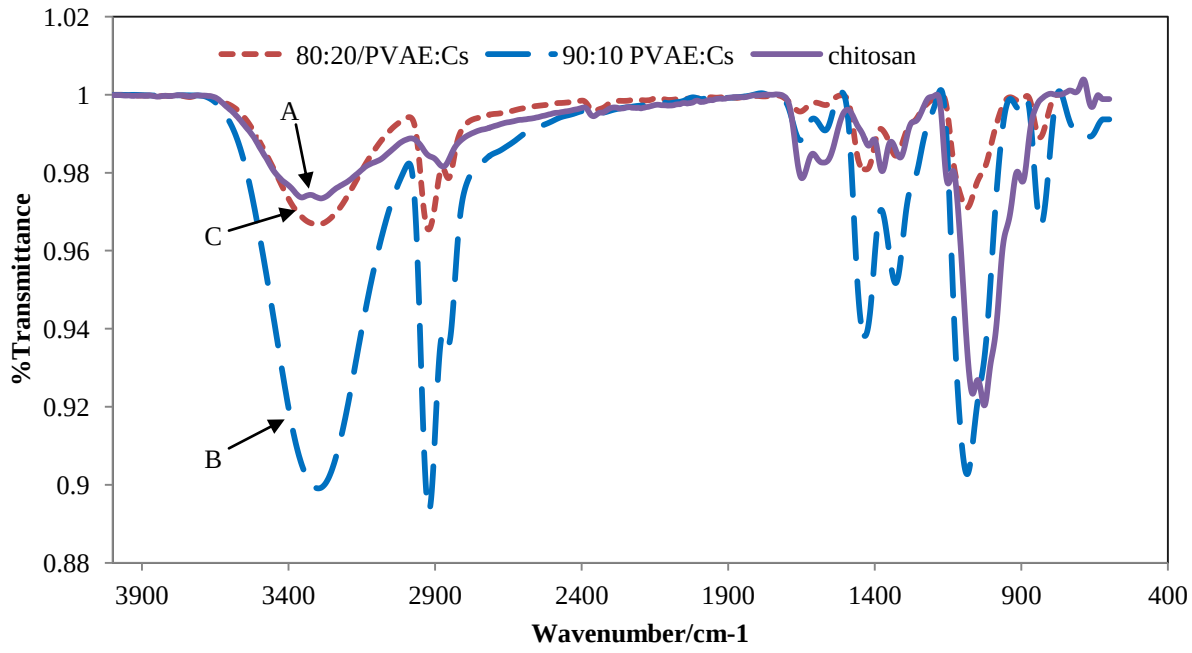

Figure 5.7: FTIR of pure chitosan and chitosan blended with PVAE

However these peaks seem to disappear in the curves B and C when chitosan is blended with PVAE at different volume percent ratios. Spectrum B where the ratio of PVAE to chitosan is 90:10 % (v/v) depicts peaks that are typical of PVAE. A broad peak in the range 3200-3400 cm^{-1} represents –OH and –NH stretching vibrations of the hydroxyl group in PVAE and amine group in chitosan. The intensity of the peaks in spectrum B is decreased when chitosan content is increased to make the volume ratio of the polymers to be 80:20 % (v/v). These observations suggest that hydrogen bonding between the two polymers occured even though most of the chitosan peaks overlapped with PVAE peaks (Krishna-Rao *et al*., 2006; Jia *et al*., 2007). The disappearance of this peak in spectra B and C can be attributed to the fact that the amount of chitosan in the blend is low compared to that of PVAE; this therefore suggests that chitosan peaks are masked.

5.2.2 TGA results

TGA analysis was employed to determine the thermal stability and degradation temperature of the synthesized nanoparticles and electrospun nanofibers. Figures 5.7, 5.8 and 5.9 shows the normal thermograms (TGA) and the differential thermograms (DTG) of PVAE:Cs polymer blends with different volume ratio. These thermograms show the degradation of the polymers as temperature is increases. All the thermograms show a multiple stage degradation with two visible weight losses or degradation stages observed around 100-120 ºC and the other in the range of 400-550 ºC. The first weight loss around 100º C corresponds to the loss of moisture and water adsorbed onto the nanofibers (Pawlak *et al*., 2003). The major weight loss observed in the range 400-460 ºC is due to the degradation of the polymer blend, mainly PVAE which is reported to degrade in one step starting from a temperature of 380 ºC (Dutra *et al*., 1996). PVAE is mainly composed of polyvinyl alcohol (PVA) which is known to undergo thermal degradation around

400 ºC, therefore the weight loss at 407.7 ºC corresponds to the breaking down of the PVA moiety in the blend (Juntanon *et al*., 2008).

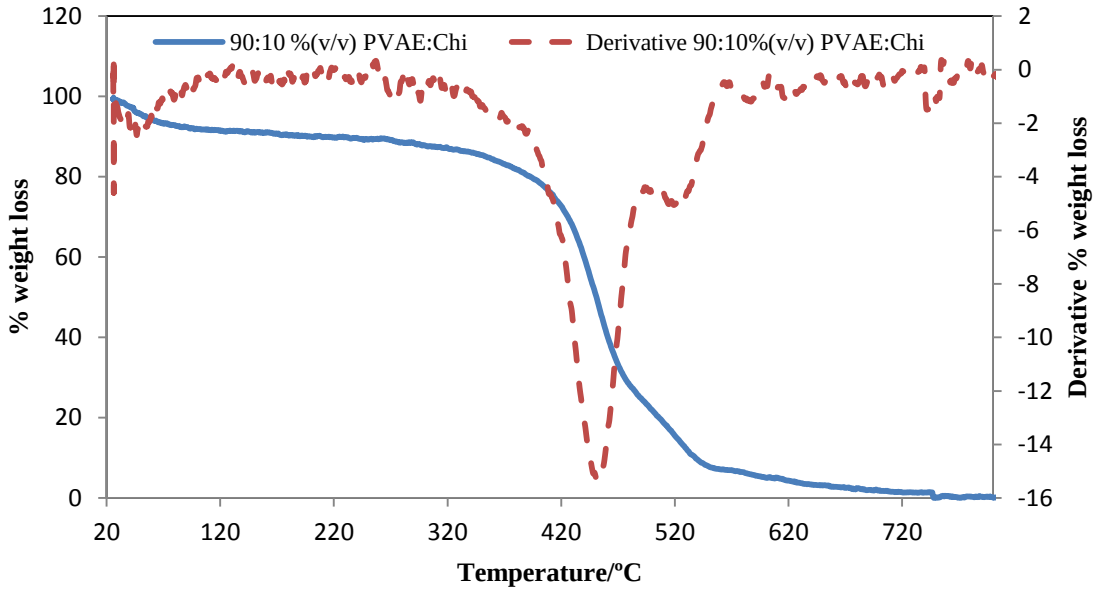

Figure 5.8: Thermogram and differential thermogram of 90:10% (v/v) PVAE:Cs polymer blend

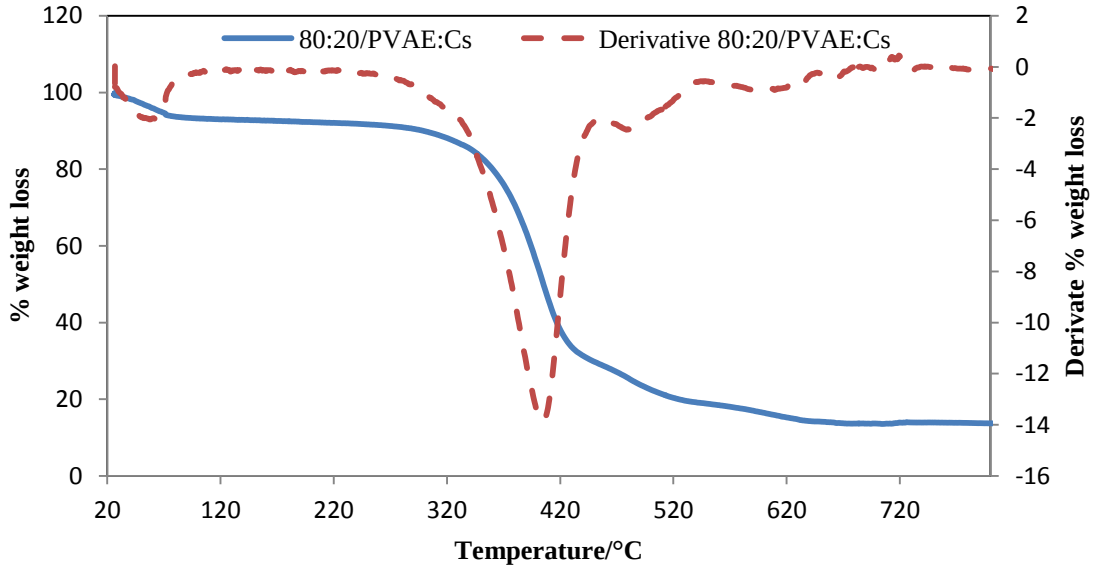

Figure 5.9: Thermogram and differential thermogram of 80:20% PVAE:Cs polymer blend

It is however observed in the DTG thermograms of the polymer blends in Figure 5.9 that as the amount of chitosan was increased from 90:10% PVAE:Cs to 80:20% (v/v) a shift in the peaks occurred. The degradation temperature of the polymer polymer blend (PVAE-Cs) decreased to a lower temperature (458 ºC to 407.7 ºC). This shift is owed to the increase in volume of chitosan because it corresponds to the thermal degradation and deacetylation of chitosan (Qu *et al*., 2000). Furthermore this change confirms the interaction between chitosan and PVAE.

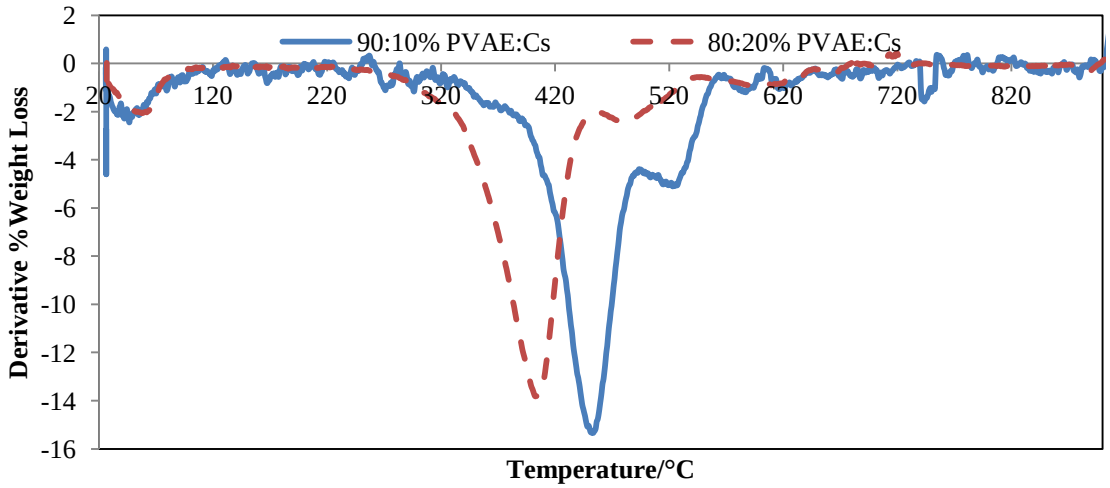

Figure 5.10: Differential thermograms of 90:10% and 80:20% (v/v) of PVAE:Cs polymer blends

5.3 Results and Discussion of Application tests

This section presents the results obtained from the evaluation of the nanomaterials synthesized in this study.

5.3.1 Photocatalytic activity

The photocatalytic activities of all the synthesized material were determined using MB as the model organic pollutant as described in Section 4.1. Figure 5.1.1 presents a graph showing change in the concentration of MB as a function of time. The graph showed a difference between

the experiments that were run under natural solar light, the N-doped ($MBNTiO_2$-solar) and the Ag-doped ($MBAgTiO_2$-solar) and the samples that had been irradiated with UV using a UV lamp, the N-doped ($MBNTiO_2UV$) and Ag-doped ($MBAgTiO_2UV$).

From the plot it could be seen that degradation of methylene blue dye was much faster for the experiments that were done under solar light compared to those irradiated with UV light. The concentration of MB decreased significantly within the first 2 hours of the experiment in samples under solar light. This can be attributed to the absorption shifts of the doped samples to higher wavelength that have been discussed in Section 5.1.6 under DRS results. Moreover, it was observed that silver doped titania samples were more efficient in degrading MB compared to the nitrogen doped samples for both the UV and solar light experiments. The experiment of silver doped titania under UV illumination showed a steady decrease for 6 hours of the experimental run, whereas the nitrogen doped titania did not show significant change in the concentration. This could imply that in the experiment of nitrogen doped titania run under UV illumination the photocatalyst was not significantly activated because of the observed red-shift to 396 nm. The contrast was observed when the same experiment with N-TiO_2 was run under solar light which constitutes 45% of visible light. The rate of colour degradation for samples under solar was faster compared to the experiments under UV light.

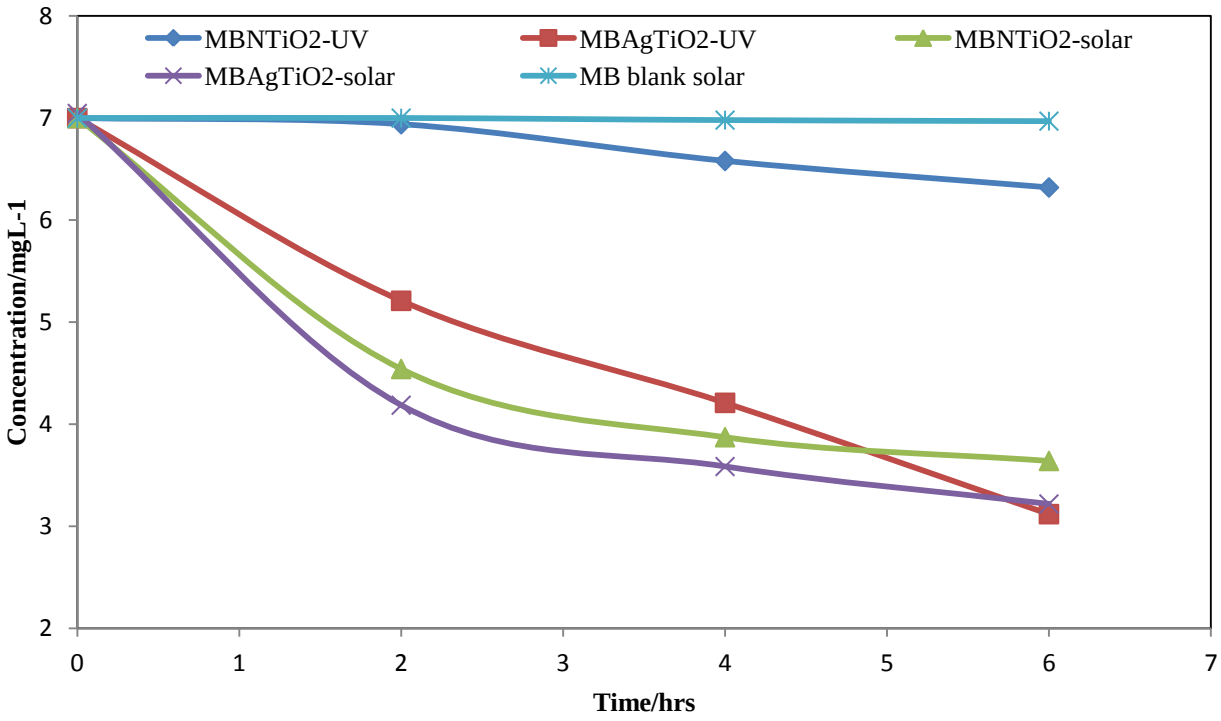

Figure 5.11: Degradation of MB using doped TiO2 nanoparticles immobilized on Chitosan-PVAE blend nanofibers

From the plot in Figure 5.11 it can be seen that the transition metal doped sample was more efficient compared to the non-metal doped one. This corresponds to what has been reported in the literature that the silver and other TM dopants have the ability to act as electron traps therefore reducing the rate of electron hole pair recombination (Sobana *et al*., 2006). These allow enough time for the photogenerated charge carriers to react with species adsorbed at the surface of titania to form reactive hydroxyl radicals and superoxide ions. A schematic diagram by Macwan *et al*., (2011) in Figure 2.2 illustrates the reaction mechanism of this process. In addition, the concentration of free holes (h^+) on the catalyst surface is increased by the electron trap phenomenon by the silver dopant leading to an increase in the generation of OH• radicals thereby resulting in increased photocatalytic activity of the titania (Rao *et al*., 2003; Kumar *et al*., 2009; Zhang *et al*., 2011).

The commercial P25 Degussa in powder form was used to degrade MB solution and it showed efficiency by decolourizing the dye within one hour. This is also observed on the images taken during the photocatalytic degradation test in Figure 4.2. A similar trend was observed with for both samples exposed to solar and UV light. However the shortfall of this commercial nanopowder photocatalyst remains the recovery process after cleaning the water. This is evident in the images, after decolorization the water remains milky due to the powdered photocatalyst.

5.3.2 Antibacterial activity

The antibacterial activity of the synthesized nanocomposites was determined using a strain of *E.coli* as a microorganic pollutant as described in Section 4.2. This was done in order to show and compare the effectiveness of the synthesized nanomaterials. Figure 5.12 presents the inactivation plots of *E. coli* by $AgTiO_2$/Cs-PVAE and $NTiO_2$/Cs-PVAE, commercial Degussa P25 TiO_2, and a mixture of broth and *E. coli* organism only which was used as the experimental blank. The tests were done under solar radiation and the control experiment was set up in a dark room.

The initial concentration of surviving colonies at t=0 was $1x10^3$; this sample was taken before the microorganism had time to interact with the antibacterial agents. Hence the number of colonies for all the plots was the same. There was a sharp decrease in the number of microorganisms during the first 30 minutes of exposure of the pathogens to the antibacterial nanomaterials, therefore suggesting immediate effectiveness of the antibacterial agents. The microorganisms went through a phase called “sudden death” due to the fact that they were introduced to a different environment. However not all the organisms were killed in each of the reaction vessels and they appeared to undergo a steady increase for about 15 minutes before reaching 60 minutes after which the pathogens seemed to die again. This is with exception to the

microorganisms exposed to the commercial P25 Degussa, possible reason for the exponential growth of the organisms in this instance could be that: the E.coli strain had developed outer membrane proteins therefore preventing the titania nanomaterials from being in contact with cell contents. Bacteria have also been reported to resist antibiotics due to genetic transformation by undergoing chromosomal changes and also by using membrane transporters (Masuda *et al*., 1995).

Ag doped TiO_2 however shows the potential to inhibit the growth of *E.coli*, this occurs within 90 minutes from t = 60. The nanomaterials exhibited higher antibacterial activity compared to all the antibacterial nanomaterials including N doped TiO_2. This corresponds to what has been reported by Zhang *et al*., (2009) that silver containing materials have good antibacterial properties. The exact mechanism of the antibacterial activity silver is not fully understood. However, it has been suggested in literature that it interacts with essential thiol (-SH) groups in bacterial proteins. Thus inhibiting DNA replication and causing damage to the cytoplasmic membranes of the bacterial cell and subsequently cell death (Martinez-Castanon *et al*., 2008; Jaiswal *et al*., 2010).

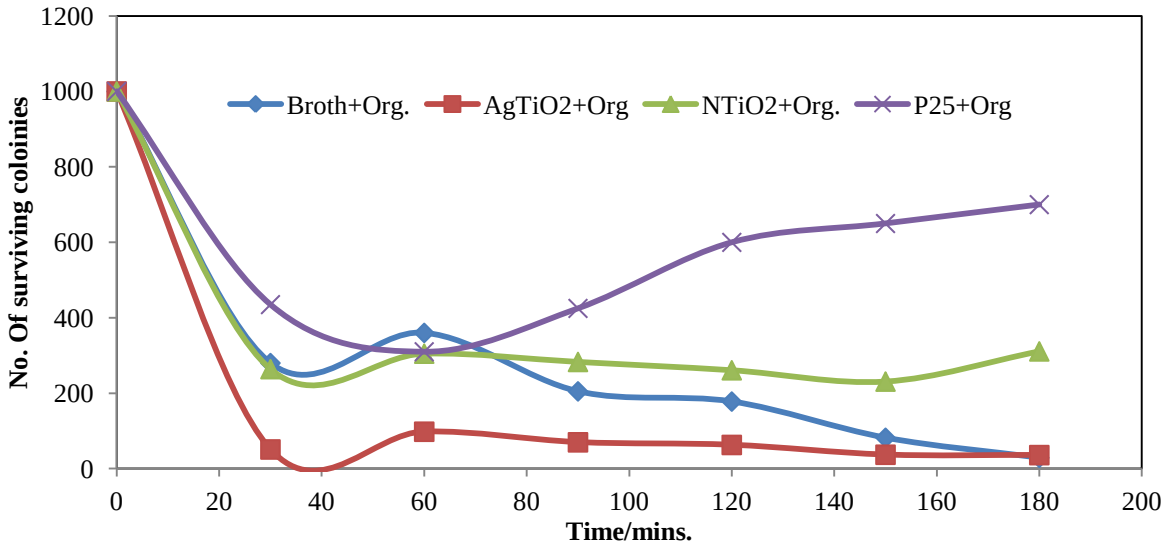

Figure 5.12: Photocatalytic inactivation of E. Coli using P25 Degussa TiO2, and undoped TiO2 nanoparticles immobilized on chitosan-PVAE blend nanofibers

On the other hand, N-TiO_2 was able to inactivate the microorganism for a while after which the number of surviving colonies increased. This might have occurred because the organism was conditioned to the nitrogen filled environment after a while and started using the environment as an energy source. Degussa P25 results showed that the growth of this Gram negative microorganism could not be inhibited. The increased antibacterial efficiency of Ag-TiO_2 compared to N-TiO_2 can be attributed to the fact that Ag alone is known to have antibacterial properties (Li *et al*., 2008; Nasr-Esfahani *et al*., 2008; Rai *et al*., 2009).

Chapter 6: Conclusion and Recommendations

6.1 Conclusions

Production of TiO_2 nanoparticles with extended optical band edge for environmental purification was achieved using a one pot sol-gel method. The sol gel synthesis method is advantageous because many parameters such as temperature, pH and concentration of dopants can be controlled during the process. Moreover sol-gel is suitable for doping reactions since it helps to develop strong interactions between the dopant and photocatalyst or support (Lopez Goeme *et al*., 2012). Nitrogen and silver doped titanium dioxide nanoparticles were successfully synthesized and this was confirmed by characterization by FTIR, TEM, SEM, DRS and EDS. From the XRD results it was deduced that the selected calcination at a temperature of 600 ºC for 2 hours was best suited for production of high crystalline nanomaterials. DRS analysis showed that there was an optical shift to higher wavelength due to the incorporation of the dopants Ag and N on titania.

Using the electrospinning method the prepared nanopowders of Ag and N doped TiO_2 were immobilized onto the nanofibers of a polymer blend of chitosan and polyvinyl alcohol co ethylene. The electrospun nanofibers were characterized by SEM to determine fibre orientation and size. The SEM images showed that the fiber had a uniform distribution and looked like mats.

The prepared functionalized nanofibers composites were tested for photocatalytic activity and antibacterial activity using methylene blue and *E. coli* respectively as model pollutants. These tests were done under solar radiation and UV light for comparison. The photocatalytic activity results in Section 5.3.1 showed that silver doped titania was a better photocatalyst because of the enhanced degradation of methylene blue dye used as a model organic pollutant. Silver and other

noble metals are said to have a strong surface Plasmon resonance (SPR) character mainly observed in the visible region. Furthermore these observations are due to the fact that silver nanoparticles doped on the photocatalyst were able to trap the photogenerated electrons, therefore preventing recombination of electron hole pairs (Kanjwal *et al*., 2010;).

The results obtained for antibacterial tests and photocatalytic activity tests show similar trends in terms of the dopants used. Silver doped titania showed high antimicrobial efficiency and high photocatalytic activity compared to nitrogen doped titania. The effect of the Cs-PVAE polymer blend matrix was mainly as a support for the photocatalyst and as an adsorbent. Blending the two polymers together improved the mechanical strength of the polymers in water hence the nanofibers could be used repeatedly with ease of removal from one reaction vessel to another. However it was also observed that the photocatalytic efficiency of titania was masked since the photocatalyst nanoparticles were encapsulated within the polymer blend instead of on the surface. This reduces the amount of TiO_2 active surface sites available for photocatalytic decolorization of MB and antibacterial degradation of *E. coli* as compared to the powdered photocatalyst.

6.2 Recommendations for Future work

It is recommended that further studies should be carried out in order to answer some of the questions which arose from this research as well as further investigation on how methods used in this study can be optimized. Specific work identified for recommendation include:

- Vary the concentration of Ag dopant to investigate whether the absorption band edge can be shifted to a longer wavelength.

- Co dope titania with Ag and N and immobilize the nanopowders on the Cs-PVAE matrix to compare if there will be any increase in the optical shift as well as the photocatalytic activity and antibacterial activity.
- A large surface area of TiO_2 provides many active sites on the photocatalyst where pollutants can be adsorbed; therefore BET analysis should be done in order to calculate the specific surface area (SSA) of the synthesized nanomaterials.
- Find a method on how to calculate the photocatalyst loading in the nanofibers materials per area of the electrospun mat.
- The efficiency of the polymer blends as adsorbents towards the pollutants should be investigated using the adsorption isotherms.
- More research work to increase the volume ratio of chitosan in the polymer blend from 20% to 80% resulting in 50:50% (v/v) chitosan to PVAE, as well as measurements of the viscosity in order to identify the one suitable for electrospining and nanofiber synthesis.

References

Akpan, U.G., Hameed, B.H. (2010). The advancements in sol–gel method of doped-TiO2 photocatalysts. *Applied Catalysis* , 1-11.

Anicuta, S., Dobre, L., Stroescu, M., Jipa, I. (2010). Fourier transform infrared (FTIR) spectroscopy for characterization of antimicrobial films containing chitosan. *Analele Universitatii din Oradea Fascicula: Ecotoxicologie, Zootehnie si Tehnologii de Industrie Alimentara* , 1234-1240.

Asahi, R., Morikawa, T., Ohwaki, T., Aoki, K., Taga, Y. (2001). Visible-Light Photocatalysis in Nitrogen-Doped Titanium Oxides. *Science* , 269-271.

Chen, X., Lou, Y., Samia, A.C.S., Burda, C., Gole, J.L. (2005). Formation of Oxynitride as the Photocataltic Enhancing Site in Nitrogen-Doped Titania Nanocatalysts: Comparison to a Commercial Nanopowder. *Advanced Functional Materials* , 15;41-49.

Choi, H., Stathatos, E., Dionysiou, D.D. . (2007). PhotocatalyticTiO2 films and membranes for the development of efficient wastewater treatment and reuse systems. *Desalination, Vol. 202* , 199-206.

Choi, J., Park, H., Hoffmann, M.R. (2009). Effects of Single Metal-Ion Doping on the Visible-Light Photo-reactivity of TiO2. *Journal of Physical Chemistry,C* , 17-55.

Christianmangun, Z., Economy, J. (2001). Removal of Chemical Contaminants from Water to below USEPA MCL using fiber glass supported activated carbon filters. *Environmental Science Technology, Vol. 35* , 2844-2848.

Coleman, H.M., Marquis, C.P., Scott, J.A., Chin, S.S., Amal, R. (2005). Bactericidal effects of titanium dioxide-based photocatalysts. *chemical Engineering Journal* , 113, 55-63.

Ding, Z., Lu, G.Q., Greenfield, P.F. (2000). Role of the Crystallite Phase of TiO2 in Heterogeneous Photocatalysis for Phenol Oxidation in water. *J. Phys. Chem B* , 104, 4815-4820.

Dutra, R.C.L., Lourenco, V.L., Diniz, M.F., Azevedo, M.F.P., Barbosa, R.V., Soares, B.G. (1996). Poly (ethylene-co-vinyl alcohol-co-vinyl mercaptoacetate) (EVALSH)-determination of the vinyl mercaptoacetate content by thermogravimetric analysis and FTIR spectroscopy. *Polymer Bulletin* , 36, 593-600.

Jagadale, T.C., Takale, S.P., Sonawane, R.S., Joshi, H.M., Patil, S.I., Kale, B.B., Ogale, S.B. (2008). N-Doped TiO2 Nanoparticle Based Visible Light Photocatalyst by Modified Peroxide Sol-Gel Method. *Journal Phys. Chem.* , 14596-14602.

Jia, Y.T., Gong, J., Gu, X.H., Kim, H.Y., Dong, J., Shen, X.Y. (2007). Fabrication and characterization of poly (vinyl alcohol)/chitosan blend nanofibers produced by electrospinning method. *Carbohydrate Polymers* , 67, 403-409.

Juntanon, K., Niamlang, S., Rujiravanit, R., Sirivat, A. (2008). electrically controlled release of sulfosalicylic acid from crosslinked poly (vinyl alcohol) hydrogel. *International Journal of Pharmaceutics* , 356, 1-2, 1-11.

Kanda-Nishikicho. *Measurement of Band Gap in Compound Semiconductors-Band Gap determination from Diffuse Reflectance Spectra.* Tokyo, Japan: SHUMADZU CORPORATION International Marketing Division.

Kong, H., Song, J., Jang, J. (2010). Photocatalytic Antibacterial Capabilities of TiO2-Biocidal Polymer Nanocomposites Synthesized by a Surface-Initiated Photopolymerization. *Environmental Science and Technology* , 44;5672-5676.

Krishna Rao, K.S.V., Vijaya Kumar Naidu, B., Subha, M.C.S., Sairam, M., Aminabhavi, T.M. (2006). Novel chitosan-based pH-sensitive interpenetrating network hydrogels for the controlled release of cefadroxil. *Carbohydrate Polymers* , 66, 333-344.

Kulkarni, A., Bambole, V.A., Mahanwar, P.A. (2010). Electrospinning of Polymers, Their Modeling and Applications. *Polymer-Plastics Technology and Engineering, 49* , 427-441.

Kumar, R.V., Raza, G. (2009). Photocatalytic disinfection of water with Ag-TiO2 nanocrystalline composite. *Ionics* , 15;579-587.

Kusumawardani, C., Kartini, I., Narsito. (2009). Synthesis of visible light active N-doped Titania photocatalyst. *International Conference on Chemical, Biological and Environmental Engineering* (pp. 115-118). Singapore: World Scientific Publishing Co. Pte. Ltd.

Liu, H.-L., Yang, T.C.-K. . (2003). Photocatalytic inactivation of Escherichia coli and Lactobacillus helveticus by ZnO and TiO2 activated with ultraviolet light. *Process Biochemistry* , 39, 475-481.

Macwan, D.P., Dave, P.N., Chaturvedi, S. (2011). A review on nano-TiO2 sol–gel type syntheses and its applications. *Journal of Material Science* , 3669-3686.

Madani, S.M., Ehteshamzadeh, M., Rafsanjani, H.H., Mansoori, S.S. (2010). The effect of calcination on the corrosion performance of TiO2 sol-gel coatings dioed with benzotriazole on steel CK45. *Materials and Corrosion* , 1-6.

Maira, A.J., Coronado, J.M., Augugliaro, V., Yeung, K.L., Conesa, J.C., Soria, J. (2001). Fourier Transform Infrared Study of the Performance of Nanostructured TiO2 Particles for the Photocatalytic Oxidation of Gaseous Toluene. *Journal of Catalysis* , 202, 413-420.

Nasr-Esfahani, M., Habibi, M.H. (2008). Silver Doped TiO2 Nanostructure Composite Photocatalyst Film Synthesized by Sol-Gel Spin and Dip Coating Technique of Glass. *International Journal of Photoenergy* , 1-11.

Park, H.K., Kim, D.K., Kim, C.H. (1997). Effect of Solvent on Titania Particle Formation and Morphology in Thermal Hydrolysis of TiCl4. *Journal American Ceramic Soc.* , 743-749.

Pawlak, A., Mucha, M. (2003). Thermogravimetric and FTIR studies of chitosan blends. *Tehmochimica Acta* , 396, 153-166.

Qu, X., Wirsen, A., Albertsson, A.-C. (2000). Effect of lactic/glycolic acide side chains on the thermal degradation kinetics of chitosan derivatives. *Polymer* , 41, 4841-4847.

Ren, L., Huang, X., Sun, F., He, X. (2007). Preparation and characterization of doped TiO2 nanodandelion. *Materials letters* , 61;427-431.

Shen, Y., Xiong, T., Du, H., Jin, H., Shang, J., Yang, K. (2009). Phosphorous, nitrogen, and molybdenum ternary co-doped TiO2: preparation and photocatlytic activities under visible light. *Journal of Sol-Gel Science Technology* , 98-102.

Sobana, N., Muruganadham, M., Swaminathan, M. (2006). Nano-Ag particles doped TiO2 for efficient photodegradation of Direct azo dyes. *Journal of Molecular Catalysis A: Chemical* , 258, 124-132.

Suwanchawalit, C., Chanhom, P., Sriprang, P., Wongnawa, S. (2011). A Ag-Doped TiO2 Photocatalyst for Dye Decolorization under UV. *Pure and Applied Chemistry International Conference* , (pp. 375-405).

Tayade, R. J., Kulkarni, R.G., Jasra, R.V. (2006). Transition Metal Ion Impregnated Mesoporous TiO2 for Photocatalytic Degradation of Organic Contaminants in Water . *Ind. Eng. Chem. Res.* , 45,5231-5238.

Zhang, J., Zhang, Y., Yu, L., Zhong, X., Wang, W. (2011). Preparation of Ag-modified nano-titanium and their photocatalytic activity. *Rare Metals* , 30; 267-270.